UNIVERSITÀ DELLA CALABRIA

UNIVERSITÀ DELLA CALABRIA

Dipartimento di Farmacia e Scienze della Salute e della Nutrizione

Dottorato di Ricerca in
Biochimica Cellulare e Attività dei Farmaci in Oncologia

CICLO
XXVI

IN VITRO MECHANISM FOR DOWNREGULATION OF ERα EXPRESSION BY EPIGALLOCATECHIN GALLATE IN ER+/PR+ HUMAN BREAST CANCER CELLS

Settore Scientifico Disciplinare BIO/13

Coordinatore: Prof. Diego Sisci

Supervisore/Tutor: Dott.ssa Francesca De Amicis

Dottorando: Dott.ssa Alessandra Russo

ABSTRACT

La prolungata esposizione agli estrogeni rappresenta un fattore di rischio per lo sviluppo e la progressione del carcinoma mammario, pertanto la terapia anti-estrogenica è considerata l'approccio terapeutico di elezione per il trattamento del carcinoma mammario ormono-dipendente a tutti gli stadi. Purtroppo, spesso ci può essere una ricomparsa del tumore che si manifesta come conseguenza dello sviluppo di una resistenza ormonale secondaria. A tal proposito, sostanze in grado di down-regolare il recettore estrogenico, in grado di esercitare una tossicità minima e di agire su bersagli multipli, stanno suscitando un notevole interesse dal punto di vista clinico.

Negli ultimi anni l'epigallocatechina-3-gallato (EGCG), un composto polifenolico presente nel tè verde, ha suscitato una significativa attenzione per le sue proprietà chemio-preventive e antitumorali.

In particolare, in questo studio si è cercato di delineare il meccanismo molecolare attraverso il quale EGCG regola l'espressione di ERα in cellule di carcinoma mammario ER+/ PR+.

I dati del presente lavoro hanno mostrato che EGCG down-regola ERα dal punto di vista di proteina, di mRNA e di attività del promotore genico con una concomitante riduzione del segnale genomico e non genomico di ERα. Noi dimostriamo che questi eventi sono mediati dall'attivazione del signaling p38MAPK/CK2 che porta al distacco dell'isoforma B di PR da hsp90 e di conseguenza alla sua traslocazione nel nucleo.

I nostri saggi EMSA e ChIP hanno rivelato che, sotto trattamento con EGCG, PR-B è reclutato all'emisito contenente elementi di risposta al progesterone (half-PRE

site) presente sul promotore di ERα. Questo avviene contemporaneamente alla formazione del complesso con i corepressori N-Cor e HDAC1 che induce quelle alterazioni nella struttura della cromatina, come la de acetilazione, che bloccano l'accessibilità al promotore da parte dell'RNA polimerasi II che viene così spiazzata.

I dati del presente lavoro permettono di delineare un nuovo modello secondo il quale EGCG down-regola ERα con una conseguente azione inibitoria sulla proliferazione delle cellule di carcinoma mammario ER+/PR+.

INDEX

Introduction 5

Estrogens and estrogen receptor in breast cancer 6

Progesterone and progesterone receptor in breast cancer 11

Role of hsp90 in the steroid hormone receptor action 15

Coregulators in steroid receptors transcriptional control 19

Hormonal therapy in breast cancer 22

Epigallocatechin-3-gallate and breast cancer 24

Materials and Methods 29

Materials 29

Cell Culture 29

Cell proliferation assays 30

MTT anchorage-dependent growth assay 30

Anchorage-independent soft agar growth assays 30

Plasmids 31

Reverse transcription and real-time PCR 31

Western blotting (WB) and immunoprecipitation 32

Immunofluorescence 33

Transfections and luciferase assays 34

Site-directed mutagenesis 34

Lipid-mediated transfection of siRNA duplexes 35

Electrophoretic mobility shift assay (EMSA) 35

Chromatin immunoprecipitation (ChIP) assays 36

Statistical analysis 36

Results 37

EGCG treatment decreases ER+ PR+ cancer cell proliferation 37

EGCG downregulates ER-α expression and transcriptional activity 39

EGCG downregulates ER-α mRNA via a region between −2769 and −1000 bp of its promoter 45

EGCG inhibits Hsp90 client proteins and promotes PR-B translocation into the nucleus 49

Downregulation of ER-α expression by EGCG is dependent on PR-B 55

The NCoR co-repressor is recruited with PR-B to the ER-α promoter upon EGCG treatment 56

Discussion 60

References 66

Scientific Publication

1. Cassano R., Trombino S., Ferrarelli T., Bergonzi M.C., Bilia A. R., De Amicis F., **Russo A.** and Picci N. Curcumin-based microspheres for azathioprine oral delivery: development, antiproliferative and antioxidant activity evaluation. *Journal of Bioactive and Compatible Polimers,* 2011.

2. De Amicis F., Santoro M, Guido C, **Russo A**, Aquila S. Epigallocatechin gallate affects survival and metabolism of human sperm. *Molecular Nutrition and Food Research,* 2012.

3. De Amicis F., **Russo A.**, Avena P., Santoro M., Vivacqua A., Bonofiglio D., Mauro L., Aquila S., Tramontano D., Fuqua S.A.W. and Andò S. In vitro mechanism for down-regulation of ERalpha expression by epigallocatechin gallate in ER+/PR+ human breast cancer cells. *Molecular Nutrition and Food Research,* 2013.

4. De Amicis F., Perri A., Vizza D., **Russo A.**, Panno M.L., Bonofiglio D., Giordano C., Mauro L., Aquila S., Tramontano D., Andò S. Epigallocatechin gallate inhibits growth and Epithelial-to-Mesenchymal Transition in human thyroid carcinoma cell lines. *Journal of Cellular Physiology,* 2013.

Introduction

Breast cancer is the most commonly diagnosed cancer among women and it is second only to lung cancer in cancer-related deaths (*Siegel et al., 2012; Aguas et al., 2005*) (Fig.1). One in nine women in the UK and USA will develop the disease in their lifetimes. It is more common in Western countries, and many factors have been implicated in its etio-pathogenesis (*Bonefeld-Jorgensen et al., 2011; Weinberg et al., 2005*).

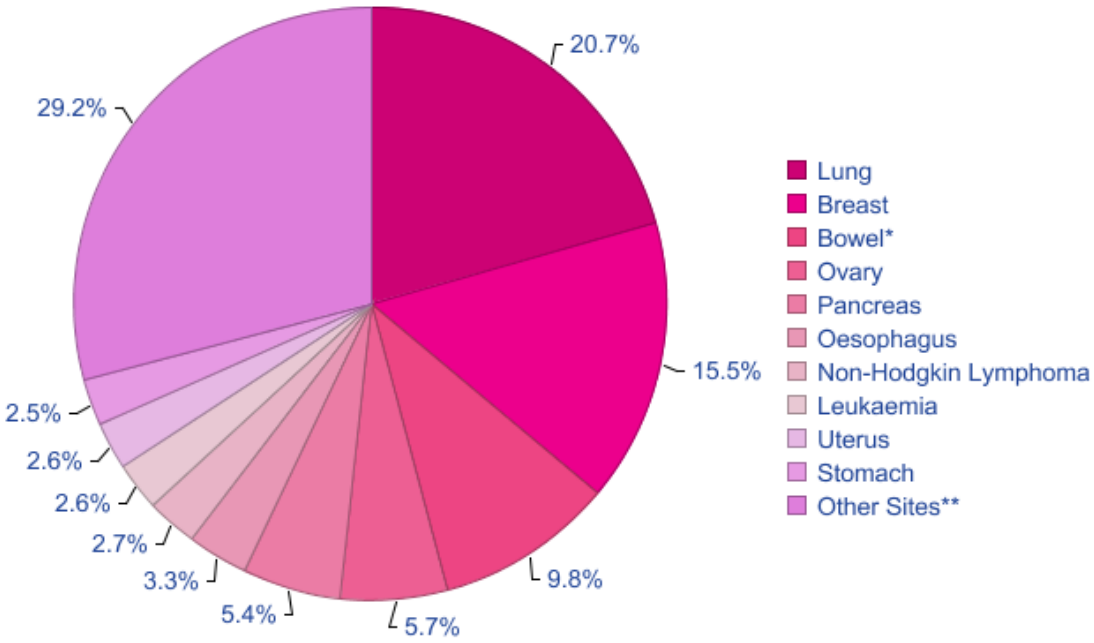

Figure 1: The ten most common causes of cancer death in females. Percentages of all cancer death, UK, 2010 (*http://www.cancerresearchuk.org*).

Breast cancer risk factors, such as early age at menarche (menstruation begins at 12 years), late age at menopause (menopause occurs after 55 years), postmenopausal hormone therapy, and high body mass index (BMI) are thought to affect breast

carcinogenesis by increasing the life-time exposure of the breast to estrogens and other sex hormones (*Herynk and Fuqua, 2004*).

Estrogens and estrogen receptor in breast cancer

The most potent and dominant estrogen in humans is 17β-estradiol (E_2), but lower levels of the estrogens estrone and estriol are also present (*Zhu and Conney, 1998*).

Estrogens particularly are mitogenic to breast epithelial cells, and since the effects of estrogens are mediated by both estrogen receptors (ERα and ERβ), the magnitude of their effects may be determined by the individual levels of ERs expressed in the breast.

Estrogen receptor (ER) belongs to a superfamily of nuclear receptors, including those of other steroid hormones, thyroid hormones, vitamin D, and retinoic acid (*Weatherman et al.,1999*). ERα and ERβ are produced by two distinct genes located on chromosome 6 and 14, respectively (*Green et al., 1986; Kuiper et al., 1996*). ERα and ERβ display a high relative tissue-specific expression, with overlapping distribution in some tissues. ERβ is more expressed in prostate, bone, ovaries (granulosa cells), lungs, and in various parts of the central and peripheral nervous system, while ERα is predominantly expressed in the pituitary gland, ovaries (thecal and interstitial cells), uterus, liver, kidneys, adrenals, and the mammary glands (*Kuiper et al., 1997; Emmen et al., 2005; Harris, 2007*).

Normally, when bound to their ligand, the ERs function as transcriptional factors of specific target genes (*Osborne et al., 2001; Osborne and Shiff, 2005*).

Like other steroid hormone receptors both the ER subtypes contain a well-defined domain organization, designated A/B through F (*Kumar et al., 1987; Evans, 1988; Nilsson, 2000; Zilli et al., 2009*) (Fig.2). The A/B domain, which is located at the N-

terminus, contains the activation function 1 (AF1) (*Tora et al.,1989*), a region responsible for the constitutive and ligand-independent transcriptional activity of ER. The C domain, referred to as DNA-binding domain (DBD), is responsible for specific DNA binding and receptor dimerization (*Mader and Chambon, 1993*). The D domain is a flexible hinge between the C and E domains and contains a nuclear localization signal (*Picard et al., 1990*). The E domain, referred to as ligand-binding domain (LBD), is a twelve-helix region involved in ligand binding and receptor dimerization. It harbors a second nuclear localization signal and the activation function 2 (AF2), responsible for the ligand-dependent activation of ER (*Tora et al., 1989*). The F domain, located at the extreme carboxy-terminus of the ERs, is a small region that although unnecessary for transcriptional activation exerts a complex modulatory role on both AF1 and AF2 activities of the receptor (*Weatherman and Scanlan, 2001; Koide et al., 2007; Skafar and Zhao, 2008*).

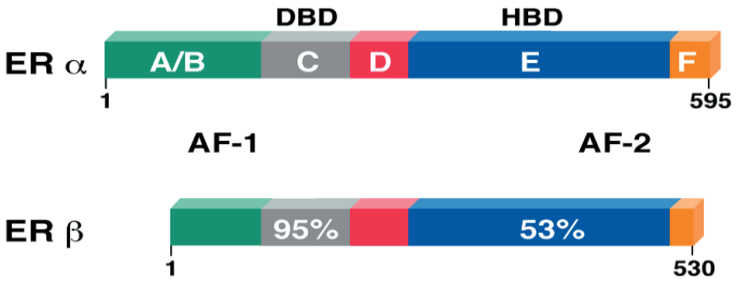

Fig. 2. Schematic representation of the structure of human ERα and ERβ nuclear receptors. Both ERα and ERβ are characterized by a well-defined domain organization: the A/B domain at the N-terminus contains the ligand-independent transcriptional activation function 1 (AF1), the C domain represents the DNA-binding domain (DBD) and contains a nuclear localization signal

(NLS), the D domain corresponds to the hinge region, the E domain harbors the ligand-binding domain and the ligand-dependent transcriptional activation function 2 (AF2) and the F domain at the C-terminus. Numbers outside each box refer to amino-acid number. Percentage of amino-acid homology for each domain is also shown. (*Journal of Clinical Oncology, Vol 18, 2000: pp 3172-3186*).

The classical mechanism of ER action involves estrogen binding to receptors in the nucleus, after which the receptors dimerize and bind to specific response elements known as estrogen response elements (EREs) located in the promoters of target genes (*Nilsson et al., 2001*). Hormone binding also induces a conformational change within the ligand binding domain of the receptors, and this conformational change allows coactivator proteins to be recruited (*Rosenfeld and Glass, 2001*). However, evidence for signaling pathways that deviate from this classical model has emerged, and it is now accepted that ERs can regulate gene expression by a number of distinct mechanisms. Around one third of the genes in humans that are regulated by ERs do not contain ERE-like sequences (*O'Lone et al., 2004*). The molecular mechanisms by which ERs regulate transcription at alternative response elements are not fully understood but are becoming increasingly clear. ERs can regulate gene expression without binding directly to DNA by modulating the function of other classes of transcription factors through protein-protein interactions in the nucleus (*Gottlicher et al., 1998*). The interaction of ERs with the activator protein 1 (AP-1) transcription factor complex is a typical example of such ERE-independent genomic actions (*O'Lone et al., 2004*).

Estrogens exert some of their effects through the action of ERs on gene expression, but a number of other effects of estrogens are so rapid that they cannot depend on the activation of RNA and protein synthesis. These actions are known as non-genomic

actions and are believed to be mediated through membrane-associated ERs. The actions are frequently associated with the activation of various protein-kinase cascades (*Losel and Wehling, 2003*). However, non-genomic actions of estrogens may indirectly influence gene expression, through the activation of signal transduction pathways that eventually act on target transcription factors. The functions of many transcription factors, including AP-1, are regulated through protein kinase-mediated phosphorylation, and these transcription factors may thus be targets of non-genomic actions of estrogens. This signalling pathway can be referred to as non genomic-to-genomic signaling, and it provides for a mechanism, distinct from protein-protein interactions in the nucleus, by which ERs can modulate the functions of transcription factors, and thus regulate the expression of genes that do not contain EREs (Fig.3).

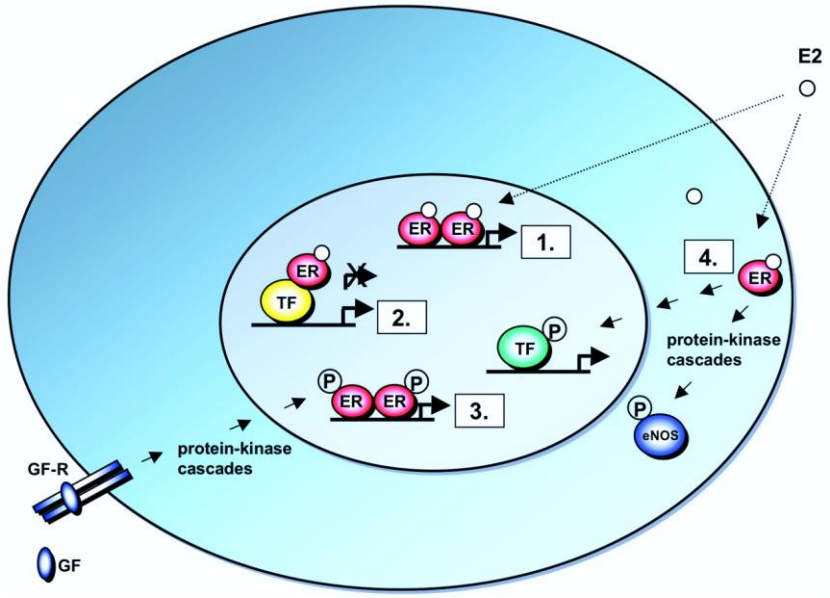

Figure 3: Schematic Illustration of ER Signaling Mechanisms. 1. Classical mechanism of ER action. Nuclear E2-ERs bind directly to EREs in target gene promoters. **2. ERE-independent genomic actions.** Nuclear E2-ER complexes are tethered through protein-protein interactions to a

transcription factor complex (TF) that contacts the target gene promoter. **3. Ligand-independent genomic actions.** Growth factors (GF) activate protein-kinase cascades, leading to phosphorylation (P) and activation of nuclear ERs at EREs. **4. Nongenomic actions.** Membrane E2-ER complexes activate protein-kinase cascades, leading to altered functions of proteins in the cytoplasm, e.g. activation of eNOS, or to regulation of gene expression through phosphorylation (P) and activation of a TF (*Molecular Endocrinology 19:833-842*).

A hypothesis is proposed that estrogens might play a dual role in affecting breast cancer risk. On one hand, there is evidence to indicate that estrogens might serve as preinitiators, initiators, and promoters of breast cancer. We generally associate estrogens with promotion of the growth of existing malignancies in the breast. However, these hormones and their metabolic products are also shown to induce direct and indirect free radical-mediated DNA damage, genetic instability, and mutations in cells in culture and *in vivo* (*Liehr, 2000*), suggesting a role for estrogens in cancer initiation. Furthermore, estrogens may serve as preinitiators. For example, elevated fetal estrogen levels can permanently alter the morphology of the mammary gland (*Hilakivi-Clarke, 1997*) and cause a persistent presence of epithelial structures (TEBs) that are known to be sites of malignant growth (*Russo J. and Russo I.H., 1987*). Data obtained in animal models and indirect evidence in humans indicate that high *in utero* estrogenicity increases breast cancer risk (*Potischman and Troisi, 1999; Hilakivi-Clarke, 1997; Trichopoulos, 1990*).

Up-regulated ERα expression in mice produces ductal hyperplasia, lobular hyperplasia, and ductal carcinoma in situ, demonstrating the consequences of unregulated ERα levels at all stages of breast cancer development (*Frech et al., 2005*); in contrast ERβ acts to regulate the degree of estrogen action by negatively modulating ERα, and the estrogen independent transcriptional activity of ERβ isoforms is inhibited by ERα (*Poola et al., 2005*). Further evidence shows that ERα levels in both hyperplastic lesions and ER-

positive tumors are greatly elevated as compared with adjacent normal tissue (*van Agthoven et al., 1995*) . Therefore it is not surprising that elevated levels of ERα in benign breast epithelium is, itself, considered a risk factor for progression to invasive breast disease (*Khan et al., 1994*).

Several studies demonstrated that ERβ expression is a favorable prognostic factor, correlating with low histological grading, longer disease-free survival and response to tamoxifen (*Fuqua et al., 2003; Jarvinen et al.,2000*).

Several studies have reported an increase in ERα/ERβ ratio in breast cancer as compared with benign tumors and normal tissues (*Roger et al., 2001; Shaw et al., 2002; Park et al., 2003*), suggesting that ERα is most closely associated with carcinogenesis, while ERβ can protect against the mitogenic activity of estrogens in mammary premalignant lesions. There is evidence that the estrogen-induced proliferation of ERα-positive breast cancer cells can be inhibited by ERβ overexpression (*Ström et al., 2004; Paruthiyil et al., 2004; Williams et al., 2008*). Routinely the evaluation of the ER expression in breast cancer, as determined by immunohistochemistry refers to ERα; consequently, the available information on the prognostic and predictive value of ER are related to this receptor form.

Progesterone and progesterone receptor in breast cancer

The steroid hormone, progesterone, is a key modulator of normal reproductive functions. These include ovulation, uterine and mammary gland development and the neurobehavioral expression associated with sexual responsiveness (*Clarke and Sutherland, 1990; Lydon et al., 1995*). The physiological effects of progesterone are mediated by interaction of the hormone with two specific intracellular progesterone

receptors (PRs) termed PR-A and PR-B that are transcribed from a single gene under the control of separate promoters (*Kastner et al., 1990*).

Binding of progesterone to PRs induces a significant conformational change on the receptor proteins (*Allan et al., 1992 a,b*) that results in dimerization of two ligand-receptor complexes (*Tsai et al., 1988; O' Malley et al., 1991*), increased receptor phosphorylation (*Weigel et al., 1995*), binding of receptor dimers to specific hormone responsive DNA elements located in the promoter regions of target genes (*Gronemeyer 1991, Tsai and O'Malley 1994*), and interaction of the receptor complex with specific coactivator proteins and general transcription factors (*Onate et al., 1995; Kamei et al., 1996*) to form a productive transcription initiation complex on specific target gene promoters.

In human breast cancer the PR-A and B proteins, characterized *in vitro* (*Lessey et al., 1983*) and *in vivo* (*Horwitz et al., 1983*), are detected with molecular masses of approximately 81 kDa and 115 kDa, respectively.

Despite structural similarities, PR-A and PR-B regulate different subsets of genes and, although PR-B is transcriptionally more active, there are genes, known to be involved in breast cancer progression, that are uniquely regulated by the PR-A isoform (*Kraus et al., 1993, Richer et al., 2002*).

Approximately 75% of primary breast cancers express ERα, and more than half of these cancers coexpress PR.

Increased expression of ERα is an early event in breast carcinogenesis; in contrast, a decrease of PR levels is associated with breast cancer progression (*Gross et al., 1984*). PR is able to inhibit the growth of ER+ breast cancer cells in ovariectomized nude mice despite Progesterone (Pg) deficiency, addressing a specific inhibitory role of PR

independent of its natural ligand (*Sartorius et al., 2003*). It emerges from experimental models that ER+/PR+ breast cancers are well differentiated, presenting as low-risk, well-defined lesions whereas ER+/PR- metastatic tumors display a much more aggressive course after loss of PR compared with tumors retaining PR (*Gross et al., 1984*).

Importantly, in multivariate analyses including lymph node involvement, tumor size, and age, PR status was independently associated with disease-free and overall survival (*Bardou et al., 2003*).

In vivo the two PR isoforms are usually coexpressed at similar levels in normal cells, but their ratio varies dramatically in different tissues, in varying physiological states, and disease sites (*Boyd-Leinen et al., 1982, Kato et al., 1993*). With regard to the mammary gland, 3:1 overexpression of PR-A over PR-B in transgenic mice results in extensive epithelial cell hyperplasia, excessive ductual branching, and disorganized basement membrane, all features associated with neoplasia. In contrast, overexpression of PR-B leads to premature ductal growth arrest and inadequate lobulo-alveolar differentiation (*Shymala et al., 2000, Shymala et al., 1998*). Moreover the loss of coordinated PR-A and PR-B expression is thought to be an early event in carcinogenesis and is evident in premalignant breast lesions (*Mote et al., 2002*). A significant proportion of carcinomas express a predominance of the PR-A isoform, and elevated PR-A has been associated with poor clinical outcomes in endometrial cancer, indicating a direct association between PR-A isoform predominance and poor prognosis (*Arnett-Mansfield et al., 2001*).

Although ER and PR are members of different steroid hormone receptor subfamilies and recognize distinct hormone response elements, there is considerable biological evidence for cross-talk between their receptor-signaling pathways. For instance, progestins can suppress the stimulatory effects of estrogens in target cells; estrogen increases the expression of both c-*fos* and PR mRNA in uterine cells, and progestins block these

effects (*Loose-Mitchell et al., 1988, Kirkland et al., 1992*). This blockade appears to be mediated via the PRs, but it is unclear whether ER or some other component of the estrogen-ER signaling pathway is the target for repression. It is also known that liganded PRs can suppress E_2-stimulated ER activity, with the magnitude of repression dependent on the PR isoform, progestin ligand, promoter and cell type (*Katzenellenbogen 2000, Weigel et al., 1993*). The exact molecular mechanisms regulating ERα expression in breast tumors are unclear, but studies suggest that they are partly at the level of transcription (*Martin et al., 1994*). PR-B ablation studies using small interfering RNA further demonstrated that endogenous PR-B levels are determinant in regulating ERα.

Our previous studies have shown that PR-B overexpression repressed ERα levels in breast cancer cells in a ligand-independent manner as it emerges from data obtained on cells transiently overexpressing PR-B truncated in LBD. This inhibitory effect is mediated by the recruitment of NCoR bound to PR-B on ERα promoter (*De Amicis et al., 2009*). Furthermore we demonstrated previously that PR-B overexpression, but not PR-A, inhibited ERα transactivation together with the expression of estrogen-dependent genes such as pS2, cyclin D1, and IRS1. These effects correlate well with the inhibition of E_2-induced cell proliferation by Pg through endogenous PR-B isoform. Our findings corroborate previous clinical studies (*Hopp et al., 2004; Graham et al. 1996*) illustrating that high PR-A/PR-B ratios in breast tumors predict shorter disease-free survival. The protective action of PR-B in breast cancer is further reinforced by studies showing that PR is inversely associated with HER-2/neu, the signaling of which is known to drive estrogen-independent breast cancer cell growth (*Huang et al., 2005, Bamberger et al., 2000*). Also of note are the findings that the levels of Her-2 are significantly higher in ER+/PR-A+ xenografts, than in ER+/PR-B+ xenografts (*Hopp et al., 2004*). To clarify the molecular mechanisms through which PR-B may interfere with ERα gene

transcription, we analyzed previously the ERα promoter sequence and identified a PRE half-site located at -1757 bp to -1752 bp. Functional experiments using five deletion constructs of the ERα promoter showed that the down-regulatory effects induced by PR-B overexpression on ERα promoter activity were through the half-site and were not detected in the deletion constructs lacking the half-PRE site. Moreover site directed mutagenesis of the above region completely reversed down-regulation of ERα promoter activity. ChIP assay results further confirmed the specific recruitment of the PR-B isoform to the half-PRE site within the ERα gene promoter because recruitment was prevented in PR-B knockdown experiments. The inhibitory effects on the ERα promoter transcriptional machinery addressed the ability of PR-B to recruit corepressors interfering with ERα gene transcription (*De Amicis et al., 2009*).

Role of hsp90 in the steroid hormone receptor action

Steroid receptors form large oligomeric complexes in the absence of hormone (*Toft and Gorski, 1966*). Most of the receptor associated proteins belong to chaperoning proteins. In eukaryotes molecular chaperones are essential proteins that take part in then regulation of steroid receptors. Chaperones bind and stabilize unstable forms of protein and facilitate the folding of the protein, oligomeric assembly, transport in the cell compartment, switch between active and inactive conformations and assist in the regulation of signal transduction pathways. Their function is to ensure that the assembly of other polypeptide chains occurs correctly. They do not determine the tertiary structure of the folding protein and prevent incorrect interactions of protein folding intermediates. Chaperone-bound receptor is stabilized so that it has high affinity for hormone but cannot bind DNA. Many molecular chaperones are called heat shock proteins (hsps) (*Hartl, 1996).*

The heat shock response was first described in 1962 (*Ritossa, 1962*), and heat shock proteins (HSPs) are named for their increased synthesis after heat shock that is contrary to the reduced synthesis of most cellular proteins under these conditions. In addition to heat, these proteins are modulated by nutrient deprivation, and oxidative and other stresses where protein denaturation might otherwise occur (*Zuehlke and Johnson, 2009*). Many HSPs form multimolecular complexes that act as molecular chaperones binding other proteins, denoted as client proteins. These complexes play a regulatory role in the fate of proteins in several different ways including: folding of proteins in the cytosol, endoplasmic reticulum and mitochondria; intracellular transport of proteins; repair or degradation of proteins partially denatured by exposure to various environmental stresses; control of regulatory proteins; and refolding of misfolded proteins (*Johnson and Brown, 2009)*. HSPs differ in their cellular localization and functions and mammalian HSPs have been classified into several families according to their molecular size: Hsp90, Hsp70, Hsp60 and Hsp40, and the small HSPs such as Hsp27 (*Jackson, 2013*).

Hsp90 defines a family of molecular chaperones that are highly conserved from prokaryotes to eukaryotes (*Pearl et al., 2008; Wegele et al., 2004*). Nonessential for normal growth in most bacteria, Hsp90 is abundantly expressed in higher eukaryotes where it has been shown to be necessary for viability (*Zhao et al., 2005; McClellan et al., 2007*). It functions as a homodimer that associates with co-chaperones to catalyze the maturation and/or activation of over 100 substrate proteins that are known to be involved in cell regulatory pathways (*Theodoraki and Caplan, 2012*). These ‘client proteins’ include protein kinases, nuclear hormone receptors, transcription factors, and an array of other essential proteins (*Street et al., 2011*).

It has been suggested that nuclear receptors as ER and PR are found in the cytoplasm in the form of heterocomplex with hsp90. Hormone binding stimulates hsp90 dissociation, and this leads to receptor dimerization, interaction with co-activators, DNA binding and target gene activation (*Manninen et al., 2005*).

Hsp90 forms a direct contact with the receptor and it acts on the ligand-binding domain of the steroid receptors (*Pratt et al., 2004 a*).

In humans, there are two hsp90 isoforms in the cytosol, hsp90α and hsp90β. These proteins are closely related. They are both induced by stress and no differences in their activities have been identified (*Chen et al., 2005*). Hsp90 is a phosphorylated homodimer containing two to three covalently bound phosphate molecules on each monomer. Hsp90 contains a highly conserved ATP binding domain near its N-terminus and the chaperoning activity of hsp90 requires both the binding and hydrolysis of ATP at this site (*Mayer et al., 2009*). A second nucleotide binding site appears to be present near the C-terminus, but this is less well characterized (*Pratt and Toft, 2003*). HSP90 functions as a part of a multichaperone complex, involving the dynamic association with various accessory cochaperones and client proteins. In an ATP-bound state, HSP90 adopts a closed conformation and becomes a mature complex that is essential for it to perform its function of client protein folding and stabilization.

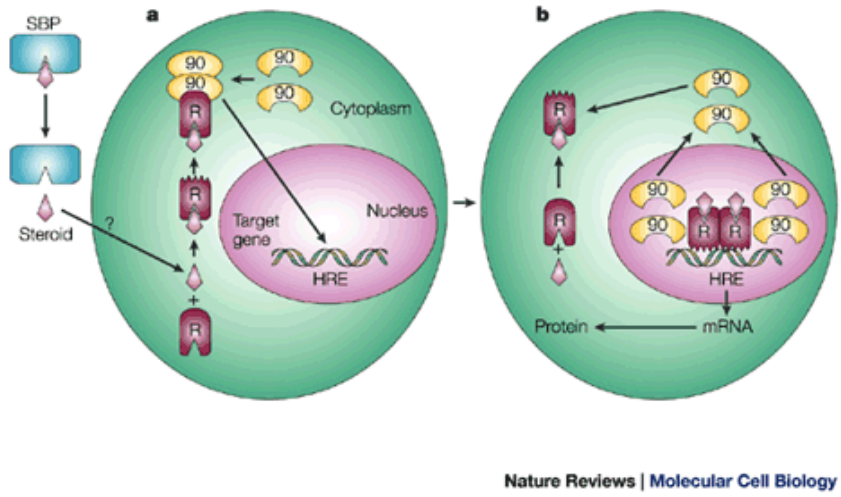

Figure 4: a The extracellular steroid released from its circulating steroid-binding protein (SBP) is transported into the cytoplasm of the target cell by passive diffusion or active transport. When bound to the non-ligand-bound receptor (R) it induces a conformational change that allows it to bind the Hsp90 dimer, which acts as its chaperone. The nuclear localization signal of the receptor allows the R–Hsp90 complex to translocate into the nucleus. **b** Once in the nucleus, the ligand–receptor complex dissociates from Hsp90 and itself dimerizes. The removal of Hsp90 unmasks the DNA-binding site of the receptor, which allows it to interact with the hormone response element (HRE) in the target gene promoter to activate transcription. This mechanism is only applicable to oestrogen receptor, progesterone receptor, glucocorticoid receptor and mineralocorticoid receptor, which do not heterodimerize with other nuclear receptors .

The association of hsp90 and breast cancer is of considerable interest, following studies showing the association of hsp90 and steroid receptors (*Pratt, 1987; Shymala et al., 1989*).

Inhibition of the Hsp90 chaperone cycle causes client proteins to undergo ubiquitination and subsequent degradation by the proteasome (*Mimnaugh et al., 2004*). Because many

of its clients include oncoproteins with important functions in the development and promotion of cancer, hsp90 is an important target in cancer therapy (*Whitesell and Lindquist, 2005*).

Levels of the heat shock proteins (hsp) molecular chaperones are elevated in many cancers, and hsp overexpression signals a poor prognosis in terms of survival and response to therapy in specific cancer types (*van 't Veer et al., 2002; Cornford et al., 2000; Ciocca et al., 1993*). Elevated hsp expression in malignant cells plays a key role in protection from spontaneous apoptosis associated with malignancy as well as the apoptosis generated by therapy, mechanisms which may underlie the role of hsp in tumor progression and resistance to treatment (*Gyrd-Hansen et al., 2004; Nylandsted et al., 2000; Volloch and Sherman, 1999).*

In particular, the discovery of hsp90 as the target of anticancer activity of geldanamycin (GM) sparked much interest in the inhibition of hsp90 as a strategy for the treatment of cancer (*Nickers and Workman, 2012*).

Coregulators in steroid receptors transcriptional control

The activities of nuclear receptors are modulated by coregulators that are divided into coactivators and corepressors (*Gao et al., 2002*).

Coactivators are factors that can interact with nuclear receptors (NRs) in a ligand-dependent manner and enhance their transcriptional activity. Corepressors are factors that interact with NRs, either in the absence of hormone or in the presence of antihormone, and repress their transcriptional activity. Both types of coregulators are required for efficient modulation of target gene transcription by steroid hormones. Therefore, changes in the expression level and pattern of steroid receptor coactivators or

corepressors can affect the transcriptional activity of the steroid hormones and hence cause disorders of their target tissues.

The SRC (steroid receptor coactivator) family is composed of three distinct but structurally and functionally related members, which are named SRC-1 (NcoA-1), SRC-2 (TIF2/GRIP1/NcoA-2), and SRC-3 (p/CIP/RAC3/ACTR/AIB1/TRAM-1), respectively (*McKenna et al.,1999*). Histone acetyltransferase (HAT) activity was identified in the C-terminal region of SRC members. The acetylation of histones results in a less restrictive chromatin structure that is generally associated with transcriptional activation (*Liu and Bagchi, 2004*).

Although there are far fewer nuclear receptor corepressors, these molecules serve important roles in negatively regulating receptor-dependent gene expression (*Smith and O'Malley, 2004*).

Two corepressors, nuclear receptor corepressor (N-CoR) and silencing mediator for retinoid and thyroid hormone receptors (SMRT), were initially identified as a component of repression complexes associated with unliganded retinoic acid receptor (RAR) and thyroid-hormone receptor (TR) (*Chen et al., 1996; Horlein et al.,1995*).

It has been recently documented that NCoR and SMRT are also recruited by both ER and PR in the presence of ligand antagonist to repress their transcriptional activations (*Agoulnik et al., 2003*). The N-CoR and SMRT are thought to recruit histone deacetylase complex (HDAC) in the nuclear receptor complex to reduce the level of histone acetylation and repress transcription (*Jones and Shi, 2003; Nagy et al., 1997*).

For instance, our previous ChIP experiments showed that among potential corepressor molecules that are able to interact with PR, NCoR was the only one present on the PR-B/DNA complex regardless of its natural ligand. These results are consistent with

evidence reporting that corepressors have different preferences and determinants for interactions with nuclear receptors and transcription factors at specific genes (*Hu and Lazar, 2001; Jepsen and Rosenfeld 2002*). Moreover we show that formation of this bipartite complex leads to hypoacetylation of histone H4, which causes stabilization of nucleosome structure, limiting accessibility to the basal transcriptional machinery and thus repressing ERα gene expression. All these data support a model in which elevated expression levels of PR-B increase the interaction of the receptor with NCoR on the half-PRE site of the ERα promoter, an event incompatible with PR-coactivator interactions. The crucial role of NCoR emerges from our previous data showing that silencing of this corepressor was able to reverse the down-regulation of ERα expression induced by PR-B overexpression.

E_2 is known to down-regulate the levels of ERα in breast cancer cell line through an increased turnover of E_2-bound receptor and via reduced transcription of its own gene (*Pink and Jordan, 1996*). This down-regulation represents a classical feature of ERα transactivation. Our previous findings showed that PR-B is a determinant of these down-regulatory effects, because PR-B knockdown attenuated the feedback inhibition of ERα levels after estrogenic stimulus. Therefore we proposed that ERα modulation by E_2 could be due to early events independent from PR expression, and later transcriptional events leading to PR-B overexpression, which in turn can produce a decrease in ERα transcription, via recruitment of a corepressor complex containing NCoR and displacing RNA polymerase II (Pol II). Thus, in our previous study, we demonstrated that the E_2 enhanced PR-B is crucial in determining the concomitant ERα down-regulation (*De Amicis et al., 2009*).

Hormonal therapy in breast cancer

Approximately 70% of breast cancer patients are positive for estrogen receptor (ER) or progesterone receptor (PR) expression at diagnosis. These patients are therefore suitable candidates for hormonal therapy, which aims to block estrogen stimulation of breast cancer cells (*Normanno et al, 2005*).

Although introduced more than 100 years ago, endocrine therapy is still an integral component in the systemic treatment of ER-positive breast cancer at any stage. Endocrine therapy is based on different approaches, including: (i) block of ER by the use of selective ER modulators (SERMs), such as tamoxifen; (ii) reduction of estrogen levels through aromatase inhibitors (AIs), such as anastrozole and letrozole; (iii) induction of ER degradation by selective estrogen receptor down-regulators (SERDs), such as fulvestrant.

Endocrine therapy is the most important component of adjuvant therapy for patients with early stage hormone receptor–positive breast cancer. Tamoxifen, a selective estrogen receptor modulator (SERM), binds to ERα and it blocks the estrogen action (*Jordan and Morrow, 1999*). Tamoxifen has been shown to improve relapse-free and overall survival in the adjuvant setting and to reduce the incidence of contralateral breast cancers (*Moy and Goss, 2006*). More recently, randomized data has shown that aromatase inhibitors (AI) as anastrozole, which deplete extragonadal peripheral estrogen synthesis, substantially improve disease-free survival in postmenopausal women with operable breast cancer in the adjuvant setting (*Thurlimann et al., 2005; Coombes et al., 2004; Goss et al., 2003; Baum at al., 2002*) (Fig. 5). In addition to these benefits in early stage disease, endocrine therapy is also of significant importance in the treatment of advanced metastatic disease (*Moy and Goss, 2006)*. Recently fulvestrant has been reported to be as active as AIs in tamoxifen-resistant metastatic breast cancer patients (*Howell et al.,*

2005) and also shows a certain efficacy in patients progressing to AIs (*Perey et al., 2007*).

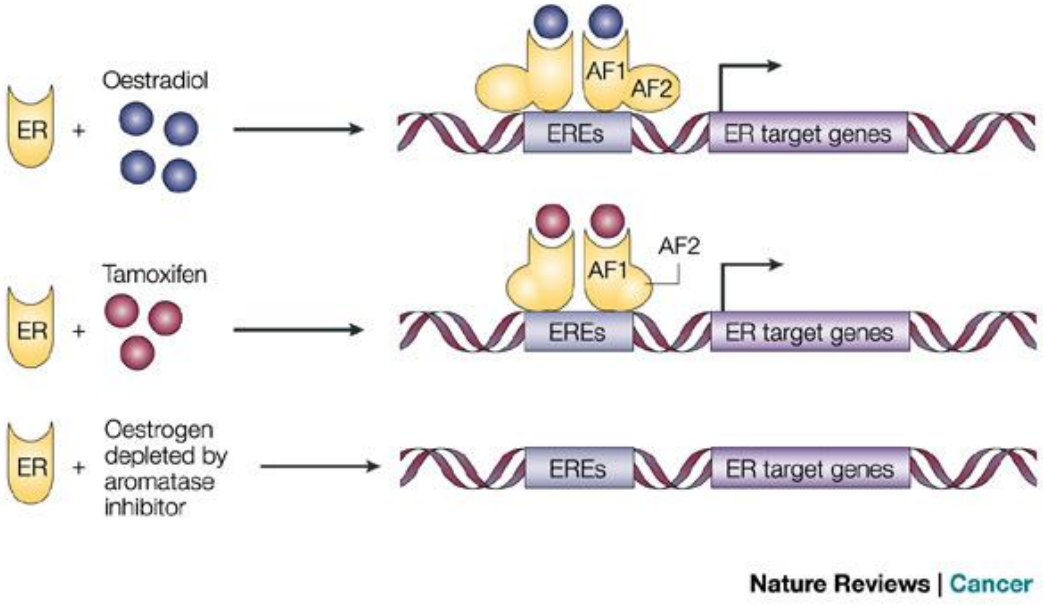

Figure 5: Both oestradiol and tamoxifen bind to the oestrogen receptor (ER) and lead to dimerization, conformational change in the activating function-2 (AF2) domain of ER and binding to oestrogen-response elements (EREs). The conformational change with tamoxifen is different from that with oestradiol and leads to persistent but less efficient transcription of most oestrogen-dependent genes. Oestrogen depletion leads to an absence of oestrogen-dependent transcription. Aromatase inhibitors block the enzyme aromatase and thus prevent the conversion of androgens into oestrogen. This decreases the level of oestrogen and the binding of oestrogen receptors. Finally, it stops the growth of cancer cells. (Nature Reviews Cancer 3, 821-831).

Despite these obvious benefits in a proportion of patients, acquired resistance to endocrine therapies frequently occurs; in fact, resistance to all forms of endocrine therapy remains a major problem. Furthermore, long-term use of tamoxifen is associated with several important side effects (increased incidence of endometrial cancer due to its

undesirable agonistic activity in the uterus, bone fractures and thrombo-embolism) (*Coombes et al., 2004*). Chemotherapy, in these cases, remains the treatment of choice, but is associated with severe adverse effects (*Budzar, 2007*).

Thus, looking for new antitumoral drugs with low toxicity to approach endocrine-related cancers treatment need to be considered as one of the most important priorities for research.

Epigallocatechin-3-gallate and breast cancer

The strong correlation between ERα expression, breast disease patho-physiology, and therapeutic response have justified the use of estrogen receptor down-regulators as attractive intervention, with significant clinical interest in their use. In this regard, many naturally occurring compounds, commonly present in the diet have gained considerable attention as well (*De Amicis et al., 2011; Hong and Sporn, 1997*). In recent years epigallocatechin gallate (EGCG), a polyphenolic compound found in green tea, has demonstrated chemo-preventative and antitumor properties (*Mukhtar et al., 1992*).

Green tea is a form of tea commonly consumed in Asia, derived from the leaf of the plant *Camellia sinensis* and its habitual consumption has long been associated with health benefits (*Cabrera et al., 2006; Brown, 1999; Zloch, 1996*). Most of the beneficial effects of green tea are attributed to its polyphenolic flavonoids, known as catechins, including epicatechin (EC), epigallocatechin (EGC), epicatechin-3- gallate (ECG) and the major flavonoid (−)-epigallocatechin-3-gallate (EGCG) (Fig.6) (*Singh et al., 2011*). These polyphenols account for up to 40% of the dry weight of green tea, and purified EGCG has been the focus of research in recent years (*Kanwar et al., 2012*).

Extensive research on green tea has taken place over the last decade, especially on the isolated catechin EGCG; however, most are based on in vitro and animal experiments. Green tea polyphenols are known antioxidants and it is proposed that these phytochemicals modulate biochemical and physiological processes leading to the initiation and propagation of carcinogenesis (*Yuan et al., 2011*).

The polyphenolic structure of EGCG consists of 4 rings, A, B, C and D (Fig.7). A and C rings constitute the benzopyran ring. This benzopyran ring has a phenyl group at C2 and gallate group at C3 positions. The B ring of EGCG has vicinal 3,4,5-trihydroxy groups, and the D ring galloyl moiety in EGCG is in the form of an ester at C3. The presence of this ester carbon makes EGCG highly susceptible to nucleophilic attack (*Kanwar et al., 2012*).

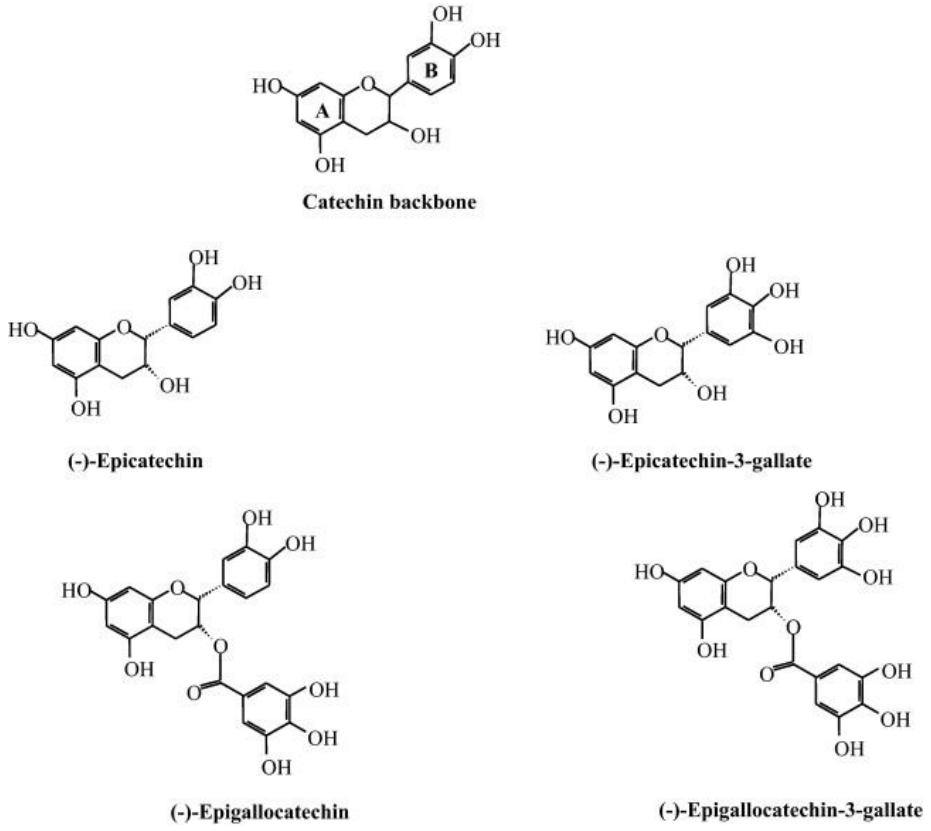

Figure 6: The structure of the green tea catechins (*Oncogene, 2006, 25, 1922–1930*).

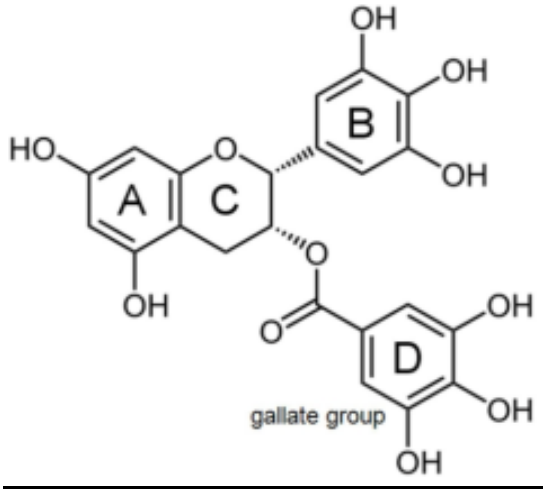

Figure 7: Chemical structure of EGCG *(Int. J. Mol. Sci, 2011)*.

Epidemiological studies have suggested that green tea consumption is linked to a decrease in the incidence and recurrence of breast cancer (*Nakachi et al., 1998*). Additionally, treatment with EGCG (50 mg/kg/day, 14 days) reduced the growth of MCF-7 implanted breast tumors in athymic nude mice by 40% (*Liao et al., 1995*), and it has been reported that catechin inhibited the proliferation of human breast cancer cells *in vitro* (*Belguise et al., 2007*). This is partly attributable to its effects on modulating the activity of mitogen-activated protein kinases (MAPKs), IGF/IGF-1 receptor, AKT, NF-κB, and CDKs (Cyclin-Dependent Kinases) (Fig.7) (*Sah et al., 2004; Gupta et al., 2001*). EGCG reduced angiogenesis and both local and distant invasion, and it could inhibit DNA methyltransferas and reactivate methylation-silenced genes in cancer cell lines (*Fang et al., 2003*).

EGCG also inhibits growth factor receptor extracellular signaling, the proteasome, mitochondrial depolarization, and fatty acid synthase (*Siddiqui et al., 2011; Qanungo et al., 2005; Liang et al.,1997*). However, the precise molecular targets and the exact anti-cancer mechanism of EGCG are not clearly defined.

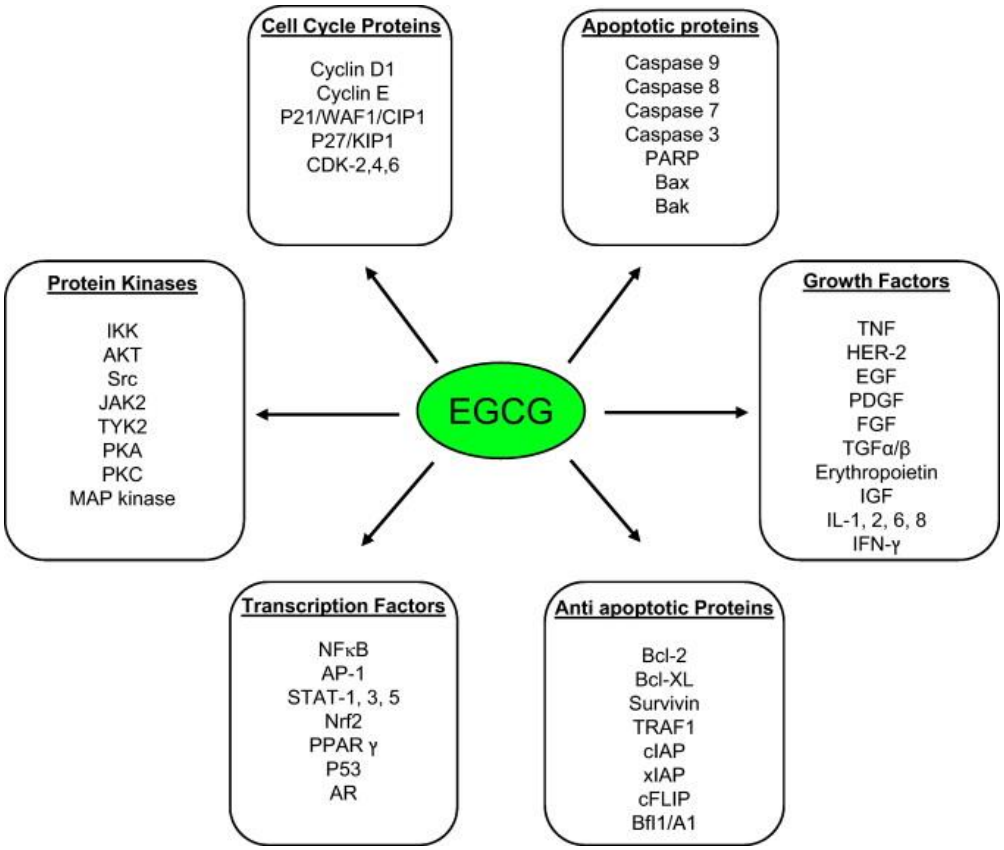

Figure 8: Mechanism of actions of EGCG (*Biochemical Pharmacology, Volume 82, Issue 12, 2011, 1807-1821*).

Recent studies report that the anti-tumor activity of EGCG is mediated by targeting HSP70 and HSP90 *in vitro* and *in vivo,* through a mechanism that involves direct binding of EGCG to the C-terminal region of HSP90 (*Tran et al., 2010*), a chaperone protein that is constitutively expressed at high levels in many cancer cells. HSP90 is assembled into heterocomplexes with unliganded steroid receptors, such as GR and PR, thus influencing their cellular distribution and activity (*Carson-Jurica et al., 1990*).

Particularly recent studies on breast cancer models have implicated EGCG in the regulation of ERα. Since the catechin family is structurally similar to isoflavones, it has been shown that catechins, such as EGCG, were co-estrogenic for ERα at lower doses

(<5μM) but antiestrogenic at higher doses (100-150 μM) and eliciting a concomitant massive cell death at the higher levels (*Belguise et al., 2007; Farabegoli et al., 2007*).

We considered that the interaction between EGCG and ERα might be potentially important and may have therapeutic implications.

In the present study we report that EGCG produces a significant inhibition of ER+ PR+ breast cancer cell proliferation and we define the molecular mechanisms associated with this growth effect. Concomitant with nuclear localization of PR, EGCG treatment causes a down-regulation of ERα protein, mRNA and gene promoter activity. We demonstrate that these effects are crucially mediated by PR-B via its recruitment to the ERα proximal promoter.

Materials and Methods

Materials

Epigallocatechin 3 gallate (EGCG), aprotinin, leupeptin, phenylmethylsulfonyl fluoride (PMFS), and sodium orthovanadate were from Sigma (Milan, Italy). PD 169316 and TBB from Calbiochem (Darmstadt, Germany). ICI 182,780 (ICI, ER antagonist), was purchased from Zeneca Pharmaceuticals (Cheshire, UK). Antibodies used in this study were GAPDH, laminin B, NCoR, RNA Pol II, HDAC1, total p38, phosphorylated p38, ERα, progesterone receptor B (PR-B), EGFR, Raf1, Her2, Hsp90, CK2 from Santa Cruz Biotechnology (Santa Cruz, CA); progesterone receptors (PR-B, PR-A), total MAPK, total AKT, phosphorylated p42/44 MAPK (Thr202/Tyr 204) and pAKT (Ser437), from Cell Signaling Technology (Beverly, MA).

Cell Culture

Cells utilized in the studies were obtained from American Type Culture Collection (Manassas, VA, USA). MCF-7 cells were maintained in DMEM/F-12 medium containing 5% fetal bovine serum (5% FBS), 1% L-glutamine, 1% Eagle's nonessential amino acids, and 1 mg/ml penicillin/streptomycin in a 5% CO_2 humidified atmosphere at 37 °C. T47D cells were routinely maintained in RPMI 1640 supplemented with 10% FBS, 1 mg/ml insulin (Sigma), 1 mg/ml penicillin /streptomycin (Sigma), 1% L-glutamine (Sigma), 2.5 mg/ml D-glucose (Sigma), 1% Sodium Pyruvate (Sigma), 10 nM Hepes Buffer (Sigma). Ishikawa endometrial cancer cells (ISK) were maintained in DMEM without phenol red supplemented with 10% fetal bovine serum (FBS), 1 mg/ml penicillin /streptomycin (Sigma), 1% L-glutamine. SkBr3 cells were cultured in RPMI 1640 with 10% FBS, 1 mg/ml penicillin /streptomycin (Sigma), 1% L-glutamine. Treatments were performed,

after 48 hours of serum starvation, in 1% dextran charcoal stripped (CS) FBS to reduce steroid concentration (*De Amicis et al., 2009*).

Cell proliferation assays

MTT anchorage-dependent growth assay. Cells (3×10^4 cells/mL) were plated in 24-well plates and serum-starved for 48 hours before the addition of treatment for 4 days. The MTT assay was performed as the following: 100 µL of MTT (3-(4,5-Dimethylthiazol-2-yl)-2,5-diphenyltetrazolium bromide) (2 mg/mL) (Sigma Aldrich, Milan, Italy) were added to each well, and the plates were incubated for 2 hours at 37 °C. Then, 500 µL of DMSO (Dimethyl sulfoxide) were added. The absorbance was measured with the Ultrospec 2100 Prospectrophotometer (Amersham-Biosciences, Milan, Italy) at a test wavelength of 570 nm.

Anchorage-independent soft agar growth assays. T47D cells (5000/well) were plated in 4 mL of 0.35% agarose with 5% CS FBS in phenol red free media, on a 0.7% agarose base in 6-well plates. Two days after plating, media containing control vehicle or hormonal treatments was added to the top layer, and the appropriate media was replaced every 2 days. After 14 days, 150 µL of MTT was added to each well and allowed to incubate at 37 °C for 4 hours. Plates were then placed in 4 °C overnight and colonies ≥50 µm diameter from triplicate assays were counted. Data are the mean colony number of three plates and representative of two independent experiments analyzed for statistical significance ($p < 0.05$) using a two-tailed student's test, performed by Graph Pad Prism 5 (GraphPad Software, San Diego, CA, USA). SDs are shown.

Plasmids

XETL (*Bunone et al., 1996*) , the wild-type human ER-α (HEGO) (*Tora et al., 1989 b*), the full-length PR-B consisting of the full-length PR-B cDNA fused with the SV40 early promoter (a gift from Dr. D. Picard, University of Geneve, Switzerland) (*De Amicis et al., 2009*), the PR DNA-binding mutant C587A (mDBD PR) previously described by *Faivre and Lange (2007)* (gift from Dr. C. Lange, University of Minnesota Cancer Center, Minneapolis, MN, USA), the full-length PRA (*Kastner et al., 1990*), and the deletion fragments of the ER-α gene promoter (*deGraffenried et al., 2002*). The Renilla luciferase expression vector pRL-TK (Promega, Milan, Italy) was used as a transfection standard.

Reverse transcription and real-time PCR

Cells (6×10^6) were treated as indicated and processed as described (*Vivacqua et al., 2009*). cDNA diluted were analyzed in triplicates by real-time PCR in an iCycler iQ Detection System (Bio-Rad, USA). The primers were:

(ER-α forward) 5'-AGAGGGCATGGTGGAGATCTT-3';

(ER-α reverse) 5'-CAAACTCCTCTCCCTGCAGATT-3';

(pS2 forward) 5'-TTCTATCCTAATACCATCGACG- 3';

(pS2 reverse) 5'-TTTGAGTAGTCAAAGTCAGAGC- 3';

(IRS1 forward) 5'- AGGATATTTAATTTGCCTCGG-3';

(IRS1 reverse) 5'- AAGCGTTTGTGCATGCTCTTG-3';

(CD1 forward) 5'-TCTAAGATGAAGGAGACCATC-3';

(CD1 reverse) 5'-GCGGTAGTAGGACAGGAAGTTGTT-3';

(18S forward) 5'- GGCGTCCCCCAACTTCTTA-3';

(18S reverse) 5'-GGGCATCACAGACCTGTTATT-3'.

Each sample was normalized on its GAPDH mRNA content. The relative gene expression levels were normalized to a calibrator that was chosen to be the basal, untreated sample. Final results were expressed as n-fold differences in gene expression relative to GAPDH mRNA and calibrator, calculated using the ΔCt method as follows:

$$\text{n-fold}=2^{-(\Delta Ctsample-\Delta Ctcalibrator)}$$

where ΔCt values of the sample and calibrator were determined by subtracting the average Ct value of the GAPDH mRNA reference gene from the average Ct value of the gene analysed.

Western blotting (WB) and immunoprecipitation

Protein expression or complex formation were assessed as described (*De Amicis et al., 2010*) by Western blotting (WB) or immunoprecipitation (IP) followed by WB, using total protein lysates, cytoplasmic, or nuclear protein lysates, where appropriate. Cells (6×10^6) were harvested to be analyzed using 500 µL of lysis buffer containing 50 mmol/L HEPES (pH 7.5), 150 mmol/L NaCl, 1% Triton X-100, 1.5 mmol/L $MgCl_2$, 10 mmol/L EGTA (pH 7.5), 10% glycerol, and inhibitors (0.1 mmol/L Na_3VO_4, 1% PMSF, and 2.0 mg/mL aprotinin) to obtain cytoplasmic proteins. After the collection using a scraper, incubation of 30' on ice, we lysed the nuclei for 15' at 4 °C using 250 µL of nuclear buffer containing 20 mmol/L HEPES (pH 8), 0.1 mmol/L EDTA, 5 mmol/L $MgCl_2$, 0.5 mol/L NaCl, 20% glycerol, 1% NP-40, and inhibitors (1.7 mg/mL aprotinin, 1 mg/mL leupeptin 200 mmol/L PMSF, 200 mmol/L sodium orthovanadate, and 100 mmol/L sodium fluoride). Then lysates were collected and centrifuged at 10 000 × g for 10' at 4 °C.

For total protein extracts, 500 µL RIPA buffer (50 mM Tris-HCl, pH 7.4, 150 mM NaCl, 1% NP-40, 0.25% Na deoxycholate, plus inhibitors 1.7 mg/mL aprotinin, 1 mg/mL

leupeptin 200 mmol/L PMSF, 200 mmol/L sodium orthovanadate, and 100 mmol/L sodium fluoride) was added to the 100 mL cell culture plate for 15' at 4 °C. Then lysates were collected and centrifuged at 10 000 × g for 10' at 4 °C. The protein content was determined using Bradford dye reagent (Bio-Rad). For WB, 50 µg of total, cytoplasmic or nuclear lysates were separated on an 11% polyacrylamide denaturing gel (SDS-PAGE) and transferred to nitrocellulose membranes. Proteins of interest were detected with specific Abs, recognized by peroxidase-coupled secondary Abs, and developed using the ECL PlusWestern Blotting detection system (Amersham Pharmacia Biotech, UK). For IP, 500 µg of protein of cytoplasmic or nuclear lysates were precleared for 1 hour with protein A/G-agarose (Santa Cruz), incubated with primary Abs at 4 °C for 18 hours in HNTG buffer (20 mmol/L HEPES, pH 7.5, 150 mmol/L NaCl, 0.1% Triton X-100, 10% glycerol, and 0.1 mmol/L Na_3VO_4), and then the antigen–Ab complexes were precipitated with protein A/G agarose for 2 h in HNTG buffer. The immunoprecipitated proteins were washed three times with HNTG buffer, separated on SDS-PAGE, and processed by WB. The images were acquired by using an Epson Perfection scanner (Epson, Japan) using Photoshop software (Adobe). The optical densities of the spots were analyzed by using ImageJ software (NIH; http://rsb.info.nih.gov/IJ). Images are representative of three different experiments.

Immunofluorescence

T47D cells seeded on glass cover-lips were treated with 40 µM EGCG for 12 h, washed with PBS, and then fixed with 4% paraformaldehyde in PBS for 20' at room temperature. Next, cells were permeabilized with 0.2% Triton X-100 in PBS for 5', blocked with 5% BSA for 30', and incubated with anti-PR-B antibody (1:50) in PBS overnight at 4 °C. The day after the cells were washed three times with PBS and incubated with the secondary antibody anti-rabbit IgG-FITC (1:200) for 1 hour at room temperature. To

check the specificity of immunolabeling, the primary antibody was replaced by normal rabbit serum (negative control). The blue fluorescent DAPI was used for nuclear stain. Immunofluorescence analysis was carried out on an OLYMPUS BX51 microscope using a ×40 objective. Images are representative of three different experiments.

Transfections and luciferase assays

Cells (1 x10^5) were plated into 24-well dishes with 500µl of regular growth medium per well the day before transfection. The medium was replaced with that lacking serum on the day of transfection, which was done using Fugene 6 reagent as recommended by the manufacturer (Roche Diagnostics, Milan, Italy) with a mixture containing 0.5 µg of reporter plasmid, alone or in combination plasmids as indicated in the figure legends, and 5 ng of pRL-TK. Medium was renewed after which cells were treated for 24 hours. Luciferase activity was measured with the Dual Luciferase kit (Promega, Milan, Italy) according to the manufacturer's recommendations.

TK Renilla luciferase plasmid was used to normalize the efficiency of the transfection. Firefly and Renilla luciferase activities were measured by Dual Luciferase kit. The firefly luciferase data for each sample were normalized based on the transfection efficiency measured by Renilla luciferase activity (*De Amicis et al., 2009*). Results represent mean of luciferase activities observed in three independent experiments done in triplicate.

Site-directed mutagenesis

Site-directed mutagenesis ia s method that is used to make specific and intentional changes to the DNA sequence of a gene and any gene products. Mutagenesis was performed on Fragment D of the ER-α promoter using the QuikChange mutagenesis kit (Stratagene, La Jolla, CA, USA) following the manufacturer's instructions. The sequence for the sense primer was:

5’-AGCAGGGAGATGAGGATTGCTGAAGTCCATGGGGGTATGT-3’.

The plasmids were then sequenced to confirm the mutation of the desired site.

Lipid-mediated transfection of siRNA duplexes

Custom-synthesized siRNA (Invitrogen) annealed duplexes (25-bp double-stranded RNA) were used for effective depletion of PR-B. A nonspecific siRNA (NS) (Invitrogen) that lacked identity with known gene targets was used as a control for nonsequence-specific effects. Cells were transfected using Lipofectamine 2000 reagent (Invitrogen, Paisley, UK) according to the manufacturer’s instructions and then treated as indicated.

Electrophoretic mobility shift assay (EMSA)

EMSA was carried out as previously described (*deGraffenried et al., 2002*), with a few modifications. Cells were treated for 6 hours before harvesting for the assay. The sequence of ER-α-half-PRE oligonucleotide used as probe or the unlabeled competitor was

5’-AGGATTGTGTTCTCCATGGG-3’,

mutated 5’- AGGATTGTTAAGTCCATGGG-3’.

The probe was generated by annealing single-stranded oligonucleotides, labelled with [γ^{32} P] ATP using T4 polynucleotide kinase, and purified using Sephadex G50 spin columns. To test specific binding, nuclear extracts were pre-incubated with rabbit polyclonal PR antibody or normal rabbit IgG. The reactions were separated on 6% polyacrylamide gel in 0.25× Tris borate–EDTA for 3 hours at 150 V. The gel was then dried for autoradiography. Images are representative of three different experiments.

Chromatin immunoprecipitation (ChIP) assays

Cells were treated for 12 hours before harvesting for the assay performed as described (*Guido et al., 2012*). DNA/protein complexes were cross-linked with 1% formaldehyde at 37 °C for 10' and sonicated. Supernatants were immunocleared with salmon sperm DNA/protein A agarose for 1 hour at 4°C. The precleared chromatin was immunoprecipitated with specific antibodies. A normal mouse serum IgG was used as negative control. Pellets were washed, eluted with elution buffer (1% SDS, 0.1 M $NaHCO_3$) and digested with proteinase K. DNA was obtained by phenol/chloroform/isoamyl alcohol extractions and precipitated with ethanol. A 5µl volume of each sample and input were used for PCR.

ER-α promoter primers used for PCR: forward, 5'-ACGTTCTTGATCCAGCAGGGTA-3' and reverse, 5'-ACCTGCCAAATTATATGCAAATGGCAG- 3' containing the half-PRE site; and forward, 5'-GTGGCCATTGTTGACCTACAG-3' and reverse, 5'CTGTAGGTCAACAATGGCCAC-3' upstream the half-PRE site.

Images are representative of three different experiments.

Statistical analysis

Each datum point represents the mean ±SD of three different experiments. Data were analyzed by Student's t-test using the GraphPad Prism 4 software program. $p<0.05$ was considered as statistically significant.

Results

EGCG treatment decreases ER+ PR+ cancer cell proliferation

We first investigated whether EGCG affects cancer cell proliferation following extended treatments with low doses of the catechin. We tested ER**+** PR**+** breast cancer cell lines, including T47D cells, which are known to express ER-α and elevated levels of endogenous PRs (*De Amicis et al., 2009*), MCF-7 cells that express ER-α and low levels of PR, and a well-differentiated ER**+** PR**+** human endometrial adenocarcinoma cell line (Ishikawa cells). Proliferating cells were exposed to different nontoxic concentrations of EGCG (10 μM; 20 μM; 40 μM) and then analyzed in MTT growth assays (Fig. 1A). After 4-day treatment, 10 μM EGCG inhibited basal cell proliferation of both T47D (50%), and MCF-7 (20%). With increasing doses of EGCG (20 and 40 μM), T47D cell number was further reduced by 52 to 67%, respectively. MCF-7 (25–50%) and ISK (55–68%) cells growth was also significantly decreased. EGCG inhibitory action was still present after pre-treatment with 1 μM ICI 182 780, a potent and specific antagonist with excellent growth inhibitory effects in several cell and animal models of human breast cancer, which induce ER-α degradation through ubiquitin-mediated mechanism (*Hu et al., 1993*). This suggests that growth inhibition was not mediated by binding of EGCG to ER. Of note is that the antiproliferative effects produced by EGCG occur earlier in T47D cells with respect of those observed in MCF-7 and ISK. Consistent with MTT assay results, 40 μM EGCG treatment also markedly reduced basal and E2-induced colony formation of T47D cells growing in soft agar (Fig. 1B).

A

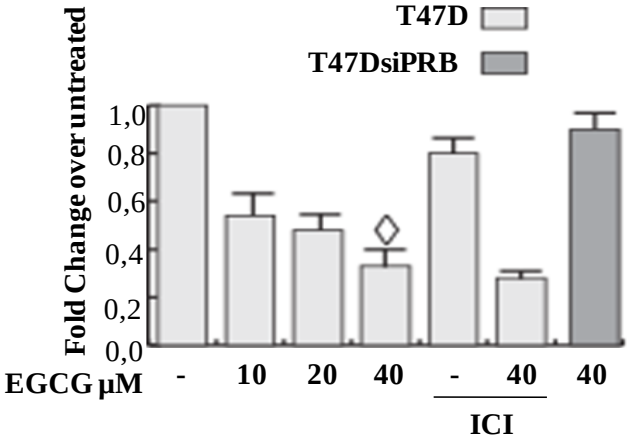
T47D
T47DsiPRB
Fold Change over untreated
1,0
0,8
0,6
0,4
0,2
0,0
EGCG µM
-
10
20
40
-
40
40
ICI

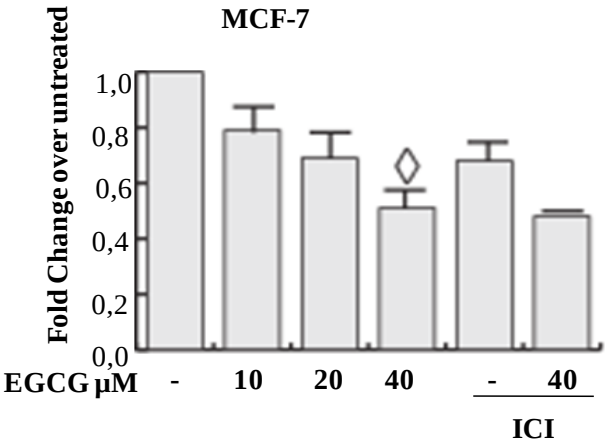
MCF-7
Fold Change over untreated
1,0
0,8
0,6
0,4
0,2
0,0
EGCG µM
-
10
20
40
-
40
ICI

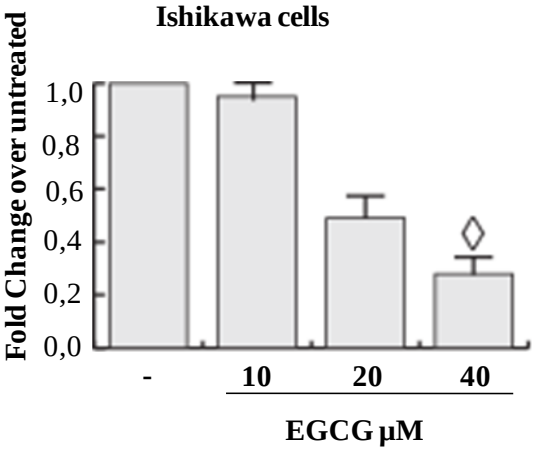
Ishikawa cells
Fold Change over untreated
1,0
0,8
0,6
0,4
0,2
0,0
-
10
20
40
EGCG µM

B

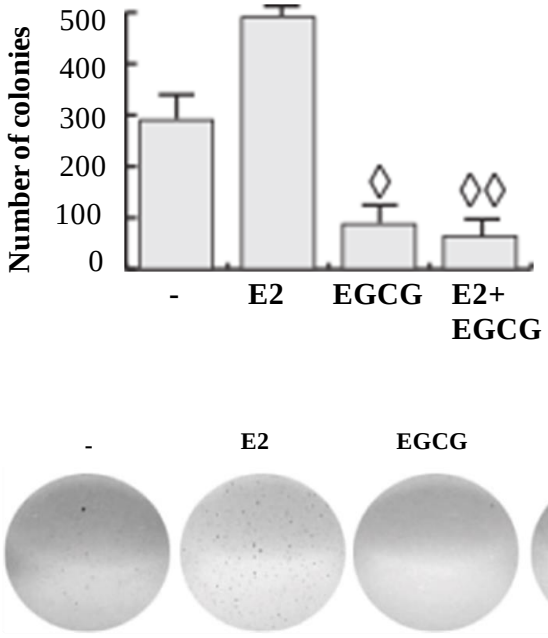

Figure 1. EGCG inhibits ER+ PR+ cancer cell proliferation (A) MTT assay. Cells, serum starved, were exposed to vehicle (−), or 1 μM ICI and/or different concentrations of EGCG in medium containing 1% dextran charcoal-stripped FBS for 4 days (treatments were renewed every 2 days). Results indicate mean of three independent experiments done in triplicate; bars SD; ◊ $p < 0.05$ compared with untreated cells. **(B) EGCG blocks E_2-induced anchorage independent growth of T47D.** Soft agar colony formation assay was performed in control conditions (−), or in the presence of 10 nM estrogen (E_2) and/or 40 μM EGCG. Cells were allowed to grow for 14 days and the number of colonies ≥50 μm were quantified. Bars SD; ◊ $p < 0.05$ compared with untreated cells; ◊◊ $p < 0.05$ compared with E_2-treated cells. Pictures at the bottom show typical well for each condition.

EGCG downregulates ER-α expression and transcriptional activity

It is well known that increased expression of ER-α is an early event in breast carcinogenesis, driving breast cancer cell proliferation. We thus hypothesized that

EGCG's effects in ER-α-positive breast cancer cells could involve the regulation of ER-α itself. As shown in Fig. 2A, ER-α protein expression levels were decreased after 24 hourd of increasing EGCG concentrations, in MCF-7 and T47D. E_2 treatment was used as control for downregulation of ER-α.

To investigate the functional effects of downregulation of ER-α by EGCG, we next analyzed ER-α genomic activity after treatment. To this aim, a luciferase reporter plasmid containing a consensus estrogen-responsive element (XETL) was transiently transfected into MCF-7 cells. EGCG treatment caused a significant decrease of basal, and with more intensity of E_2-induced luciferase activity (sevenfold) (Fig. 2B). To confirm these results, we also evaluated mRNA levels of known estrogen-regulated genes, such as IRS1, pS2, and cyclin D1 (CD1). As assessed by real-time PCR, EGCG at 40 μM significantly decreased basal and E_2-induced levels (Fig. 2C) of IRSI, pS2, and cyclin D1 in T47D and MCF-7 cells.

Stemming from our evidence that EGCG inhibited ER-α levels, we hypothesized that it could also influence E_2/ER-α nongenomic rapid effects within seconds to minutes (*Castoria et al., 2001*). Therefore to demonstrate the effects of EGCG on E_2-induced nongenomic activity, we pretreated T47D cells with EGCG for 24 h causing ER-α levels to decrease, and subsequently we treated the same cells with short exposures to E_2. As shown in Fig. 2D, EGCG treatment blocked E_2-induced phosphorylation of MAPK and AKT. Five percent CS treatments were used as positive controls for activation of downstream signaling. The ERK/MAPK and PI3K/AKT signaling pathways that are rapidly activated by the ER-α–E_2 complex, also have critical roles in estrogen action as survival agents. In fact, these pathways enhance the expression of the anti-apoptotic protein Bcl-2 and block the activation of p38 kinase (*Acconcia et al., 2005*). Western blot analysis in MCF-7 cells revealed that p38MAPK phosphorylation was significantly upregulated in EGCG-exposed cells, effectively opposing estrogen's effect (Fig. 2D).

These results suggest that EGCG-induced ER-α downregulation can affect nongenomic events in the E_2/ER-α signaling cascade.

A

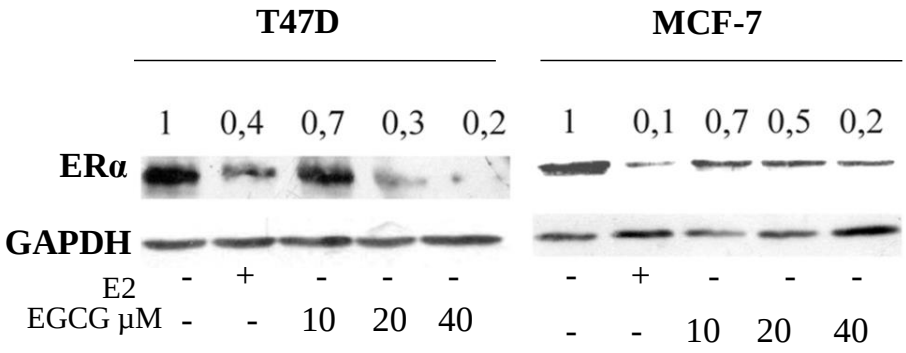

B

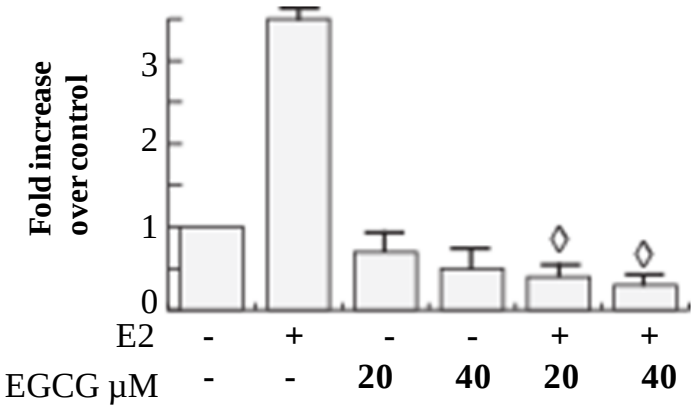

C

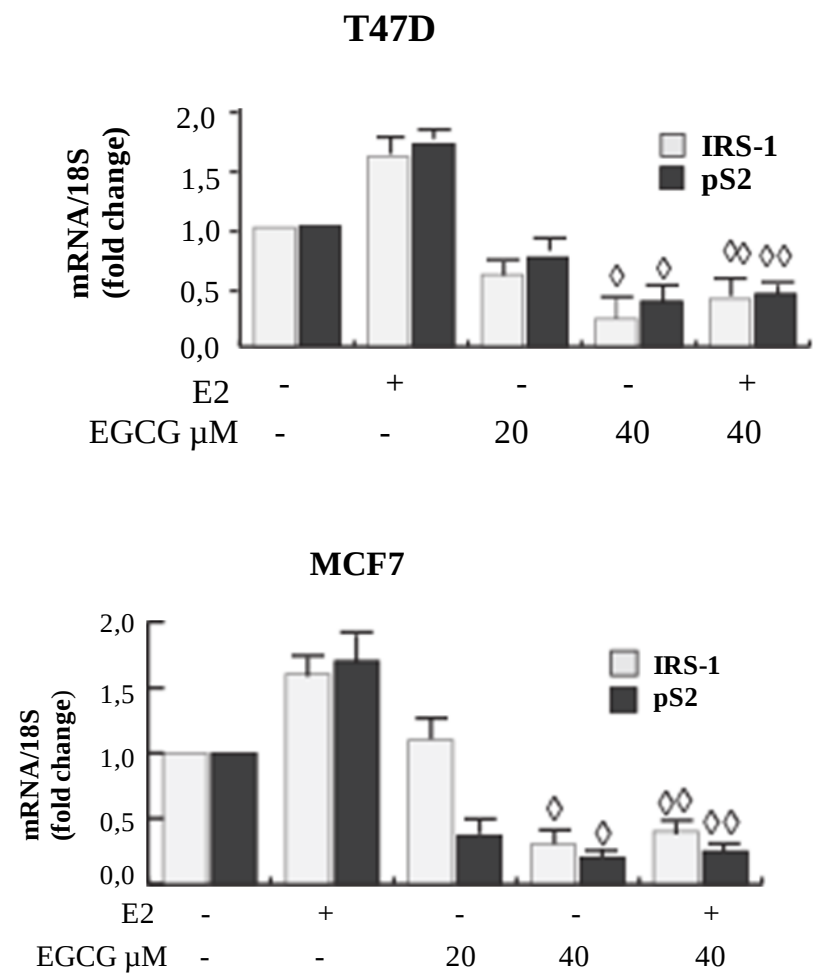
T47D
mRNA/18S (fold change)
2,0
1,5
1,0
0,5
0,0
IRS-1
pS2
E2 - + - - +
EGCG µM - - 20 40 40
MCF7
mRNA/18S (fold change)
2,0
1,5
1,0
0,5
0,0
IRS-1
pS2
E2 - + - - +
EGCG µM - - 20 40 40

D

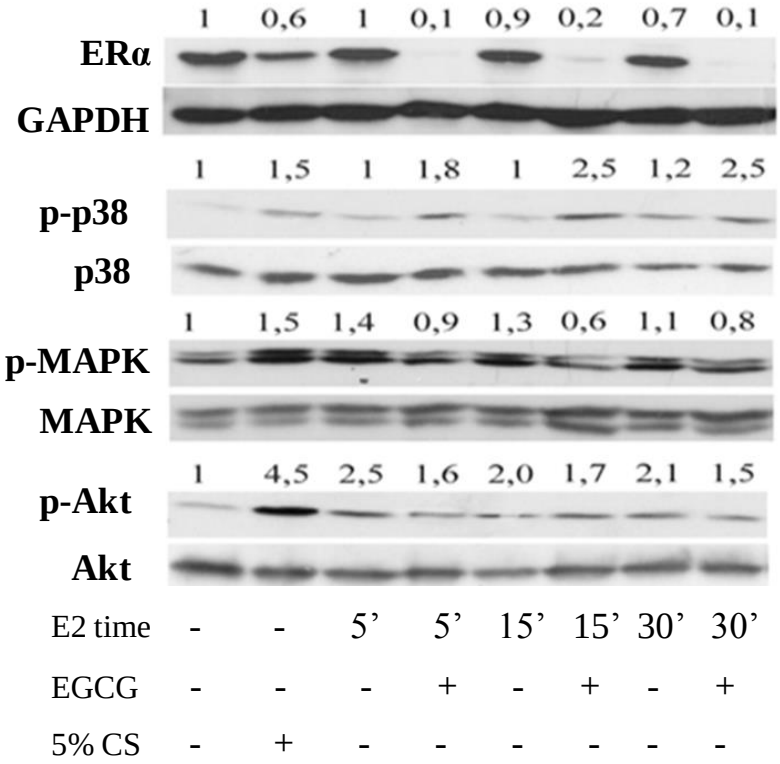
1 0,6 1 0,1 0,9 0,2 0,7 0,1
ERα
GAPDH
1 1,5 1 1,8 1 2,5 1,2 2,5
p-p38
p38
1 1,5 1,4 0,9 1,3 0,6 1,1 0,8
p-MAPK
MAPK
1 4,5 2,5 1,6 2,0 1,7 2,1 1,5
p-Akt
Akt
E2 time - - 5’ 5’ 15’ 15’ 30’ 30’
EGCG - - - + - + - +
5% CS - + - - - - - -

E

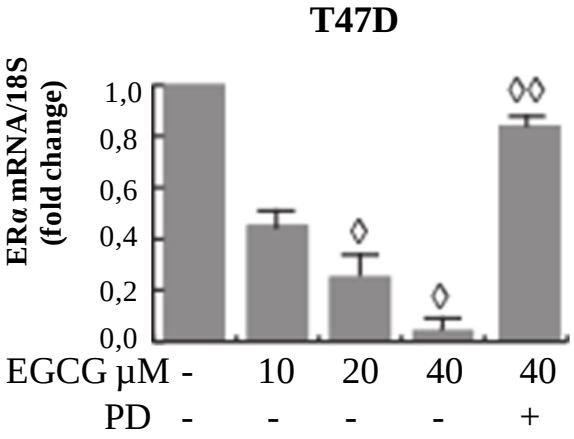
T47D
ERα mRNA/18S (fold change)
1,0
0,8
0,6
0,4
0,2
0,0
EGCG µM - 10 20 40 40
PD - - - - +

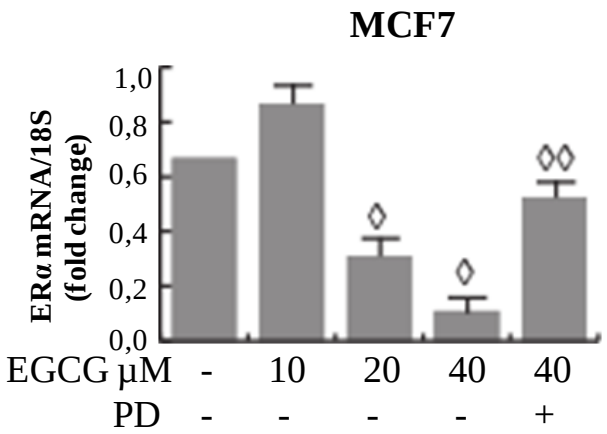

Figure 2. EGCG downregulates ER-α expression, genomic and nongenomic signal (A) Immunoblot analysis. Cells were treated with different concentrations of EGCG for 24 h. The whole-cell lysates obtained were then collected and analyzed by WB using specific Abs. Numbers represent the average fold change in ER-α and GAPDH levels. **(B) ERE luciferase reporter assay.** XETL was transiently transfected into MCF-7 cells treated with vehicle (−) or 10 nM E_2 and/or different concentrations of EGCG. Cells were then harvested, and luciferase activities were determined; Columns, mean of relative luciferase units (RLU); bars SD; ◊ $p < 0.05$ compared with E_2. **(C) Real-time PCR assay.** mRNA expression of pS2, IRS1, and CD1 in T47D and MCF-7 cells treated with vehicle (−) or 10 nM E_2 and/or different concentrations of EGCG for 24 h; 18S was determined as a control. Graphs are the mean of three independent experiments run in triplicate; bars SD; ◊ $p < 0.05$ compared with untreated cells; ◊◊ $p < 0.05$ compared with E_2-treated cells. **(D) Immunoblot analysis.** T47-D cells pretreated with 40 µM EGCG for 24 h were then treated with 10 nM E_2 for different times as indicated or with 5% CS for 24-h treatment. The whole-cell lysates obtained were then collected and analyzed by WB using specific Abs. Numbers represent the average fold change in ER-α and GAPDH, p-p38 and p38, p-MAPK and MAPK, p-AKT, and AKT levels. **(E) Real-time PCR assay.** mRNA expression of ER-α. Cells were treated with vehicle (−), different concentrations of EGCG for 24 h as indicated in presence or absence of PD. Columns mean of three independent experiments; bars, SD. ◊, $p < 0.05$ compared with untreated cells, ◊◊, $p < 0.05$ compared with 40 µM EGCG.

EGCG downregulates ER-α mRNA via a region between −2769 and −1000 bp of its promoter

To further investigate the molecular basis for regulation of ER-α expression by EGCG, we examined its effects on ER-α mRNA levels in T47D and MCF-7, treated for 24 hours. EGCG (20 μM and 40 μM) significantly downregulated ER-α as assessed by real-time-PCR (Fig. 2E). Since EGCG downregulated ER-α mRNA, we next evaluated whether it could act at the level of gene transcription through regulatory regions within the ER-α promoter. Therefore, we examined the ER-α promoter region covered from − 4100 bp to +212 bp first with a bioinformatics approach using the NCBI Genome database (www.ncbi.nlm.nih.gov). The region examined in this study contains multiple regulatory elements, including binding sites for AP-1, NF-kB, Oct-1, Sp1, CCAAT-binding proteins, CREB-2, USF1, half PRE (*De Amicis et al., 2009; deGraffenried et al., 2002*). Five overlapping ER-α promoter deletion constructs, − 245 bp to +212 bp (A), − 735 bp to +212 bp (B), − 1000 bp to +212 bp (C), − 2769 bp to +212 bp (D), and − 4100 bp to +212 bp (E), all relative to the first transcriptional ATG start site (depicted in Fig. 3A) and previously described (*deGraffenried et al., 2002*) , were transiently transfected into T47D and MCF 7 cells and the data are shown as relative promoter activity in luciferase units (Fig. 3B). We found that 40 μM EGCG had no effect on the promoter activity of fragments A, B, or C. In contrast, it reduced the activity of fragments D and E by 44% and 40%, respectively, indicating that the region between − 2769 and − 1000 bp may be responsible for downregulation of ER-α promoter activity after EGCG treatment. Precisely within this region of ER-α promoter, we also previously reported the presence of a functional half-PRE site responsible for transcriptional repression of ER-α mediated

by the B isoform of the PR (*De Amicis et al., 2009*). Green tea polyphenols have been reported to exert their biological effects through steroid receptors (*Siddiqui et al., 2011*); therefore, we hypothesized that EGCG downregulatory effects on ER-α gene transcription might involve this potential half-PRE site. To test this hypothesis, we next used site directed mutagenesis to alter this site. Mutation of 3 bp of the half-PRE site of the ER-α promoter D fragment resulted in the loss of EGCG-responsiveness, suggesting that this half-PRE site could be an effector of EGCG signalling (Fig. 3C).

To investigate DNA–protein interactions induced by EGCG within this promoter region, we next performed EMSA, using oligonucleotide from the ER-α promoter sequence bearing the half-PRE site (Fig. 3D). Cell extracts prepared in the absence of ligand (lane 1) generated double retarded bands corresponding to half-PRE complexes that were enhanced in EGCG treated extracts (lane 2), and whose appearance was effectively competed by a 100 fold molar excess of unlabeled probe (lane 3), thus demonstrating the specificity of the DNA-binding complexes. This inhibition was no longer observed using a mutated half-PRE oligonucleotide as competitor (lane 4). A rabbit antibody to PR also completely disrupted the DNA-protein complexed bands (lane 5) while normal rabbit IgG addition did not affect protein–DNA complex formation (lane 6).

A

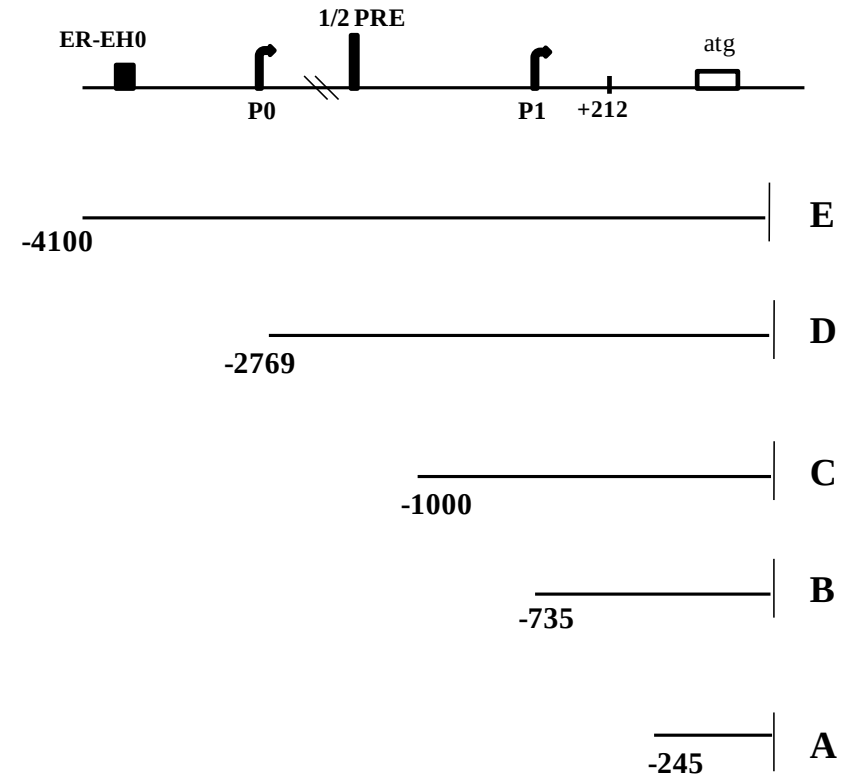
ER-EH0
1/2 PRE
atg
P0
P1
+212
-4100
E
-2769
D
-1000
C
-735
B
-245
A

B

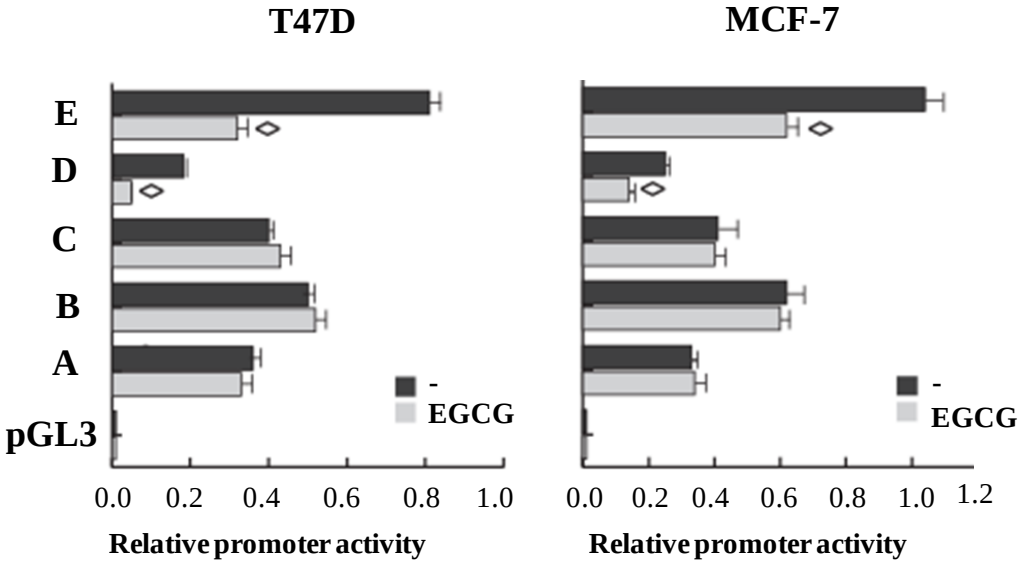
T47D
MCF-7
E
D
C
B
A
pGL3
-
EGCG
0.0
0.2
0.4
0.6
0.8
1.0
1.2
Relative promoter activity

C

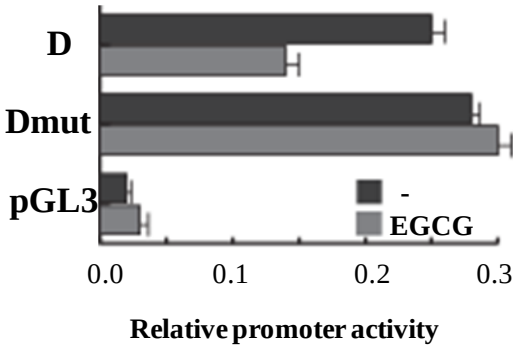

D

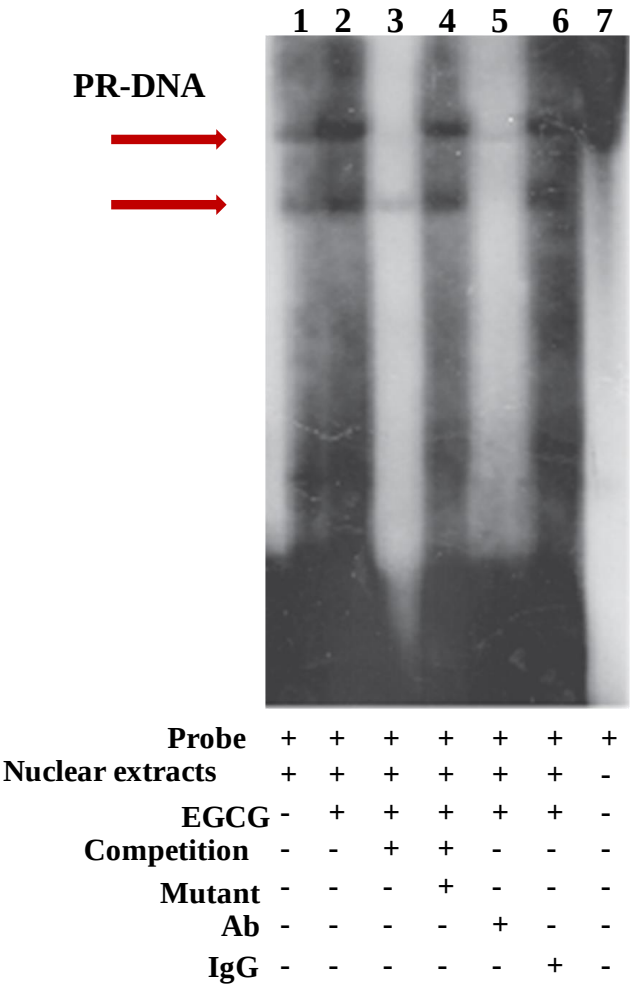

Figure 3. EGCG downregulates ER-α promoter activity through a half-PRE site. (A) Schematic representation of deletion fragments of the ER-α gene promoter. Fragments

coordinates are expressed relative to the primary transcription start site. **(B) Promoter activity of the ER-α 5'−flanking region.** Constructs depicted in panel A were transiently transfected in T47D and MCF-7 cells, treated with vehicle (−) or 40 μM EGCG. After 24 h, cells were harvested and luciferase activities were determined; bars, SD; ◊, $p < 0.05$ compared with untreated cells. **(C) Site-directed mutagenesis of the half-PRE site present in D fragment.** Fragment D and fragment D mut promoter constructs were cotransfected into MCF-7 cells, and promoter activity was assessed in the absence or presence of 40 μM EGCG; bars, SD. **(D) EMSA assay.** Nuclear extracts from T47-D cells treated with vehicle (-, lane 1) or 40 μM EGCG (lanes 2–6) were incubated with an ER-α promoter/half-PRE annealed probe (lane 2) or, for competition analysis, 100-fold excess unlabeled annealed probe (lane 3), or mutated in half-PRE site (lane 4). EGCG-treated nuclear extracts were also incubated with anti-PR Bffibf (lane 5), IgG (lane 6), or probe alone (lane 7). Picture is representative of three independent experiments.

EGCG inhibits Hsp90 client proteins and promotes PR-B translocation into the nucleus

The functions of PR are modulated by Hsp90 and its inhibition can be measured via the degradation of its many client proteins (such as c-Raf and Her2) (*Tillotson et al., 2010*). As shown in Fig. 4A, we observed depletion of Hsp90 client proteins EGFR, Raf-1, and Her 2 after EGCG treatment. Thus, we characterized the effects of EGCG on protein interaction between PR and Hsp90, performing co-IP assay from T47D cells cytosolic extracts. EGCG reduced the specific interactions between PR-B isoform and Hsp90 (Fig. 4B), while it did not affect PR-A/Hsp90 complex. We also investigated the influence of EGCG treatment on PR-B cellular localization by immunofluorescence microscopy experiments using a specific antibody. As shown in Fig. 4C, PR-B showed both a light nuclear and a stronger cytoplasmic distribution in untreated T47D cells. Interestingly, when cells were exposed to 40 μM EGCG, there was a remarkable redistribution of the PR-B from the cytosol to the nucleus. Results confirmed, by WB analysis of isolated

cellular compartments (Fig. 4D), that the PR-B nuclear isoform was specifically influenced by EGCG (7.5-fold nuclear versus 0.3 fold cytoplasmic). Therefore, we next examined the effects of a short treatment of EGCG on the activation of kinase cascades. As shown in Fig. 4E, 40 μM EGCG at different times modulated basal levels of p42/p44 MAPK and pAKT depending upon the cell type. At 15', in both cell types, EGCG induced p38MAPK phosphorylation, which remained activated in MCF-7 cells even after 24 hours of treatment (data not shown). An important effector of p38MAPK is CK2 (*Hildesheim et al., 2005*). IP assays revealed that EGCG treatment enhanced a physical interaction between CK2 and p-p38 (Fig. 4F). Stemming from these results, we next investigated the relevance of activated p38 in triggering the effects of EGCG treatment, by using a p38 inhibitor PD169316, known to block the p38 kinase activity (*Duval et al., 2004*). Pretreatment with PD or with the CK2 inhibitor TBB, strongly restored the specific interaction between Hsp90 and PR-B (Fig. 4B) indicating that activation of p38/CK2 signaling by ECGC modulates Hsp90/PR-B interaction. Moreover, PD and TBB clearly changed the cellular localization of PR-B produced by EGCG (Fig. 4C and D) demonstrating that EGCG via p38/CK2 allows PR nuclear translocation; furthermore, PD attenuated ER-α mRNA downregulation by EGCG (Fig. 2E).

A

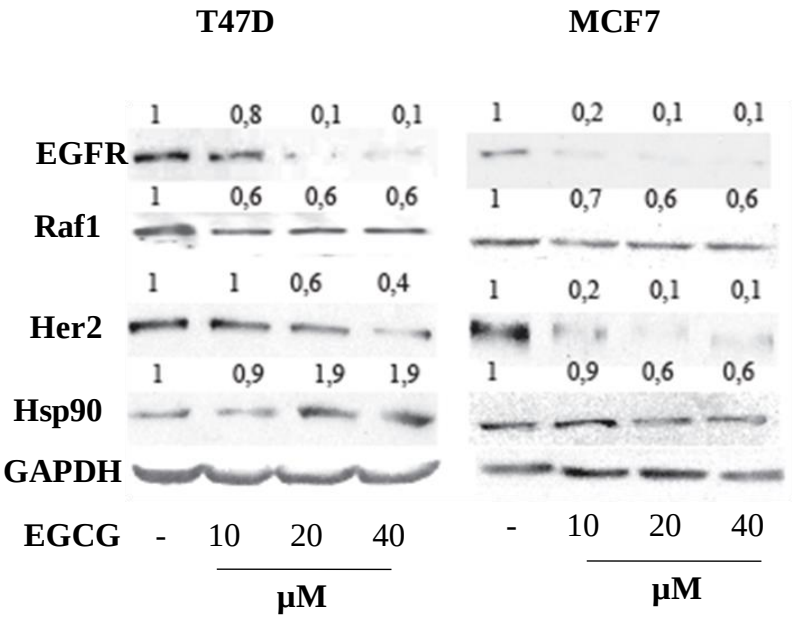
T47D
MCF7
EGFR
Raf1
Her2
Hsp90
GAPDH
1 0,8 0,1 0,1
1 0,6 0,6 0,6
1 1 0,6 0,4
1 0,9 1,9 1,9
1 0,2 0,1 0,1
1 0,7 0,6 0,6
1 0,2 0,1 0,1
1 0,9 0,6 0,6
EGCG - 10 20 40
- 10 20 40
µM
µM

B

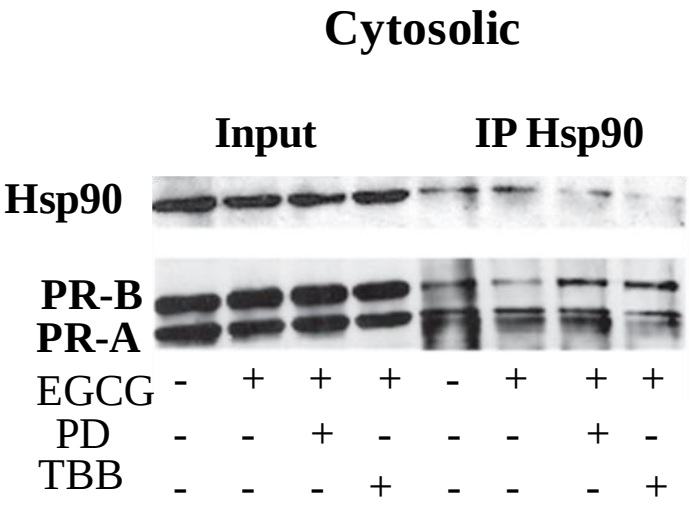
Cytosolic
Input
IP Hsp90
Hsp90
PR-B
PR-A
EGCG - + + + - + + +
PD - - + - - - + -
TBB - - - + - - - +

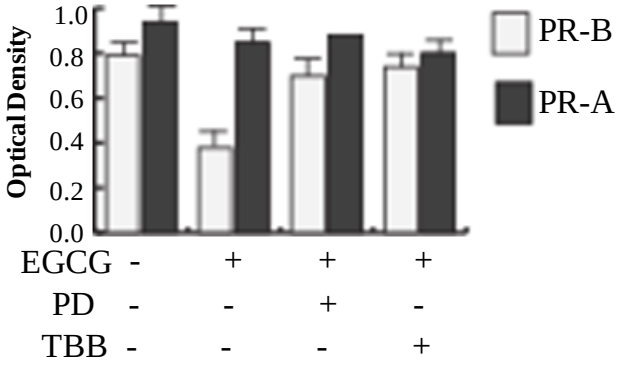
Optical Density
1.0
0.8
0.6
0.4
0.2
0.0
PR-B
PR-A
EGCG - + + +
PD - - + -
TBB - - - +

C

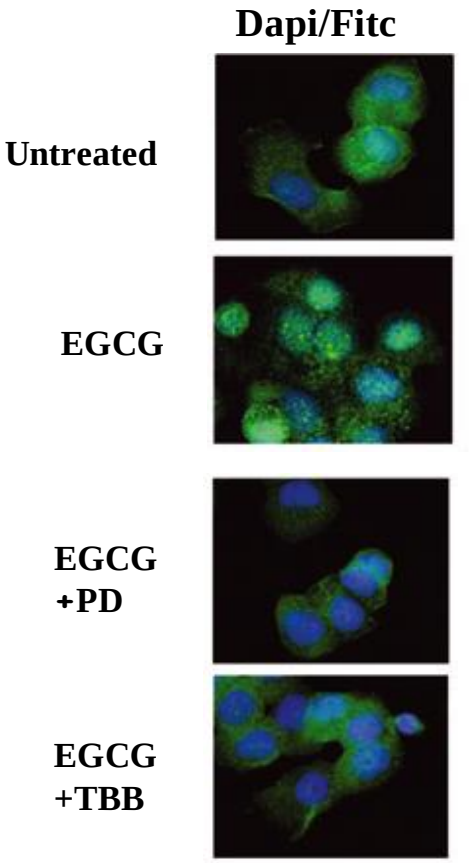
Dapi/Fitc
Untreated
EGCG
EGCG +PD
EGCG +TBB

D

Nuclear

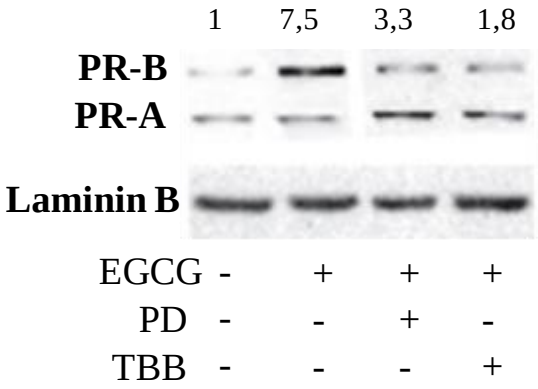

Cytosolic

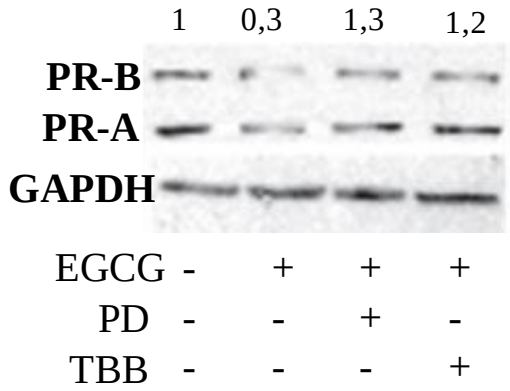

E

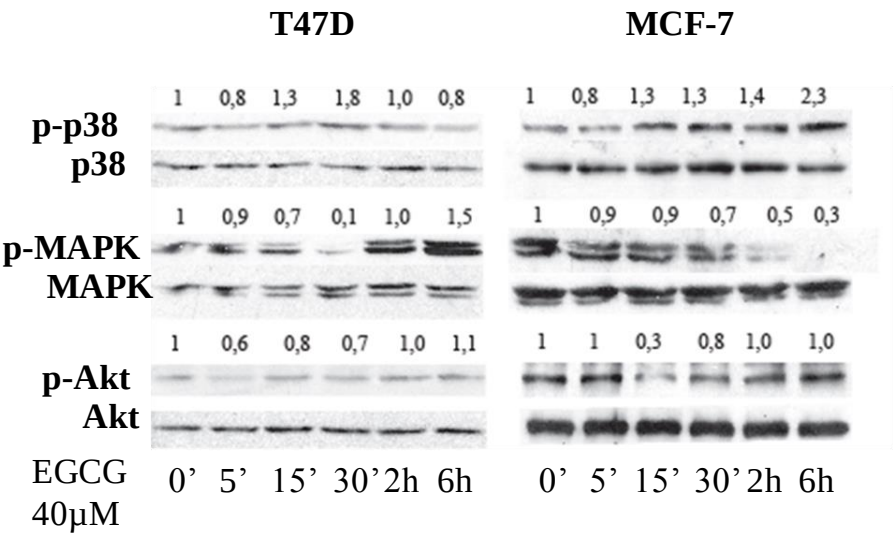

F

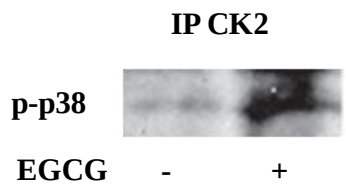

Figure 4: EGCG inhibits Hsp90 client proteins and promotes PR translocation into the nucleus via p38MAPK activation (A) Immunoblot analysis. Cells were treated with different concentrations of EGCG for 24 h. The whole-cell lysates obtained were then collected and analyzed. Numbers represent the average fold change in EGFR or Raf1 or Her2 or Hsp90 and GAPDH levels. **(B) Co-immunoprecipitation assay.** T47-D cells were treated for 24 h with vehicle (−) or 40 µM EGCG in presence or absence of PD or TBB. Cytosolic cell lysates were immunoprecipitated using anti-Hsp90 and then blotted with anti-Hsp90 or anti-PR antibody. Columns, mean of three independent experiments in which band intensities were evaluated in terms of optical density arbitrary units and expressed as IP/input; bars, SD; ◊ $p < 0.05$ compared with untreated cells. **(C) Immunofluorescence with anti-PR-B antibody.** T47-D cells were treated for

12 h with vehicle (−) or 40 μM EGCG in presence or absence of PD or TBB, then were stained (DAPI/FITC merge is presented). Immunofluorescent receptor is cytoplasmic in absence of treatment but shifted into the nucleus after EGCG administration. Pictures are representative of three independent experiments**. (D) Immunoblot analysis.** Cells were treated with 40 μM of EGCG for 12 h in presence or absence of PD or TBB, then nuclear and cytoplasmic protein extracts were analyzed. Numbers represent the average fold change in PR-B and Laminin B or GAPDH levels. **(E) Immunoblot analysis.** Cells were treated with vehicle (−) or 40 μM EGCG at different times as indicated. The whole-cell lysates obtained were then collected and analyzed. Numbers represent the average fold change in p-p38 and p38, p-MAPK and MAPK, p-AKT, and AKT levels. **(F) Co-immunoprecipitation assay.** Cells were treated for 24 h with vehicle (−) or 40 μM EGCG. Cell lysates were immunoprecipitated using anti-CK2 and then blotted with anti-p-p38.

Downregulation of ER-α expression by EGCG is dependent on PR-B

We next investigated the role of the PR-B isoform in mediating EGCG effects on ER-α.We co-transfected equal amounts of expression plasmids encoding PR-B or PR-A into the ERPR- negative SKBR3 cell line, along with the ER-α promoter reporter fragments. Only PR-B reduced ER-α promoter activity (51%) with EGCG treatment (Fig. 5A). Co-transfection of equal amounts of expression plasmids encoding either the PR-A isoform or the PR mutant with a disrupted DNA-binding domain (Cys587 to Ala, called mDBD PR) did not affect ER-α promoter activity either in presence or absence of EGCG, strongly suggesting that PR-B was responsible for EGCG downregulatory effects on ER-α, which occur at the transcriptional level. We also performed PR-B siRNA knockdown experiments during EGCG treatment of T47D cells. Addition of a PR-B-targeting siRNA resulted in a remarkable decrease in PR-B protein levels (Fig. 5B) that greatly blocked ER-α downregulation by EGCG treatment. PR-B knockdown also blocked the growth

inhibitory effect of EGCG in MTT assays (Fig. 1A). Altogether these data strongly support the hypothesis that PR-B through the half-PRE site within the ER-α promoter mediates EGCG effects on transcriptional regulation of ER-α.

The NCoR co-repressor is recruited with PR-B to the ER-α promoter upon EGCG treatment

To demonstrate the recruitment of PR to the ER-α gene promoter, we also used ChIP assays. T47D andMCF-7 cells were exposed to either control vehicle or 40 μM EGCG, after which chromatin was cross-linked with formaldehyde, and protein– DNA complexes were immunoprecipitated with antibodies directed against PR, RNA polymerase II, or the co-repressors NCoR, DAX-1, and SMRT. Results obtained demonstrate an enhanced recruitment of PR to the ER-α promoter with EGCG treatment (Fig. 5C); as a control we did not see recruitment to an unrelated ER-α promoter region located upstream of the half-PRE site (data not shown). Specific knockdown of PR-B also confirmed the recruitment of this isoform to the ER-α promoter (Fig. 5C). Concomitant with the increased recruitment of PR-B to the ER-α promoter after EGCG treatment, we saw the similar molecular events we described previously (*De Amicis et al., 2009*): displacement of RNA polymerase II, indicating that the chromatin in this region is probably in a less permissive environment for gene transcription, recruitment of NCoR in T47D and MCF7 cells (Fig. 5C). Since it is known that different co-repressor complexes contain one or more HDACs, as candidate mediators of PR action (*Jepsen and Rosenfeld, 2006*) we looked for histone deacetylases, in particular the class I HDAC-1 and HDAC-3. Our results show that HDAC-1 was the most strongly recruited following EGCG treatment. These data indicate PR-B binds to the ER-α promoter at half-

PRE site and this results in enhancement of the tripartite complex containing NCoR and HDAC1 with EGCG treatment and a concomitant release of RNAPol II, thereby inhibiting ER-α transcription. Thus the catechin may acquire pharmacological significance acting as an estrogen receptor downregulator in breast cancer cells. To further address the interaction between PR-B, HDAC1, and NCoR, we performed co-IP assays from nuclear extracts of T47D cells. EGCG induced the complex formation between PR-B, NCoR, and HDAC1 (Fig. 5D) via p-38/CK2, since pretreatment with PD or TBB prevented the interaction upon EGCG.

A

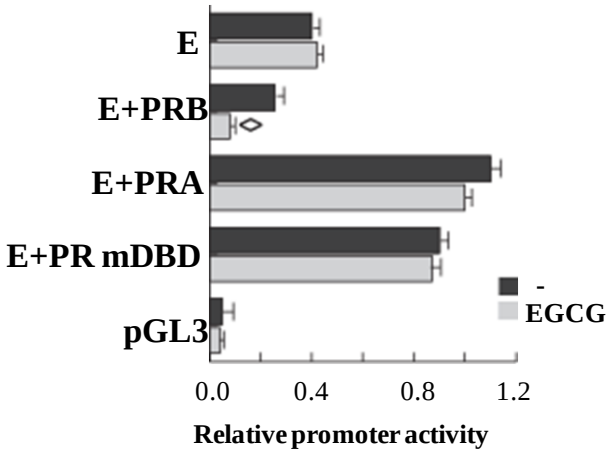

B

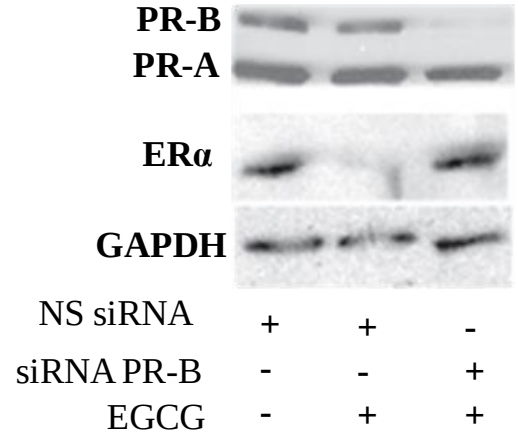
PR-B
PR-A
ERα
GAPDH
NS siRNA + + -
siRNA PR-B - - +
EGCG - + +

C

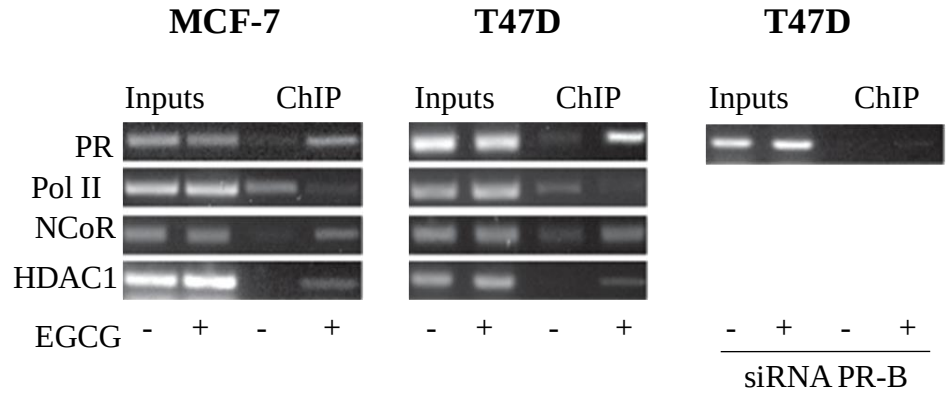
MCF-7
T47D
T47D
Inputs ChIP
Inputs ChIP
Inputs ChIP
PR
Pol II
NCoR
HDAC1
EGCG - + - + - + - + - + - +
siRNA PR-B

D

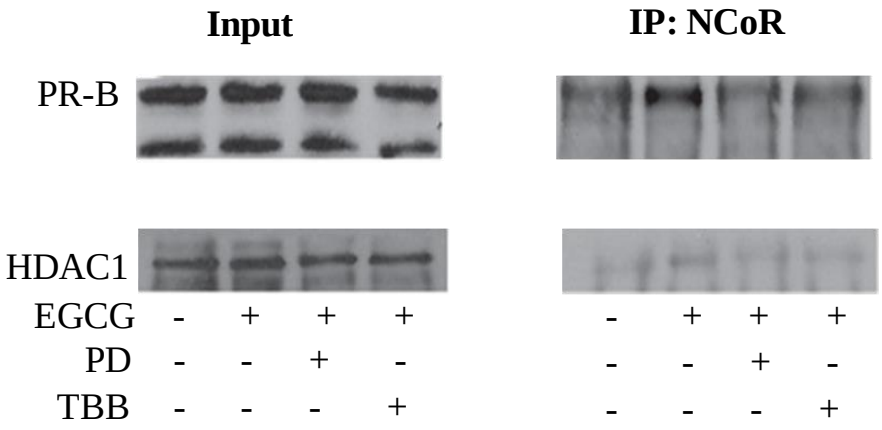

Figure 5: PR-B mediates the EGCG effects on ER-α promoter and recruits an NCoR corepressor complex. (A) Promoter activity of the ER-α 5'−flanking region. Fragment E was transiently transfected into Skbr3 cells in the presence or absence of full-length PR-B, or PR-A, or mDBD PR expression plasmid, then treated with 40 μM EGCG or left untreated. After 24 h, cells were harvested, and luciferase activities were determined; bars, SD $p < 0.05$ compared with untreated cells. **(B) Immunoblot analysis.** T47-D cells were transfected with NS siRNA or targeted against PR-B and treated with vehicle (−) or 40 μM EGCG. **(C) ChIP assay.** Cells were treated for 12 h with vehicle (−) or 40 μM EGCG and then harvested. Antibodies used to immunoprecipitate the protein DNA complex are indicated on the left. PCR primers encompass half-PRE site within the ER-α promoter. Results are representative of three independent experiments. **(D) Coimmunoprecipitation assay.** T47-D cells were treated with vehicle (−) or 40 μM EGCG in presence or absence of PD or TBB. Nuclear cell lysates were immunoprecipitated using anti-NCoR and then blotted with anti-PR or anti-HDAC1 antibody.

Discussion

Epidemiological studies have shown that breast cancer incidence rates are lowest among Asians, suggesting that Asian diets may contain phytochemicals with antibreast cancer activities. Accumulating clinical evidence indicates the protective effects of polyphenols derived from green tea in ER+/PR+/HER2− breast tumor patients (*Ogunleye et al., 2010*), while recent in vitro studies demonstrate their specific cytotoxicity toward breast cancer cells regardless of their ER status (*Thangapazham et al., 2007*). This could be due to the use of high doses of phytochemicals that may produce misleading results with regard to DNA damage and in several other respects. Specifically it was reported that dietary chemopreventive compounds can increase oxidative stress and cause DNA damage at high concentrations (*De Amicis et al., 2012*), whereas they act as antioxidants to reduce DNA damage at dietary or pharmacologic concentrations (*Moiseeva et al., 2007*). Often, the doses utilized in these studies are not achievable in vivo; therefore, whether phytochemicals might exert translational promises and benefits in clinical settings and prevention of breast cancer remain unclear. In this study, we tested EGCG doses considerably lower than the dose of 100–120 μM used for most in vitro studies and thus are closer to levels with physiological relevance (*Hsieh and Wu, 2008*). We demonstrate that at doses of 10, 20, 40 μM EGCG effectively inhibits the growth of ER+ PR+ cancer cells (Fig. 1), and it exerts its effects through multiple mechanisms of action including (i) modulation of Hsp90 chaperone activity (Fig. 4A and B) and (ii) activation of p38MAPK /CK2 signaling (Fig. 4E and F), influencing the redistribution of the PR (Fig. 4C) from the cytosol to the nucleus, (iii) recruitment of PR-B onto the ER-α promoter (Fig. 5C) leading to transcriptional inhibition of ER-α (Fig. 3B) thus reducing its expression (Fig. 2A) and E2/ER-α genomic (Fig. 2B and C) and nongenomic activity (Fig. 2D). We herein indicate that EGCG via modulation of ER-α blocks cancer cell proliferation. These studies provide a better understanding of the specific factors that can

mediate ER-α downregulation in breast cancer cells, which may be critical for future therapeutic strategies attempting to reduce its expression. A body of evidences obtained by in vivo studies demonstrate the consequences of unregulated ER-α levels at all stages of breast cancer development. For instance, transgenic mice with elevated ER-α levels can develop ductal hyperplasias, lobular hyperplasias, and ductal carcinoma in situ (*Frech et al., 2005*). Furthermore, it is shown that ESR1 is amplified in subsets of breast cancers and in precancerous breast diseases (*Holst et al., 2007*). Therefore, it is reasonable to consider ER-α downregulators of significant clinical interest. In this concern, we show that EGCG treatment decreased both ER-α genomic and rapid nongenomic activity as a consequence of ER-α content depletion that occurs through PR-B nuclear translocation. These novel findings corroborate our previous studies (*De Amicis et al., 2009*) indicating that inhibition of ER-α by PR-B is a critical regulatory pathway in ER-α-positive breast cancer cells, and highlight the protective role of PR-B as determinant of EGCG downregulatory effects, since PR-B knockdown attenuated the inhibition of ER-α levels after EGCG stimulus.

Steroid receptors such as PR in the absence of ligand, interact with Hsp90 (*Schowalter et al., 1991*). Previous studies demonstrated that EGCG interferes with Hsp90 chaperone activity for PR, by binding to Hsp90 at or near a C-terminal ATP-binding site (*Yin et al., 2009*). We demonstrate that EGCG acts at both ER-α mRNA and protein level via Hsp90/p- 38MAPK signaling to PR-B in T47D and MCF-7 cells. We also define the molecular mechanisms through which EGCG interferes with ER-α gene transcription. Our functional experiments using five deletion constructs of the ER-α promoter showed that EGCG's downregulatory effects occur through a region between −2769 and −1000 bp of the promoter (Fig. 3A) which contains a known half-PRE site that is required for repression of the ER-α promoter by PR-B (*De Amicis et al., 2009*). Our data support previous clinical and in vitro studies (*De Amicis et al., 2009; Hopp et al., 2004*)

illustrating the protective role of PR-B expression in breast cancer. This concept is further reinforced by studies showing that HER-2/neu signaling, is also inversely associated with PR levels (*Huang et al., 2005*). EGCG specifically reduced the expression of HSP70 and HSP90 (*Yin et al., 2009*) with overproduction instead, resulting in the increased incidence of cell transformation (*Ciocca and Calderwood, 2005*). Our results correlate with these data since EGCG decreased Hsp90 client proteins expression levels (Fig. 4A) with a concomitant reduction of cell proliferation and estradiol-induced colony formation of MCF-7 and T47D (Fig. 1B). Hsp90 inhibition is known to impact cellular client protein homeostasis via different mechanisms (*Tillotson et al., 2010; Basso et al., 2002*). For example, Hsp90 inhibition can arrest maturation of Hsp90-bound client proteins without disrupting the cochaperone complex, can block the release of the refolded protein, leading to ubiquitin-dependent degradation or can prevent the binding of the target client protein to Hsp90. Our results confirm that EGCG acts as an inhibitor of Hsp90 chaperone function in ER+ PR+ breast cancer cell types examined, since it produced a drastic reduction of Her 2, EGFR, raf1 levels in a dose-dependent manner (Fig. 4A).

Hsp90 functions in part as a cytoplasmic retention factor for steroid receptors (*Schowalter et al., 1991*), and our results suggest a role of Hsp90 as mediator of EGCG action in the modulation of the subcellular localization of PR-B isoforms. The nucleocytoplasmic distribution of PR-B in T47D cells was affected by EGCG treatment (Fig. 4C).

Unliganded receptors mainly localize to the cytoplasm. However, EGCG treatment leads to more PR-B nuclear localization, concomitant to a reduced cytoplasmic retention due to inhibition of the PR-B–Hsp90 interaction (Fig. 4B). EGCG treatment via p38/CK2 activation indeed resulted in destabilization ofHsp90–PR-B complexes.

We also demonstrated the specific involvement of the PR-B isoform inmediatingEGCGaction using the isoform-specific siRNA experiments (Fig. 5B and C). Our results are consistent with previous studies (*Fiskus et al., 2007*) showing that disruption of the chaperone function of Hsp90 by treatment with different drugs increased polyubiquitylation and depletion of ER-α levels and transcriptional activity resulting in growth arrest and apoptosis (*Bagatell et al., 2001; Lee et al., 2002*). EGCG may indirectly affect steroid receptors nuclear translocation influencing their ability to interact with Hsp90 clients via MAP kinase superfamily. It has been reported that PR-A and PR-B stability and transcriptional activities is selectively regulated by p38 and p42/44 MAPK through specific phosphorylation sites (*Khan et al., 2011*) and MAPKs are known to play important roles in PR subcellular trafficking via Ser294 phosphorylation (*Qiu et al., 2003*). A significant finding in our study is that sustained p38 and CK2 activation by EGCG influenced Hsp90–PR B interactions, and played a critical role in the nuclear localization of PR-B as demonstrated with specific inhibitors of p38 and CK2 (Fig. 4C and D). Dissociation of PR with its chaperones and receptor dimerization, leads to its binding to PREs in the promoters of target genes and the recruitment of specific co-regulators and general transcription factors, resulting in the modulation of transcription of those genes (*Arnett-Mansfield et al., 2007*). Recent studies in the human endometrium have demonstrated that PR-A and PR-B are distributed either evenly throughout the nucleus or into discrete nuclear foci, and that there is a link between the subnuclear distribution of PR and its transcriptional activity (*Arnett-Mansfield et al., 2007*). These data collectively indicate that these nuclear foci contain multiple activated PR-co-regulator complexes that can influence the basic transcriptional machinery. Our ChIP assays (Fig. 5C) of the ER-α promoter correlate well with these previous reports and also show a release of RNAPol II. This is concomitant to the

enhancement of the tripartite co-repressor complex PRB/ NCoR/HDAC1 (Fig. 5C) due to PR-B nuclear localization via p38/CK2 activation.

Our results support the molecular mechanism that EGCG's inhibition of ER-α gene transcription is mediated by a physical recruitment to the promoter of PR-B, which then exerts a repressive effect on chromatin by maintaining interactions between the co-repressor NCoR and HDAC1 with the ER-α gene (Fig. 5C). Thus, PR-B recruitment after EGCG treatment is to the PRE half-sites in the ER-α promoter. We also show that EGCG induces PR-B binding directly to this PRE half-site. Results from transient cell transfection assays, with ER-α reporter gene containing point mutations in the half PRE (Fig. 3C), further confirm the importance of PRDNA binding and the PRE half-site for a functional inhibitory response to EGCG. Furthermore, siRNA knockdown of PR-B confirmed that recruitment of the PR-B isoform to the half- PRE site within the ER-α gene promoter is a prerequisite in mediating EGCG downregulatory effects on ER-α expression in breast cancer cells. We propose a novel model (Fig. 6) for the inhibitory action of EGCGs on the proliferation of ER+ PR+ breast cancer cells, through regulation of ER-α gene transcription. The p38/CK2 activation by EGCG provides a mechanism for the downregulation of Hsp90–PR-B interactions, as well as PR-B nuclear localization which is necessary for its recruitment to the half-PRE site within the ER-α promoter. The formation of a tripartite complex, containing PR-B, HDAC1, and NCoR that interacts with the half PRE, induces those alterations in chromatin structure such as deacetylation which then blocks promoter accessibility to the transcriptional machinery such as RNAPol II.

In conclusion, we discovered that EGCG can function as ER-α downregulator thus inhibiting ER+/PR+ breast cancer cell growth. Our results suggest that potentiating EGCG/PRB signaling should be further exploited for clinical approach.

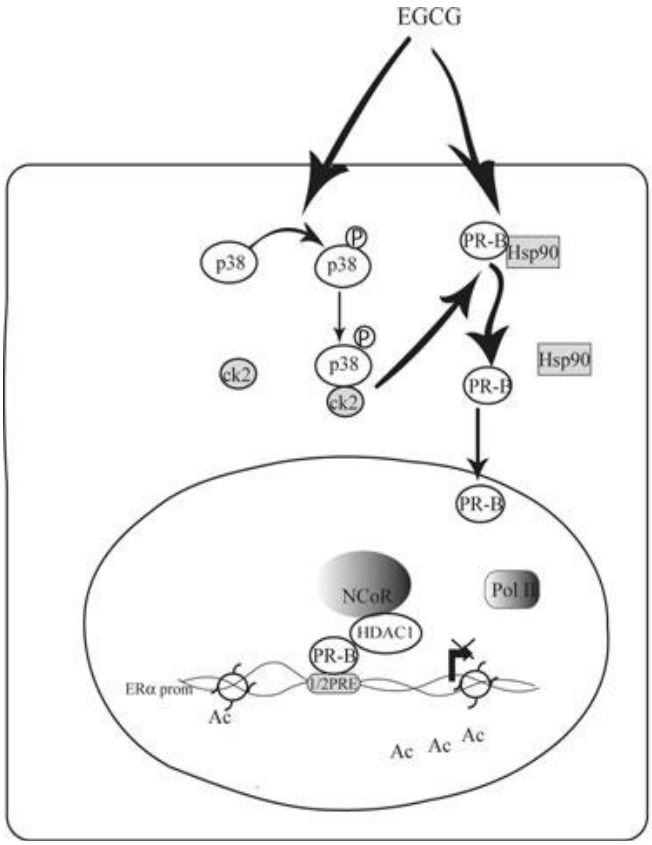

Figure 6: A proposed model for EGCG-induced repression of ER-α promoter in ER+ breast cancer cells. For details, see the text. Ac, acetylation.

References

-**Acconcia F., Totta P., Ogawa S., Cardillo I., Inoue S., Leone S., Trentalance A., Muramatsu M., Marino M.** Survival versus apoptotic 17b-estradiol effect: role of ER-α and ER-β activated nongenomic signalling. *J. Cell. Physiol. 2005, 203, 193–201*.

-**Agoulnik I.U., Krause W.C., Bingman W.E. III, Rahman H.T., Amrikachi M., Ayala G. E., Weigel N.L.** Repressors of androgen and progesterone receptor action. *J. Biol. Chem., 2003, 278, 31136–31148*.

-**Aguas F., Martins A., Gomes T.P., de Sousa M., Silva D.P., Portuguese Menopause Society and Portuguese Gynaecology Society.** Prophylaxis approach to a-symptomatic post-menopausal women: breast cancer. *Maturitas. 2005,52, 23-31*.

-**Allan G.F., Leng X., Tsai S.Y., Weigel N.L., Edwards D.P., Tsai M.J., O'Malley B.W.** Hormone and antihormone induce distinct conformational changes which are central to steroid receptor activation. *J Biol Chem, 1992, 267, 19513-19520.*

-**Allan G.F., Tsai S.Y., Tsai M.J., O'Malley B.W.** Ligand-dependent conformational changes in the progesterone receptor are necessary for events that follow DNA binding. *Proc Natl Acad Sci U S A. 1992, 89, 11750-11754.*

Annu Rev Genet, 1991, 25, 89-123.

-**Arnett-Mansfield R.L., de Fazio A., Wain G.V., Jaworski R.C., Byth K., Mote P.A., Clarke C.L.** Relative expression of progesterone receptors A and B in endometrioid cancers of the endometrium. *Cancer Res, 2001, 61, 4576–4582*.

-**Arnett-Mansfield R.L., Graham J.D., Hanson A.R., Mote P.A., Gompel A., Scurr L.L., Gava N., de Fazio A., Clarke C.L.** Focal subnuclear distribution of progesterone receptor is ligand dependent and associated with transcriptional activity. *Mol. Endocrinol. 2007, 21, 14–29*.

-**Bagatell R., Khan O., Paine-Murrieta G., Taylor C.W., Akinaga S., Whitesell L.** Destabilization of steroid receptors by heat shock protein 90-binding drugs: a ligand-independent approach to hormonal therapy of breast cancer. *Clin. Cancer Res. 2001, 7, 2076– 2084*.

-**Bamberger A.M., Milde-Langosch K., Schulte H.M., Löning T.** Progesterone receptor isoforms, PR-B and PR-A, in breast cancer: correlations with clinicopathologic tumor parameters and expression of AP-1 factors. *Horm Res, 2000, 54, 32–37*.

-**Bardou V.J., Arpino G., Elledge R.M., Osborne C.K., Clark G.M.** Progesterone receptor status significantly improves outcome prediction over estrogen receptor status alone for adjuvant endocrine therapy in two large breast cancer databases. *J Clin Oncol, 2003, 21, 1973–1979*.

-**Basso A.D., Solit D.B., Chiosis G., Giri B., Tsichlis P., Rosen N.** Akt forms an intracellular complex with heat shock protein 90 (Hsp90) and Cdc37 and is destabilized by inhibitors of Hsp90 function. *J. Biol. Chem. 2002, 277, 39858–39866*.

-**Baum M., Budzar A.U., Cuzick J., Forbes J., Houghton J.H., Klijn J.G., Sahmoud T; ATAC Trialists' Group.** Anastrozole alone or in combination with tamoxifen versus tamoxifen alone for adjuvant treatment of postmenopausal women with early breast cancer: first results of the ATAC randomised trial. *Lancet. 2002, 359, 2131–9*.

-**Belguise K., Guo S., Sonenshein G. E.** Activation of FOXO3a by the green tea polyphenol epigallocatechin-3-gallate induces estrogen receptor alpha expression reversing invasive phenotype of breast cancer cells. *Cancer Res. 2007, 67, 5763–5770*.

-**Bonefeld-Jorgensen E.C., Long M., Bossi R., Ayotte P., Asmund G., Kruger T., Ghisari M., Mulvad G., Kern P., Nzulumiki P., Dewailly E.** Perfluorinated compounds are related to breast cancer risk in Greenlandic Inuit: A case control study. *Environ. Health. 2011, 10, 88*.

-**Boyd-Leinen P.A., Fournier D., Spelsberg T.C.** Nonfunctioning progesterone receptors in the developed oviducts from estrogen-withdrawn immature chicks and in aged nonlaying hens. *Endocrinology, 1982, 111, 30–36*.

-**Brown M.D.** Green tea (Camellia sinensis) extract and its possible role in the prevention of cancer. *Altern Med Rev. 1999, 4, 360-70*.

-**Bunone G., Briand P.A., Miksicek R.J., Picard D.** Activation of the unliganded estrogen receptor by EGF involves the MAP kinase pathway and direct phosphorylation. *EMBO J, 1996, 15, 2174-2183*.

-**Buzdar A.U.** Preoperative chemotherapy treatment of breast cancer--a review. *Cancer. 2007, 110, 2394-407*.

-**Cabrera C., Artacho R., Giménez R.** Beneficial effects of green tea-a review. *J Am Coll Nutr. 2006, 25, 79–99*.

-**Carson-Jurica M.A., Schrader W.T., O'Malley B.W.** Steroid receptor family: structure and functions. *Endocr. Rev. 1990, 11, 201–220*.

-**Castoria G., Migliaccio A., Bilancio A., Di Domenico M., de Falco A., Lombardi M., Fiorentino R., Varricchio L., Barone M.V., Auricchio F.** PI3-kinase in concert with Src promotes the S-phase entry of oestradiol-stimulated MCF-7 cells. *EMBO J. 2001, 20, 6050–6059*.

-**Chen J. D., Umesono K., and Evans R.M.** SMRT isoforms mediate repression and anti-repression of nuclear receptor heterodimers. *Proc. Natl. Acad. Sci. USA, 1996, 93,7567–7571*.

-**Chen B., Piel W.H., Gui L., Bruford E., Monteiro A.** The HSP90 family of genes in the human genome: insights into their divergence and evolution. *Genomics, 2005, 86, 627-637*.

-**Ciocca D.R., Calderwood S. K.** Heat shock proteins in cancer: diagnostic, prognostic, predictive, and treatment implications. *Cell Stress Chaperones 2005, 10, 86–103*.

-**Ciocca D.R., Clark G.M., Tandon A.K., Fuqua S.A., Welch W.J., McGuire W.L.** Heat shock protein hsp70 in patients with axillary lymph node-negative breast cancer: prognostic implications. *J Natl Cancer Inst, 1993, 85, 570-574*.

-**Clarke C.L., Sutherland R.L.** Progestin regulation of cellular proliferation. *Endocr Rev, 1990, 11, 266–330*.

-**Coombes R.C., Hall E., Gibson L.J., Paridaens R., Jassem J., Delozier T., Jones S.E., Alvarez I., Bertelli G., Ortmann O., Coates A.S., Bajetta E., Dodwell D., Coleman R.E., Fallowfield L.J., Mickiewicz E., Andersen J., Lønning P.E., Cocconi G., Stewart A., Stuart N., Snowdon C.F., Carpentieri M., Massimini G., Bliss J.M., van de Velde C.;Intergroup Exemestane Study.** A randomized trial of exemestane after two to three years of tamoxifen therapy in postmenopausal women with primary breast cancer. *N Engl J Med 2004, 350, 1081–92*.

-**Cornford P.A., Dodson A.R., Parsons K.F., Desmond A.D., Woolfenden A., Fordham M., Neoptolemos J.P., Ke Y., Foster C.S.** Heat shock protein expression independently predicts clinical outcome in prostate cancer. *Cancer Res. 2000, 60, 7099–7105*.

-**De Amicis F., Giordano F., Vivacqua A., Pellegrino M., Panno M.L., Tramontano D., Fuqua S.A., Andò S.** Resveratrol, through NF-Y/p53/Sin3/HDAC1 complex

phosphorylation, inhibits estrogen receptor {alpha} gene expression via p38MAPK/CK2 signaling in human breast cancer cells. *FASEB J. 2011, 25, 3695–3707.*

-**De Amicis F., Santoro M., Guido C., Russo A., Aquila S.** Epigallocatechin gallate affects survival and metabolism of human sperm. *Mol. Nutr. Food. Res. 2012, 56, 1655–1664.*

-**De Amicis F., Zupo S., Panno M.L., Malivindi R., Giordano F., Barone I., Mauro L., Fuqua S.A., Andò S.** Progesterone receptor B recruits a repressor complex to a half-PRE site of the estrogen receptor alpha gene promoter. *Mol. Endocrinol. 2009, 23, 454–465.*

-**De Amicis F., Thirugnansampanthan J., Cui Y., Selever J., Beyer A., Parra I., Weigel N.L., Herynk M.H., Tsimelzon A., Lewis M.T., Chamness G.C., Hilsenbeck S.G., Andò S., Fuqua S.A.** Androgen receptor overexpression induces tamoxifen resistance in human breast cancer cells. *Breast Cancer Res. Treat. 2010, 121, 1–11.*

-**deGraffenried L.A., Hilsenbeck S.G., Fuqua S.A.** Sp1 is essential for estrogen receptor α gene transcription. *J. Steroid Biochem. Mol. Biol. 2002, 82, 7–18.*

-**Duval D., Malaisé M., Reinhardt B., Kedinger C., Boeuf H.** A p38 inhibitor allows to dissociate differentiation and apoptotic processes triggered upon LIF withdrawal in mouse embryonic stem cells. *Cell Death Differ. 2004, 11, 331–341.*

-**Emmen J.M., Couse J.F., Elmore S.A., Yates M.M., Kissling G.E., Korach K.S.** In vitro growth and ovulation of follicles from ovaries of estrogen receptor (ER){alpha} and ER{beta} null mice indicate a role for ER{beta} in follicular maturation. *Endocrinology, 2005, 146, 2817–2826.*

-**Evans R.M.** The steroid and thyroid hormone receptor superfamily. *Science, 1988, 13, 889–895.*

-**Faivre E.J., Lange C.A.** Progesterone receptors upregulate Wnt-1 to induce epidermal growth factor receptor transactivation and c-Src-dependent sustained activation of Erk1/2 mitogen-activated protein kinase in breast cancer cells. *Mol. Cell. Biol. 2007, 27, 466–480.*

-**Fang M.Z., Wang Y., Ai N., Hou Z., Sun Y., Lu H., Welsh W., Yang C.S.** Tea polyphenol (-)-epigallocatechin-3-gallate inhibits DNA methyltransferase and reactivates methylation-silenced genes in cancer cell lines. *Cancer Res. 2003, 63, 7563-70.*

-**Farabegoli F., Barbi C., Lambertini E., Piva R.** (-)- Epigallocatechin-3 gallate downregulates estrogen receptor alpha function in MCF-7 breast carcinoma cells. *Cancer Detect. Prev. 2007, 31, 499–504.*

-**Fiskus W., Ren Y., Mohapatra A., Bali P., Mandawat A., Rao R., Herger B., Yang Y., Atadja P., Wu J., Bhalla K.** Hydroxamic acid analogue histone deacetylase inhibitors attenuate estrogen receptor-alpha levels and transcriptional activity: a result of hyperacetylation and inhibition of chaperone function of heat shock protein 90. *Clin. Cancer Res. 2007, 13, 4882–4890.*

-**Frech M. S., Halama E. D., Tilli M. T., Singh B., Gunther EJ, Chodosh LA, Flaws JA, Furth PA.** Deregulated estrogen receptor alpha expression in mammary epithelial cells of transgenic mice results in the development of ductal carcinoma in situ. *Cancer Res. 2005, 65, 681–685*.

-**Fuqua S.A., Schiff R., Parra I., Moore J.T., Mohsin S.K., Osborne C.K., Clark G.M., Allred D.C.** Estrogen receptor beta protein in human breast cancer: correlation with clinical tumor parameters. *Cancer Res. 2003, 63, 2434-2439*.

-**Gao X., Loggie B.W., Nawaz Z.** The roles of sex steroid receptor coregulators in cancer. *Mol Cancer. 2002, 1, 7.*

-**Giannoukos G., Szapary D., Smith C.L., Meeker J.E., Simons S.S. Jr.** New antiprogestins with partial agonist activity: potential selective progesterone receptor modulators (SPRMs) and probes for receptor- and coregulator-induced changes in progesterone receptor induction properties. *Mol Endocrinol, 2001, 15, 255-270*.

-**Goss P.E., Ingle J.N., Martino S., Robert N.J., Muss H.B., Piccart M.J., Castiglione M., Tu D., Shepherd L.E., Pritchard K.I., Livingston R.B., Davidson N.E., Norton L., Perez E.A., Abrams J.S., Therasse P., Palmer M.J., Pater J.L.** A randomized trial of letrozole in postmenopausal women after five years of tamoxifen therapy for early-stage breast cancer. *N Engl J Med 2003, 349, 1793–802*.

-**Göttlicher M., Heck S., Herrlich P.** Transcriptional cross-talk, the second mode of steroid hormone receptor action. *J Mol Med (Berl). 1998, 76, 480-9*.

-**Graham J.D., Roman S.D., McGowan E., Sutherland R.L., Clarke C.L.** Preferential stimulation of human progesterone receptor B expression by estrogen in T-47D human breast cancer cells. *J Biol Chem, 1995, 270, 30693–30700*.

-**Green S., Walter P., Greene G., Krust A., Goffin C., Jensen E., Scrace G., Waterfield M., Chambon P.** Cloning of the human estrogen receptor cDNA. *J. Steroid Biochem., 1986, 24, 77–83*.

-**Gronemeyer H.** Transcription activation by estrogen and progesterone receptors. *Ann. Rev. Gen., 1991, 25:89-123*.

-**Gross G.E., Clark G.M., Chamness G.C., McGuire W.L.** Multiple progesterone receptor assays in human breast cancer. *Cancer Res, 1984, 44, 836–840*.

-**Guido C., Panza S., Santoro M., Avena P., Panno M.L., Perrotta I., Giordano F., Casaburi I., Catalano S., De Amicis F., Sotgia F., Lisanti M.P., Andò S., Aquila S.** Estrogen receptor beta (ER-β) produces autophagy and necroptosis in human seminoma cell line through the binding of the Sp1 on the phosphatase and tensin homolog deleted from chromosome 10 (PTEN) promoter gene. *Cell Cycle 2012, 11, 2911–2921*.

-**Gupta S., Hastak K., Ahmad N., Lewin J. S., Mukhtar H.** Inhibition of prostate carcinogenesis in TRAMP mice by oral infusion of green tea polyphenols. *Proc. Natl. Acad. Sci. USA 2001, 98, 10350–10355*.

-**Gyrd-Hansen M., Nylandsted J., Jäättelä M.** Heat shock protein 70 promotes cancer cell viability by safeguarding lysosomal integrity. *Cell Cycle, 2004, 3, 1484-1485*.

-**Harris H.A.** Estrogen receptor-beta: recent lessons from in vivo studies. *Mol. Endocrinol., 2007, 21, 1–13*.

-**Hartl FU.** Molecular chaperones in cellular protein folding. *Nature, 1996, 381, 571-579*.

-**Heldring N., Nilsson M., Buehrer B., Treuter E., Gustafsson J.A.** Identification of tamoxifen-induced coregulator interaction surfaces within the ligand-binding domain of estrogen receptors. *Mol Cell Biol, 2004, 24, 3445-3459*.

-**Herynk M. H., Fuqua S. A.** Estrogen receptor mutations in human disease. *Endocr. Rev. 2004, 25, 869–898*.

-**Hilakivi-Clarke L., Clarke R., Onojafe I., Raygada M., Cho E., Lippman M. E.** A maternal diet high in n-6 polyunsaturated fats alters mammary gland development, puberty onset, and breast cancer risk among female rat offspring. *Proc. Natl. Acad. Sci. USA. 1997, 94, 9372-9377*.

-**Hildesheim J., Salvador J. M., Hollander M. C., Fornace A. J. Jr.** Casein kinase 2- and protein kinase A-regulated adenomatous polyposis coli and beta-catenin cellular localization is dependent on p38 MAPK. *J. Biol. Chem. 2005, 280, 17221–17226*.

-**Holst F., Stahl P.R., Ruiz C., Hellwinkel O., Jehan Z., Wendland M., Lebeau A., Terracciano L., Al-Kuraya K, Jänicke F, Sauter G, Simon R.** Estrogen receptor alpha (ESR1) gene amplification is frequent in breast cancer. *Nat. Genet. 2007, 39, 655–660*.

-**Hong W. K., Sporn M. B.** Recent advances in chemoprevention of cancer. *Science 1997, 278, 1073–1077*.

-**Hopp T.A., Weiss H.L., Hilsenbeck S.G., Cui Y., Allred D.C., Horwitz K.B., Fuqua S.A.** Breast cancer patients with progesterone receptor PR-A-rich tumors have poorer disease-free survival rates. *Clin Cancer Res, 2004, 10, 2751–2760*.

-**Hopp T.A., Weiss H.L., Hilsenbeck S.G., Cui Y., Allred D.C., Horwitz K.B., Fuqua S.A.** Breast cancer patients with progesterone receptor PR-A-rich tumors have poorer disease-free survival rates. *Clin. Cancer Res. 2004, 10, 2751–2760*.

-**Horlein A.J., Naar A.M., Heinzel T., Torchia J., Gloss B., Kurokawa R., Ryan A., Kamei Y., Soderstrom M., Glass C. K., Rosenfeld M. G.** Ligand-independent repression by the thyroid hormone receptor mediated by a nuclear receptor co-repressor. *Nature, 1995, 377, 397–404*.

-**Horwitz K.B., Alexander P.S.** In situ photolinked nuclear progesterone receptors of human breast cancer cells: subunit molecular weights after transformation and translocation. *Endocrinology, 1983, 113, 2195-2201*.

-**Howell A., Pippen J., Elledge R.M., Mauriac L., Vergote I., Jones S.E., Come S.E., Osborne C.K., Robertson J.F.** Fulvestrant versus anastrozole for the treatment of advanced breast carcinoma: a prospectively planned combined survival analysis of two multicenter trials. *Cancer 2005, 104, 236–239*.

-**Hsieh T. C., Wu J. M.** Suppression of cell proliferation and gene expression by combinatorial synergy of EGCG, resveratrol and gamma-tocotrienol in estrogen receptorpositive MCF-7 breast cancer cells. *Int. J. Oncol. 2008, 33, 851–859*.

-**Hu X.F., Veroni M., De Luise M., Wakeling A., Sutherland R., Watts C.K., Zalcberg JR.** Circumvention of tamoxifen resistance by the pure anti-estrogen ICI 182,780. *Int. J. Cancer 1993, 55, 873–876*.

-**Hu X., Li Y., Lazar M.A.** Determinants of CoRNR-dependent repression complex assembly on nuclear hormone receptors. *Mol Cell Biol, 2001, 21, 1747-1758*.

-**Huang H.J., Neven P., Drijkoningen M., Paridaens R., Wildiers H., Van Limbergen E., Berteloot P., Amant F., Christiaens M.R., Vergote I.** Association between HER-2/neu and the progesterone receptor in oestrogen-dependent breast cancer is age-related. *Breast Cancer Res Treat, 2005, 91, 81–87*.

-**Jackson S.E.** Hsp90: structure and function. *Top Curr Chem, 2013, 328, 155-240*.

-**Jarvinen T.A., Pelto-Huikko M., Holli K., Isola J.** Estrogen receptor beta is coexpressed with ERalpha and PR and associated with nodal status, grade, and proliferation rate in breast cancer. *Am J Pathol. 2000, 156, 29-35*.

-**Jepsen K., Rosenfeld M.G.** Biological roles and mechanistic actions of co-repressor complexes. *J. Cell. Sci. 2006, 115, 689–698*.

-**Johnson J.L., Brown C.** Plasticity of the Hsp90 chaperone machine in divergent eukaryotic organisms. *Cell Stress Chaperones. 2009, 14, 83-94*.

-**Jones P.L., Shi Y.B.** N-CoR-HDAC corepressor complexes: roles in transcriptional regulation by nuclear hormone receptors. *Curr. Top. Microbiol. Immunol., 2003, 274, 237–268*.

-**Jordan V.C., Morrow M.** Tamoxifen, raloxifene, and the prevention of breast cancer. *Endocr Rev. 1999, 20, 253-78*.

-**Kamei Y., Xu L., Heinzel T., Torchia J., Kurokawa R., Gloss B., Lin S.C., Heyman R.A., Rose D.W., Glass C.K., Rosenfeld M.G.** A CBP integrator complex mediates transcriptional activation and AP-1 inhibition by nuclear receptors. *Cell, 1996, 85, 403-414*.

-**Kanwar J., Taskeen M., Mohammad I., Huo C., Chan T.H., Dou Q.P.** Recent advances on tea polyphenols. *Front Biosci (Elite Ed). 2012, 4, 111-31*.

-**Kastner P., Krust A., Turcotte B., Stropp U., Tora L., Gronemeyer H., Chambon P.** Two distinct estrogen-regulated promoters generate transcripts encoding the two functionally different human progesterone receptor forms A and B. *EMBO J. 1990, 9, 1603–1614.*

-**Kastner P., Krust A., Turcotte B., Stropp U., Tora L., Gronemeyer H., Chambon P.** Two distinct estrogen-regulated promoters generate transcripts encoding the two functionally different human progesterone receptor forms A and B. *EMBO J, 1990, 9,1603–1614*.

-**Kato J., Hirata S., Nozawa A., Mouri N.** The ontogeny of gene expression of progestin receptors in the female rat brain. *J Steroid Biochem Mol Biol, 1993, 47, 173–182*.

-**Katzenellenbogen B.S.** Mechanisms of action and cross-talk between estrogen receptor and progesterone receptor pathways. *J Soc Gynecol Investig, 2000, 7, 33–37*.

-**Khan J.A., Amazit L., Bellance C., Guiochon-Mantel A., Lombès M., Loosfelt H.** p38 and p42/44 MAPKs differentially regulate progesterone receptor A and B isoform stabilization. *Mol. Endocrinol. 2011, 25, 1710–1724*.

-**Khan S. A., Rogers M. A., Obando J. A., Tamsen A.** Estrogen receptor expression of benign breast epithelium and its association with breast cancer. *Cancer Res. 1994, 54, 993–997*.

-**Kirkland J.L., Murthy L., Stancel G.M.** Progesterone inhibits the estrogen-induced expression of c-fosmessenger ribonucleic acid in the uterus. *Endocrinology, 1992, 130, 3223–3230.*

-**Koide A., Zhao C., Naganuma M., Abrams J., Deighton-Collins S., Skafar D.F., Koide S.** Identification of regions within the F domain of the human estrogen receptor alpha that are important for modulating transactivation and protein–protein interactions. *Mol. Endocrinol., 2007, 21, 829–842.*

-**Kraus W.L., Katzenellenbogen B.S.** Regulation of progesterone receptor gene expression and growth in the rat uterus: modulation of estrogen actions by progesterone and sex steroid hormone antagonists. *Endocrinology, 1993, 132, 2371–2379.*

-**Kuiper G.G., Carlsson B., Grandien K., Enmark E., Häggblad J., Nilsson S., Gustafsson J.A**. Comparison of the ligand binding specificity and transcript tissue distribution of estrogen receptors alpha and beta. *Endocrinology, 1997, 138, 863-870.*

-**Kuiper G.G., Enmark E., Pelto-Huikko M., Nilsson S., Gustafsson J.A**. Cloning of a novel receptor expressed in rat prostate and ovary. *Proc. Natl. Acad. Sci. U.S.A., 1996, 93, 5925–5930.*

-**Kumar V., Green S., Stack G., Berry M., Jin J.R., Chambon P**. Functional domains of the human estrogen receptor. *Cell, 1987, 51, 941–951.*

-**Lee M.O., Kim E.O., Kwon H.J., Kim Y.M., Kang H.J., Kang H., Lee J.E.** Radicicol represses the transcriptional function of the estrogen receptor by suppressing the

stabilization of the receptor by heat shock protein 90. *Mol. Cell. Endocrinol. 2002, 188, 47–54.*

-**Lessey B.A., Alexander P.S., Horwitz K.B.** The subunit structure of human breast cancer progesterone receptors:characterization by chromatography and photoaffinity labeling. *Endocrinology, 1983, 112,1267-1274.*

-**Liang Y. C., Lin-shiau S. Y., Chen C. F., Lin J. K.** Suppression of extracellular signals and cell proliferation through EGF receptor binding by (−)-epigallocatechin gallate in human A431 epidermoid carcinoma cells. *J. Cell. Biochem. 1997, 67, 55–65.*

-**Liao S., Umekita Y., Guo J., Kokontis J. M., Hiipakka R.A.** Growth inhibition and regression of human prostate and breast tumors in athymic mice by tea epigallocatechin gallate. *Cancer Lett. 1995, 96, 239–243.*

-**Liehr J.G**. Is estradiol a genotoxic mutagenic carcinogen? *Endocr. Rev. 2000, 21,40-54.*

-**Liu X.F., Bagchi M.K.** Recruitment of Distinct Chromatin-modifying Complexes by Tamoxifen complexed Estrogen Receptor at Natural Target Gene Promoters in Vivo. *J. Biol. Chem. 2004, 279, 15050-15058.*

-**Loose-Mitchell D.S., Chiappetta C., Stancel G.M.** Estrogen regulation of c-fosmessenger ribonucleic acid. *Mol Endocrinol, 1988, 2, 946–951.*

-**Lösel R., Wehling M.** Nongenomic actions of steroid hormones. *Nat Rev Mol Cell Biol. 2003, 4, 46-56.*

-**Lydon J.P., DeMayo F.J., Funk C.R., Mani S.K., Hughes A.R., Montgomery C.A. Jr, Shyamala G., Conneely O.M., O'Malley B.W.** Mice lacking progesterone receptor exhibit pleiotropic reproductive abnormalities. *Genes Dev., 1995, 9, 2266-2278.*

-**Mader S., Chambon P., White J.H.** Defining a minimal estrogen receptor DNA binding domain. *Nucleic Acids Res., 1993, 21, 1125–1132.*

-**Manninen T., Purmonen S., Ylikomi T.** Interaction of nuclear receptors with hsp90 in living cells. *J Steroid Biochem Mol Biol, 2005, 96, 13-18.*

-**Martin M.B., Saceda M., Garcia-Morales P., Gottardis M.M.** Regulation of estrogen receptor expression. *Breast Cancer Res Treat, 1994, 31, 183–189.*

-**Mayer M.P., Prodromou C., Frydman J.** The Hsp90 mosaic: a picture emerges.

-**McClellan A.J., Xia Y., Deutschbauer A.M., Davis R.W., Gerstein M., Frydman J.** Diverse cellular functions of the hsp90 molecular chaperone uncovered using systems approaches. *Cell, 2007, 131, 121-135.*

-**McKenna N.J., Lanz R.B., O'Malley B.W.** Nuclear receptor coregulators: cellular and molecular biology. *Endocr Rev 1999, 20, 321-344.*

-**Mimnaugh E.G., Xu W., Vos M., Yuan X., Isaacs J.S., Bisht K.S., Gius D., Neckers L.** Simultaneous inhibition of hsp90 and the proteasome promotes protein ubiquitination, causes endoplasmic reticulum-derived cytosolic vacuolization and enhances antitumor activity. *Mol Cancer Ther, 2004, 3, 551-566.*

-**Moiseeva E. P., Almeida G. M., Jones G. D., Manson M. M.** Extended treatment with physiologic concentrations of dietary phytochemicals results in altered gene expression, reduced growth, and apoptosis of cancer cells. *Mol. Cancer Ther. 2007, 6, 3071–3079.*

-**Mote P.A., Bartow S., Tran N., Clarke C.L.** Loss of co-ordinate expression of progesterone receptors A and B is an early event in breast carcinogenesis. *Breast Cancer Res Treat, 2002, 72, 163–172.*

-**Moy B., Goss P.E.** Estrogen receptor pathway: resistance to endocrine therapy and new therapeutic approaches. *Clin Cancer Res. 2006, 12, 4790-3.*

-**Mukhtar H., Wang Z.Y., Katiyar S. K., Agarwal R.** Tea components: antimutagenic and anticarcinogenic effects. *Prev. Med. 1992, 21, 351–360.*

-**Nagy L., Kao H.Y., Chakravarti D., Lin R.J., Hassig C.A., Ayer D.E., Schreiber S. L., Evans R. M.** Nuclear receptor repression mediated by a complex containing SMRT, mSin3A, and histone deacetylase. *Cell, 1997, 89, 373– 380.*

-**Nakachi K., Suemasu K., Suga K., Takeo T., Imai K., Higashi Y.** Influence of drinking green tea on breast cancer malignancy among Japanese patients. *Jpn. J. Cancer. Res. 1998, 89, 254–261.*

-**Neckers L., Workman P.** Hsp90 molecular chaperone inhibitors: are we there yet? *Clin Cancer Res, 2012, 18, 64-76.*

-**Nilsson S., Gustafsson J.A.** Estrogen receptor transcription and transactivation: basic aspects of estrogen action. *Breast Cancer Res., 2000, 2, 360–366.*

-**Nilsson S., Mäkelä S., Treuter E., Tujague M., Thomsen J., Andersson G., Enmark E., Pettersson K., Warner M., Gustafsson J.A.** Mechanisms of estrogen action. *Physiol Rev. 2001, 81,1535-65.*

-**Normanno N., Di Maio M., De Maio E., De Luca A., de Matteis A., Giordano A., Perrone F; NCI-Naple Breast Cancer Group.** Mechanisms of endocrine resistance and novel therapeutic strategies in breast cancer. *Endocr Relat Cancer. 2005, 12, 721-47.*

-**Nylandsted J., Brand K., Jaattela M.** Heat shock protein 70 is required for the survival of cancer cells. *Ann N Y Acad Sci. 2000a, 926,122–125.*

-**Ogunleye A. A., Xue F., Michels K. B.** Green tea consumption and breast cancer risk or recurrence: a meta-analysis. *Breast Cancer Res. Treat. 2010, 119, 477–484.*

-**O'Lone R., Frith M.C., Karlsson E.K., Hansen U.** Genomic targets of nuclear estrogen receptors. *Mol Endocrinol. 2004, 18, 1859-75.*

-**O'Malley B.W., Tsai S.Y., Bagchi M., Weigel N.L., Schrader W.T., Tsai M.J.** Molecular mechanism of action of a steroid hormone receptor. *Recent Prog Horm Res, 1991, 47, 1-24.*

-**Onate S.A., Tsai S.Y., Tsai M.J., O'Malley B.W.** Sequence and characterization of a coactivator for the steroid hormone receptor superfamily. *Science 1995, 270, 1354-1357*.

-**Osborne C.K., Schiff R.** Estrogen-receptor biology: continuing progress and therapeutic implications. *J. Clin. Oncol., 2005, 23, 1616–1622*.

-**Osborne C.K., Schiff R., Fuqua S.A., Shou J.** Estrogen receptor: current understanding of its activation and modulation. *Clin. Cancer Res., 2001, 7, 4338–4342*.

-**Park B.W., Kim K.S., Heo M.K., Ko S.S., Hong S.W., Yang W.I., Kim J.H., Kim G.E., Lee K.S.** Expression of estrogen receptor-beta in normal mammary and tumor tissues: is it protective in breast carcinogenesis? *Breast Cancer Res. Treat., 2003, 80, 79–85*.

-**Paruthiyil S., Parmar H., Kerekatte V., Cunha G.R., Firestone G.L., Leitman D.C.** Estrogen receptor beta inhibits human breast cancer cell proliferation and tumor formation by causing a G2 cell cycle arrest. *Cancer Res., 2004, 64, 423–428*.

-**Pearl L.H., Prodromou C., Workman P.** The Hsp90 molecular chaperone: an open and shut case for treatment. *Biochem J, 2008, 410, 439-453*.

-**Perey L., Paridaens R., Hawle H., Zaman K., Nolé F., Wildiers H., Fiche M., Dietrich D., Clément P., Köberle D., Goldhirsch A., Thürlimann B.** Clinical benefit of fulvestrant in postmenopausal women with advanced breast cancer and primary or acquired resistance to aromatase inhibitors: final results of phase II Swiss Group for Clinical Cancer Research Trial (SAKK 21/00). *Ann. Oncol., 2007, 18, 64–69*.

-**Picard D., Kumar V., Chambon P., Yamamoto K.R.** Signal transduction by steroid hormones: nuclear localization is differentially regulated in estrogen and glucocorticoid receptors. *Cell Regul., 1990, 1, 291–299*.

-**Pink J.J., Jordan V.C.** Models of estrogen receptor regulation by estrogens and antiestrogens in breast cancer cell lines. *Cancer Res, 1996, 56, 2321-2330*.

-**Poola I., Abraham J., Baldwin K., Saunders A., Bhatnagar R.** Estrogen receptors beta4 and beta5 are full length functionally distinct ERbeta isoforms: cloning from human ovary and functional characterization. *Endocrine. 2005, 27, 227-38*.

-**Potischman N., Troisi R.** In utero and early life exposures in relation to risk of breast cancer. *Cancer Causes Control. 1999, 10, 561-573*.

-**Pratt W.B.** Transformation of glucocorticoid and progesterone receptors to the DNA-binding state. *J Cell Biochem, 1987, 35, 51-68*.

-**Pratt W.B., Galigniana M.D., Morishima Y., Murphy P.J.** Role of molecular chaperones in steroid receptor action. *Essays Biochem, 2004, 40, 41-58*.

-**Pratt W.B., Toft D.O.** Regulation of signaling protein function and trafficking by the hsp90/hsp70-based chaperone machinery. *Exp Biol Med, 2003, 228, 111-133*.

-**Qanungo S., Das M., Haldar S., Basu A.** Epigallocatechin-3-gallate induces mitochondrial membrane depolarization and caspase-dependent apoptosis in pancreatic cancer cells. *Carcinogenesis 2005, 26, 958–967*.

-**Qiu M., Olsen A., Faivre E., Horwitz K.B., Lange C.A.** Mitogen-activated protein kinase regulates nuclear association of human progesterone receptors. *Mol. Endocrinol. 2003, 17, 628–642*.

-**Richer J.K., Jacobsen B.M., Manning N.G., Abel M.G., Wolf D.M., Horwitz K.B.** Differential gene regulation by the two progesterone receptor isoforms in human breast cancer cells. *J Biol Chem, 2002, 277, 5209–5218*.

-**Ritossa F.** A new puffing pattern induced by temperature, shock and DNP in Drosophila. *Experientia, 1962, 18, 571-573*.

-**Roger P., Sahla M.E., Mäkelä S., Gustafsson J.A., Baldet P., Rochefort H.** Decreased expression of estrogen receptor beta protein in proliferative preinvasive mammary tumors. *Cancer Res., 2001, 61, 2537–2541*.

-**Rosenfeld M.G., Glass C.K.** Coregulator codes of transcriptional regulation by nuclear receptors. *J Biol Chem. 2001, 276, 36865-8*.

-**Russo J., Russo I.H.** Biological and molecular bases of mammary carcinogenesis. *Lab. Invest. 1987, 57,112-137*.

-**Sah J. F., Balasubramanian S., Eckert R. L., Rorke E. A.** Epigallocatechin 3-gallate inhibits epidermal growth factor receptor signaling pathway. Evidence for direct inhibition of ERK1/2 and AKT kinases. *J. Biol. Chem. 2004, 279, 12755–12762*.

-**Sartorius C.A., Shen T., Horwitz K.B.** Progesterone receptors A and B differentially affect the growth of estrogen-dependent human breast tumor xenografts. *Breast Cancer Res Treat, 2003, 79, 287–299*.

-**Schowalter D.B., Sullivan W.P., Maihle N.J., Dobson A.D., Conneely O.M., O'Malley B.W., Toft D.O.** Characterization of progesterone receptor binding to the 90- and 70-kDa heat shock proteins. *J. Biol. Chem. 1991, 266, 21165–21173*.

-**Shaw J.A., Udokang K., Mosquera J.M., Chauhan H., Jones J.L., Walker R.A.** Oestrogen receptors alpha and beta differ in normal human breast and breast carcinomas. *J. Pathol., 2002, 198, 450–457*.

-**Shyamala G., Yang X., Cardiff R.D., Dale E.** Impact of progesterone receptor on cell-fate decisions during mammary gland development. *Proc Natl Acad Sci USA, 2000, 97, 3044–3049*.

-**Shyamala G., Yang X., Silberstein G., Barcellos-Hoff M.H., Dale E.** Transgenic mice carrying an imbalance in the native ratio of A to B forms of progesterone receptor exhibit

developmental abnormalities in mammary glands. *Proc Natl Acad Sci USA, 1998, 20, 696–701*.

-**Shyamala G., Gauthier Y., Moore S.K., Catelli M.G., Ullrich S.J.** Estrogenic regulation of murine uterine 90-kilodalton heat shock protein gene expression. *Mol Cell Biol, 1989, 9, 3567-3570*.

-**Siddiqui I. A., Asim M., Hafeez B. B., Adhami V. M., Tarapore R.S., Mukhtar H.** Green tea polyphenol EGCG blunts androgen receptor function in prostate cancer. *FASEB J. 2011, 25, 1198–1207*.

-**Siegel R., DeSantis C., Virgo K., Stein K., Mariotto A., Smith T., Cooper D., Gansler T., Lerro C., Fedewa S., Lin C., Leach C., Cannady R.S., Cho H., Scoppa S., Hachey M., Kirch R., Jemal A., Ward E.** Cancer treatment and survivorship statistics, 2012. *CA Cancer J Clin. 2012, 62:220-41*.

-**Singh B.N., Shankar S., Srivastava R.K.** Green tea catechin, epigallocatechin-3-gallate (EGCG): mechanisms, perspectives and clinical applications. *Biochem Pharmacol. 2011, 82,1807-21*.

-**Skafar D.F., Zhao C.** The multifunctional estrogen receptor- alpha F domain. *Endocrine, 2008, 33, 1–8*.

-**Smith C.L., O'Malley B.W.** Coregulator function: a key to understanding tissue specificity of selective receptor modulators. *Endocr. Rev., 2004, 25, 45-71*.

-**Street T.O., Lavery L.A., Agard D.A.** Substrate binding drives large-scale conformational changes in the Hsp90 molecular chaperone. *Mol Cell, 2011, 4296-105*.

-**Ström A., Hartman J., Foster J.S., Kietz S., Wimalasena J., Gustafsson J.A.** Estrogen receptor beta inhibits 17beta-estradiol-stimulated proliferation of the breast cancer cell line T47D. *Proc. Natl. Acad. Sci. U.S.A., 2004, 101, 1566–1571*.

-**Thangapazham R. L., Passi N., Maheshwari R. K.** Green tea polyphenol and epigallocatechin gallate induce apoptosis and inhibit invasion in human breast cancer cells. *Cancer Biol. Ther. 2007, 6, 1938–1943*.

-**Theodoraki M.A., Caplan A.J.** Quality control and fate determination of Hsp90 client proteins. *Biochim Biophys Acta, 2012, 1823, 683-688*.

-**Thurlimann B.J., Keshaviah A., Mouridsen H, et al.** Randomized double-blind phase III study to evaluate letrozole (L) vs. tamoxifen (T) as adjuvant endocrine therapy for postmenopausal women with receptor-positive breast cancer. *Orlando (FL): American Society of Clinical Oncology; 2005, 1-98*.

-**Tillotson B., Slocum K., Coco J., Whitebread N., Thomas B., West K.A., MacDougall J., Ge J., Ali J.A., Palombella V.J., Normant E., Adams J., Fritz C.C.** Hsp90 (heat shock protein 90) inhibitor occupancy is a direct determinant of client protein degradation and tumor growth arrest in vivo. *J. Biol. Chem. 2010, 285, 39835–39843*.

-**Toft D., Gorski J.** A receptor molecule for estrogens:isolation from the rat uterus and preliminary characterization. *Proc Natl Acad Sci U S A, 1966, 55, 1574-1581*.

-**Tora L., Mullick A., Metzger D., Ponglikitmongkol M., Park I., Chambon P.** The cloned human oestrogen receptor contains a mutation which alters its hormone binding properties. *EMBO J. 1989, 8, 1981–1986.*

-**Tora L., White J.,. Brou C, Tasset D., Webster N., Scheer E., Chambon P.** The human estrogen receptor has two independent nonacidic transcriptional activation functions. *Cell, 1989, 59, 477–487*.

-**Tran P.L., Kim S.A., Choi H. S., Yoon J. H., Ahn S.G.** Epigallocatechin-3-gallate suppresses the expression of HSP70 and HSP90 and exhibits anti-tumor activity in vitro and in vivo. *BMC Cancer 2010, 10, 276*.

-**Trichopoulos D.** Hypothesis: does breast cancer originate in utero? *Lancet. 1990, 355, 939-940*.

-**Tsai M.J., O'Malley B.W.** Molecular mechanisms of action of steroid/thyroid receptor superfamily members. *Annu Rev Biochem, 1994, 63, 451-486*.

-**Tsai S.Y., Carlstedt-Duke J., Weigel N.L., Dahlman K., Gustafsson J.A., Tsai M.J., O'Malley B.W.** Molecular interactions of steroid hormone receptor with its enhancer element: evidence forreceptor dimer formation. *Cell, 1988, 55, 361-369*.

-**van Agthoven T., Timmermans M., Dorssers L.C., Henzen-Logmans S.C.** Expression of estrogen, progesterone and epidermal growth factor receptors in primary and metastatic breast cancer. *Int. J. Cancer. 1995, 63, 790–793.*

-**van 't Veer L.J., Dai H., van de Vijver M.J., He Y.D., Hart A.A., Mao M., Peterse H.L., van der Kooy K., Marton M.J., Witteveen A.T., Schreiber G.J., Kerkhoven R.M., Roberts C., Linsley P.S., Bernards R., Friend S.H.** Gene expression profiling predicts clinical outcome of breast cancer. *Nature. 2002, 415, 530–536.*

-**Vivacqua A., Lappano R., De Marco P., Sisci D., Aquila S., De Amicis F., Fuqua S.A., Andò S., Maggiolini M.** G protein-coupled receptor 30 expression is up-regulated by EGF and TGF alpha in estrogen receptor alpha-positive cancer cells. *Mol. Endocrinol. 2009, 23, 1815–1826.*

-**Volloch V.Z., Sherman M.Y.** Oncogenic potential of Hsp72. *Oncogene. 1999, 18, 3648-3651.*

-**Weatherman R.V., Fletterick R.J., Scanlan T.S.** Nuclear-receptor ligands and ligand-binding domains. *Annu. Rev. Biochem., 1999, 68, 559–581.*

-**Weatherman R.V., Scanlan T.S.** Unique protein determinants of the subtype selective ligand responses of the estrogen receptors (ERalpha and ERbeta) at AP-1 sites. *J. Biol. Chem., 2001, 276, 3827–3832.*

-**Wegele H., Müller L., Buchner J.** Hsp70 and Hsp90--a relay team for protein folding. *Rev Physiol Biochem Pharmacol, 2004, 151, 1-44.*

-**Weigel R.J., deConinck E.C.** Transcriptional control of estrogen receptor in estrogen receptor negative breast carcinoma. *Cancer Res, 1993, 53, 3472–3474.*

-**Weigel N.L., Bai W., Zhang Y., Beck C.A., Edwards D.P., Poletti A.** Phosphorylation and progesterone receptor function. *J Steroid Biochem Mol Biol, 1995, 53, 509-514.*

-**Weinberg O.K., Marquez-Garban D.C., Pietras R.J.** New approaches to reverse resistance to hormonal therapy in human breast cancer. *Drug Resist Updat. 2005, 8, 219-33.*

-**Whitesell L., Lindquist S.L.** Hsp90 and the chaperoning of cancer. *Nat Rev Cancer, 2005, 5, 761-772.*

-**Williams C., Edvardsson K., Lewandowski S.A., Ström A., Gustafsson J.A.** A genome-wide study of the repressive effects of estrogen receptor beta on estrogen receptor alpha signaling in breast cancer cells. *Oncogene, 2008, 27, 1019–1032.*

-**Yin Z., Henry E. C., Gasiewicz T. A.** Epigallocatechin-3-gallate is a novel Hsp90 inhibitor. *Biochemistry 2009, 48, 336–345.*

-**Yuan J.M., Sun C., Butler L.M.** Tea and cancer prevention: epidemiological studies. *Pharmacol Res. 2011, 64, 123-35.*

-**Zhao R., Davey M., Hsu Y.C., Kaplanek P., Tong A., Parsons A.B., Krogan N., Cagney G., Mai D., Greenblatt J., Boone C., Emili A., Houry W.A.** Navigating the

chaperone network: an integrative map of physical and genetic interactions mediated by the hsp90 chaperone. *Cell, 2005, 120, 715-727*.

-**Zhu B.T., Conney A.H.** Functional role of estrogen metabolism in target cells: review and perspectives. *Carcinogenesis. 1998, 19, 1–27*.

-**Zilli M., Grassadonia A., Tinari N., Di Giacobbe A., Gildetti S., Giampietro J., Natoli C., Iacobelli S.** Molecular mechanisms of endocrine resistance and their implication in the therapy of breast cancer. *Biochim Biophys Acta., 2009, 1795, 62-81*.

-**Zloch Z.** The role of dietary plant polyphenols in health maintenance. *Cas Lek Cesk. 1996, 135, 84-88*.

-**Zuehlke A., Johnson J.L.** Hsp90 and co-chaperones twist the functions of diverse client proteins. *Biopolymers, 2010, 93, 211-217*.

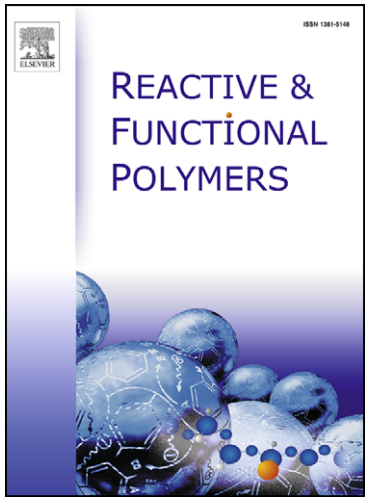

Preparation, characterization and *in vitro* activities evaluation of curcumin based microspheres for azathioprine oral delivery

Roberta Cassano, Sonia Trombino, Teresa Ferrarelli, Anna Rita Bilia, Maria Camilla Bergonzi, Alessandra Russo, Francesca De Amicis, Nevio Picci

PII: S1381-5148(12)00096-X
DOI: 10.1016/j.reactfunctpolym.2012.04.003
Reference: REACT 3015

To appear in: *Reactive & Functional Polymers*

Received Date: 5 March 2012
Revised Date: 2 April 2012
Accepted Date: 4 April 2012

Please cite this article as: R. Cassano, S. Trombino, T. Ferrarelli, A.R. Bilia, M.C. Bergonzi, A. Russo, F.D. Amicis, N. Picci, Preparation, characterization and *in vitro* activities evaluation of curcumin based microspheres for azathioprine oral delivery, *Reactive & Functional Polymers* (2012), doi: 10.1016/j.reactfunctpolym.2012.04.003

Preparation, characterization and *in vitro* activities evaluation of curcumin based microspheres for azathioprine oral delivery

Roberta Cassano[1], Sonia Trombino[1,*], Teresa Ferrarelli[1], Anna Rita Bilia[2], Maria Camilla Bergonzi[2], Alessandra Russo[3], Francesca De Amicis[3], Nevio Picci[1]

[1]Department of Pharmaceutical Sciences, [3]Department of Pharmaco-Biology University of Calabria, 87036 Arcavacata di Rende, Cosenza, Italy

[2]Department of Pharmaceutical Sciences, University of Florence, I-50019 Sesto Fiorentino, Firenze, Italy

[*]**Corresponding author**: Tel.: +39 984 493203; Fax: +39 984 493163.
E-mail address: sonia.trombino@unical.it

Abstract

The main target of this study was the preparation, characterization and *in vitro* activities evaluation of microspheres curcumin-based able to incorporate azathioprine, useful for psoriasis treatment. Curcumin was derivatized with acryloyl chloride in order to introduce polymerizable groups in its structure. The obtained polymerizable drug was characterized by Fourier transorm infrared (FT-IR), to confirm ester linkages, and by ^{1}H-NMR, to establish the functionalization degree. The ability of curcumin derivative to inhibit cell proliferation, in human breast cancer cells, gave an IC_{50} value for viability of 20μM. Acrylated curcumin also showed a strong antioxidant activity against lipid peroxidation induced in rat liver microsomal membranes. Then, spherical microparticles, based on curcumin derivative, were prepared by suspension radical copolymerization. The obtained microparticles were characterized by FT-IR spectroscopy, dimensional and morphological analysis. Particle size investigation revealed a mean diameter of around 5.8 μm. Microspheres showed a very good swelling behaviour in simulating intestinal fluids. Their azathioprine loading efficiency, determined by spectophotometric analysis was equal to 80%. Release profile of azathioprine showed an initial dot of around 60% and a further release for 24 h.

Keywords: curcumin, azathioprine, microsphere, antioxidant, antiproliferative.

1. Introduction

The use of polymeric materials for biomedical applications has been increasing rapidly in the last years. Polymers have found applications in different biomedical fields such as drug delivering systems, developing scaffolds in tissue engineering, implantation of medical devices and artificial organs, prosthesis, ophthalmology, dentistry, bone repair, and many other medical fields. For almost four decades, both natural and synthetic polymers have been investigated as carriers for controlled drug dosage. The role of the polymers in such a system is to deliver drugs to target tissue in order to increase their effectiveness thus reducing undesirable side effects. Besides, the polymer core also protects the drugs from the physiological *in vivo* environment and thus increases the drug bioavailability. Hence, polymeric drug delivering systems offer some unambiguous advantages such as localized and sustained delivery of the drug. This

becomes especially important for toxic drugs which are related to various systemic side effects. In addition, for polymers to be used as drug carriers, they should have a well defined structure, should be biocompatible and non toxic. These last properties can be also conferred by functional groups and active moieties properly located in polymer structure. Natural substances, possessing as well pharmaceutical activity, could be used to prepare materials with desired physiochemical properties and able to exhibit, other than biocompatibility, a synergic and/or additional action to vehiculated active substances. An interesting natural substance useful for the preparation of the materials described above is curcumin, a yellow pigment derived from *Curcuma longa L.*, characteristic representative of natural polyphenols, employable in medicinal and cosmetic preparations for its antiproliferative, anti-inflammatory and antioxidant properties [1-13]. Clinical studies demonstrate curcumin positive effects promoting skin regeneration, inhibition of cyclooxygenase activity and regulation of pro-inflammatory cytokines. Recently many clinical trials suggest the efficacy and safety of oral administered curcumin for psoriasis treatment [14-16]. Generally, moderate psoriasis is treated with corticosteroids, also used in combination with calcipotriene, tazarotene and other retinoids derived from vitamin A [17,18]. On the other hand, all these drugs can cause serious side effects and, for these reasons, a great deal of researchers proposed both the associations of conventional drugs, to obtain synergistic effects, that of alternative molecules such as antioxidant polymers receiving ever-increasing attention. Although *in vitro* curcumin has been shown to block pathways necessary to develop psoriasis, it is possible that, after oral administration, it will not produce a desired clinical effect because of low bioavailability [19] due to its conjugation in the intestinal tract [20]. For all these reasons we projected a new drug delivery system covalently linking acrylic moieties to curcumin (Scheme 1) to produce a polymeric carrier that can act both against oxidative stress in the bowel, frequent in psoriasis, and to entrap another antipsoriatic drug, like azathioprine. The use of this last substance has been limited due to its toxicity, thus, its vehiculation through curcumin acrylated-based microspheres, has the purpose, not only to obtain an azathioprine targeted delivery, but also the potential advantage of providing a local therapeutic effect reducing systemic azathioprine bioavailability [21].

Scheme 1

The present paper reports on: (i) the synthesis and characterisation of acrylated curcumin and of microspheres curcumin acrylated-based; (ii) the evaluation of their antiproliferative and antioxidant activities [22]; (iii) microspheres swelling degree, azathioprine loading efficiency and release behaviour.

2. Experimental

2.1. Chemicals

All solvents were obtained from Carlo Erba Reagents (Milan, Italy). N,N'-ethylene bis-acrylamide (EBA) and acryloyl chloride, were supplied by Sigma (Sigma Chemical Co, St. Louis, MO). Acryloyl chloride was distilled before using. Curcumin (C) from *Curcuma longa*, azathioprine, potassium carbonate (K_2CO_3), ammonium persulfate [$(NH_4)_2S_2O_8$], sorbitan trioleate (Span 85), polyoxyethylene sorbitan monolaureate (Tween 85), N,N,N',N'-tetramethylethylenediamine (TMEDA), potassium chloride (KCl), ethylenediaminetetraacetic acid (EDTA), sucrose, 4-(2-hydroxyethyl-1-piperazineethanesulfonic acid (HEPES), trichloroacetic acid (TCA), hydrochloric acid, butylated hydroxytoluene (BHT), *tert*-butyl hydroperoxide (*tert*-BOOH), and 2-thiobarbituric acid (TBA) were purchased from Aldrich Chemical Co. and used as received. DMEM/F-12, L-glutamine, Eagle's nonessential amino acids, penicillin, streptomycin, fetal calf serum, BSA, and PBS were purchased from Gibco (USA).

2.2. Measurements

NMR spectra were acquired on Bruker VM-300 ACP using $CDCl_3$ as solvent. FT-IR spectra were measured on a Jasco 4200 using KBr disks. UV-VIS spectra were performed by V-530 JASCO spectrophotometer. The GC-MS spectra were obtained by Hewlett Packard 5972 instrument. Morphological studies were performed using optical microscopy. Light scattering analyses were performed with a Brookhaven 90 plus particle size analyser at 25°C by measuring the autocorrelation function at 90° scattering angle. Cuvettes were filled with 100 mL of sample solution and diluted to 4 mL with filtered (0.22 mm) water. The polydispersity index (PI), which indicates the measure of the distribution of nanoparticle populations, was also determined. Six separate measurements were made in order to obtain the average. Data were fitted by the method of inverse ''Laplace transformation'' and Contin. Samples were lyophilized

using a "Freezing-drying" Micro moduly apparatus, Edwards. Scanning electron microscopy (SEM) photographs of microspheres were obtained with a JEOL JSMT 300 A; the surface of the samples was made conductive by deposition of a gold layer in a vacuum chamber.

2.3. Synthesis of Acrylated Curcumin (CA)

Curcumin (1 g, 2.71 mmol), dissolved in dry tetrahydrofuran, was treated with potassium carbonate (K_2CO_3) in equimolar ratio (0.374 g) to avoid disubstitution and then with acryloyl chloride (2.71 mmol, 0.218 ml) using Et_3N as a base (0.379 ml, 2.71 mmol) [23-24]. The reaction was left under reflux at 40°C for 48 h under magnetic stirring. The monosubstituted derivative was obtained from a raw product by chromatographic column (silica gel 60-230 mesh, eluent mixture $CHCl_3/CH_3OH$ (1:1) Subsequently, the target molecule was investigated by GC/MS, FT-IR and ^{1}H-NMR spectroscopies [25].

2.4. Antiproliferative Activity Evaluation of CA

The antiproliferative effect of CA was evaluated in MCF-7 human breast cancer cells gifts from Dr. B. Van der Burg (Utrecht, The Netherlands). These cells were maintained in DMEM/F-12 medium containing 5% fetal calf serum, 1% L-glutamine, 1% Eagle's nonessential amino acids, and 1 mg/ml penicillin/streptomycin in a 5% CO_2 humidified atmosphere. 48 h before each experiment, the cells were maintained in phenol red-free DMEM/F-12, 0.5% BSA and 2 mM L-glutamine. Treatment was performed in phenol red-free DMEM/F12 containing 5% charcoal-treated fetal calf serum to reduce the endogenous steroid concentration [26]. For our purposes MCF-7 human breast cancer cells were assessed by the MTT assay [27]. The experiment was repeated in triplicate (n=3).

2.5. Antioxidant Activity Evaluation of CA

The ability of curcumin derivative to protect against lipid peroxidation induced by *tert*-BOOH, was examined in rat liver microsomal membranes during 120 min of incubation. Aliquots of curcumin and CA were added to the microsomal suspension.

The suspension was then incubated at 37 °C in a shaking bath under air in the dark. After incubation, the thiobarbituric acid-malondialdehyde complex (TBA-MDA) formation was monitored by the use of UV-VIS spectrophotometry at 535 nm [28-30]. The experiment was repeated in triplicate (n=3).

2.6. Microspheres Preparation

Curcumin-based microspheres were produced by radical copolymerization technique. Briefly, a cylindrical glass reactor of 100-150 ml, equipped with a mechanical stirrer and dripping funnel, screw cap with puncture-proof rubber septum was flamed in a nitrogen flow and after cooling was immersed in a thermostatically controlled bath at 40° C. Then, a required amount of *n*-hexane (20 ml) and chloroform (18 ml) were introduced into the reactor as dispersing phase. After 30 min of N_2 bubbling, this mixture was treated with distilled water containing CA, EBA (comonomer) and ammonium persulfate such as radical initiator. Whilst stirring at 1000 rpm, the mixture was treated with Span85 and Tween85, then after 10 min with TMEDA and the stirring was continued for another 60 min [31].

The amounts of all reagents used in these experiments are reported in Table 1. The microspheres obtained were filtered, washed with 50 ml portions of 2-propanol, ethanol, acetone and diethyl ether and dried overnight under vacuum at 40 ºC. Their characterization was effected by light scattering, FT-IR spectrometry, optical microscopy and SEM.

Table 1

2.7. Swelling Studies

Swelling behaviour was investigated in order to check the hydrophilic affinity of spherical microparticles. Typically, aliquots (50 mg) of dried materials were placed in a tared 5-ml sintered glass filter (Ø 10 mm; porosity G3), weighed, and left to swell by immersing the filter in a beaker containing the swelling media (phosphate buffer pH 6.8, simulated intestinal fluid). At fixed times (1, 6, 12 and 24 h), the excess of water was removed by percolation and then the filter was centrifuged at 3500 rpm for 15 min and weighed. The filter tare was determined after centrifugation with only water. The

weights recorded at different times were averaged and used to give the equilibrium swelling degree (Wt (%)) by the Eq. (1) where Ws and Wd are the weights of swollen and dried microspheres, respectively. Each experiment was carried out in triplicate and the results were in agreement within ±4% standard error.

$$W_t\,(\%) = \left(W_s - W_d\right)/W_s \cdot 100 \quad (1)$$

2.8. Azathioprine Loading by Soaking Procedure

150 mg of preformed empty microspheres were wet with 10 ml of distilled water in a concentrated azathioprine solution (0.03 g). The amount of dissolved drug was chosen in order to have a drug loading of 20% (w/w). After 3 days, under slow stirring at 37 °C, the microspheres were filtered and dried at reduced pressure in presence of P_2O_5 to constant weight. The loading efficiency percentage (LE, %) of all samples were determined by spectrophotometric analysis (λ = 280 nm) of filtered solvent according to Eq. (2):

$$LE\,(\%) = \left(C_i - C_o\right)/C_i \cdot 100 \quad (2)$$

Here C_i was the concentration of the drug in solution before the loading study, while C_o is the concentration of drug in solution after the loading study.

2.9. Drug Release Studies

Dried microspheres (10 mg) were dispersed in 6 ml of swelling media (phosphate buffer pH 6.8, simulated intestinal fluid). The test tubes were maintained at 37°C in an horizontal-shaking bath and shaked at a rate of 100 rpm. At fixed intervals, samples were centrifuged, 5 ml of supernatant were removed and the medium was replaced with fresh solutions to maintain the same total volume throughout the study. The concentration of azathioprine was determined by UV spectrophotometry at 280 nm. The experiment was repeated in triplicate (n=3). The release was calculated in terms of cumulative drug release percentage.

2.10. Statistical Analysis

Each datum point represents the mean ± SD of three different experiments. Data were analyzed by Student's t test using the GraphPad Prism 4 software program. $P<0.05$ was considered as statistically significant.

3. Results and Discussion

Chemical groups susceptible of radical polymerization were introduced onto curcumin structure by esterification with acryloyl chloride in THF. Acrylated curcumin structure was confirmed by GC/MS, FT-IR and ^{1}H-NMR analysis [25]. Initial cell proliferation assays were performed with different concentrations (from 20 to 40 μM) of curcumin and CA, in MCF-7 human breast cancer cell lines. Proliferating cells were exposed to the compounds for 4 days and then analyzed in MTT growth assays. 20μM curcumin significantly inhibited basal cell proliferation (40%). With increasing doses (30 and 40μM), MCF-7 cell number was reduced by 56% to 77% respectively (IC_{50} value for viability was 30 μM). Moreover, cell growth was also markedly reduced with CA treatment and it is worth to notice that the inhibitory activity on cell proliferation of CA (IC_{50} value for viability was 20 μM) was more effective than curcumin itself (Fig. 1).

Fig. 1

The evaluation of its antioxidant activity revealed that its effect on lipid peroxidation was time-dependent. Results are given as the percentage (%) of malondialdehyde (MDA) inhibition (Fig. 2) and demonstrated that CA was also a strong antioxidant in protecting the membranes from *tert*-BOOH, induced lipid peroxidation, showing a higher efficiency than that of curcumin itself (C) at 60 and 120 min of incubation, and the preservation of antioxidant activity up to 2 h (Fig. 2). This behaviour was probably due to the major stability of the radical formed by abstraction of a hydrogen atom from the hydroxylic group of phenolic ring. The explanation is the delocalization of the unpaired radical electron on the whole structure that is increased by the presence of the acrylic group that gives higher conjugation.

Fig. 2

Microspheres curcumin-based were prepared by a reverse phase suspension copolymerization of CA with EBA. The reaction was started by using TMEDA and ammonium persulfate as initatior system. The obtained materials were characterized by Fourier Transform IR spectrophotometry, particle size distribution analysis and morphological analysis. The FT-IR spectra of curcumin, CA and microparticles curcumin based are compared in Fig. 3. Monomer FT-IR spectrum shows the characteristic peak due to C=O stretching vibration belonging to the carboxylic group of the ester at 1746 cm^{-1}. Additionally, microspheres spectrum shows the appearance of a band awardable to C=O stretching vibration of comonomer amidic group (1650 cm^{-1}). In all spectra the peaks between 3000 and 3100 cm^{-1} are assigned to C–H (aromatic) stretching vibration due to the phenyl group of curcumin itself.

Fig. 3

Using optical microscopy we were able to check that microparticles had a spherical shape (Fig. 4).

Fig. 4

In Fig. 4a the spherical shape is evident. In our experiments a mean particle diameter of around 5.8 ± 0.876 μm was calculated by using dimensional light scattering. Morfological analysis by using scanning electron microscopy (SEM) that confirmed the spherical shape and showed a homogeneous surface morphology was also performed (Fig. 4b). Microspheres swelling studies were also conducted and showed a very good swelling behaviour in simulating intestinal fluids (Table 2).

Table 2

Investigation of the applicability of curcumin based particles in controlled release was done by studying their swelling behaviour. The value of contained water percentage was determined in aqueous media which simulates some biological fluids, such as gastric (pH 1.2) and intestinal (pH 6.8) at 37 ºC. Data reported in Table 2 illustrate the water uptake, in grams per grams of dry copolymer, for each pH studied. The prepared materials showed different water affinity at pHs 6.8 and 1.2 due to pendant ionizable groups in the polymeric chains. In particular, at pH 1.2 there is a considerable decrease of the water affinity due to pendant groups unionized at this pH value. When the pH is 6.8, the water content is greater than that found at pH 1.2. It is possible to explain this behaviour as a consequence of electrostatic repulsions between polymeric chains due to the increase of dissociated groups at pH 6.8. The pendant groups responsible of this behaviour are the acidic ones of comonomer (EBA) having pKa 6.1-7.1. In order to estimate the ability of prepared matrices to release encapsulated drug, the microspheres were loaded with azathioprine by soaking procedure and their loading efficiency (LE, %) was determined by spectrophotometric analysis such as reported in the experimental section. Data showed that azathioprine was efficiently loaded on the polymeric beads (LE (%)=80). It is possible to explain this behaviour as a consequence of strong interactions between polymeric matrix and drug molecules. Drug release profile was determined by spectrophotometric analyses. Drug release was expressed as the percentage of drug delivered, related to the effectively entrapped total dose, as a function of time. These experiments were carried out the *in vitro* at 37°C. Considering the poor swelling degree at pH 1.2, the release study was effected by simulating the intestine pH value (6.8). Data showed a significative azathioprine release in these conditions (Fig. 5): the total amount of azathioprine, released in 24 h in the dissolution medium, was about 88%. It is possible to observe an initial massive release after 1 h due both to the desorption of drug trapped on the surface than to the release of the loaded one through the matrix. After 4 h the percent of drug released remains considerable showing that loaded microspheres could be useful to target azathioprine to the intestinal environment thus reducing its systemic toxicity. In these same conditions of pH, curcumin was not released from matrix (data not shown); for this reason it is possible to conclude that the polymerized substance could potentially act as a prodrug too.

Fig. 5

4. Conclusion

Curcumin, a natural antioxidant and anti-inflammatory substance, was successfully derivatized by reaction with acryloyl chloride in order to obtain a sample which contains chemical groups able to undergo radical polymerization. The antioxidant activity of new monomer was evaluated *in vitro* through rat-liver microsomal membranes and the results suggested that curcumin, linked to acrylic moieties, maintains its excellent antioxidant efficiency. The increased conjugation in the acrylic derivative is responsible for its better lipid peroxidation inhibition after 30 min respect to the unconjugated curcumin. Additionally, curcumin derivative inhibits cell proliferation more than commercial curcumin, as examined in human breast cancer cells *in vitro*. Using the radical copolymerization technique healing beads with a spherical shape and an omogeneous diameter of about 5.8 μm were obtained. Such materials could be used to transport other active substances such as azathioprine and act also as an antioxidant. In fact, the release profile of azathioprine, in a medium that simulates the intestinal environment, showed that the drug was quite massively released (87.8%) during 24 h.

Acknowledgments

This work was financially supported by Academic Funds, MIUR (Programma di Ricerca di Rilevante Interesse Nazionale 2008) and Ente Cassa di Risparmio di Firenze. The authors thanks Ms. Anna Internò, an English lecturer of Faculty of Pharmacy, for her assistance.

References

[1] J. Jagur-Grodzinski, React. Funct. Polym. 39 (1999) 99-138.

[2] D. Eigner, D.Schulz, J. Ethnopharmacol. 67 (1999) 1-6.

[3] A. Goel, A.B. Kunnumakkara, B.B. Aggarwal, Biochem. Pharmacol. 75 (2008) 787-809.

[4] V.P. Menon, A.R. Sudheer, Adv. Exp. Med. Biol. 595 (2007) 105-125.

[5] M.M. Chan, H.I. Huang, M.R. Fenton, D. Fong, Biochem. Pharmacol. 55 (1998) 1955-1962.

[6] T. Choudhuri, S. Pal, M.L. Agwarwal, T. Das, G. Sa, FEBS Lett. 512 (2002) 334–340.

[7] M.L. Bondi', E.F. Craparo, P. Picone, M. Di Carlo, R. Di Gesu', G. Capuano, G. Giammona, Current Nanosci. 6 (2010) 439-445.

[8] A. Gulcubuk, K. Altunatmaz, K. Sonmez, D. Haktanir-Yatkin, H. Uzun, A. Gurel, S. Aydin, J. Vet. Med. A Physiol. Pathol. Clin. Med. 53 (2006) 49-54.

[9] R.J. Anto, J. George, K.V. Babu, K.N. Rajasekharan, R. Kuttan, Mutai Res. 370 (1996) 127-131.

[10] W. Wongcharoen, A. Phrommintikul, Int. J. Cardiol. 133 (2009) 145-151.

[11] J.M. Ringman, S.A. Frautschy, G.M. Cole, D.L. Masterman, J.L. Cummings. Curr. Alzheimer Res. 2 (2005) 131-136.

[12] J. Dujic, S. Kippenberger, S. Hoffmann, A. Ramirez-Bosca, J. Miquel, J. Diaz-Alperi, J. Bereiter-Hahn, R. Kaufmann, A. Bernd. J. Invest. Dermatol. 127 (2007) 1992-2000.

[13] M. Panchatcharam, S. Miriyala, V. Gayathri, L. Suguna, Mol. Cell. Biochem. 290 (2006) 87-96.

[14] S.K. Kurd, N. Smith, A. VanVoorhees, A.B. Troxel, V. Badmaev, J.T. Seykora, J.M. Gelfand, J. Am. Acad. Dermatol. 58 (2008) 625-31.

[15] M.C. Heng, M.K. Song, J. Harker, M.K. Heng, Dermatol. 143 (2000) 937-949.

[16] G.D. Weinstein, G.G. Krueger, N.J. Lowe, M. Duvic, D.J. Friedman, B.V. Jegasothy, J.L. Jorizzo, E. Shmunes, E.H. Tschen, D.A. Lew-Kaya, J.C. Lue, J.

Sefton, J.R. Gibson, R.A. Chandraratna, J. Am. Acad. Dermatol. 37 (1997) 85-92.

[17] M. Lebwohl, J. Am. Acad. Dermatol. 37 (1997) 55-58.

[18] B. Patel, S. Siskin, R. Krazmien, M. Lebwohl, J. Am. Acad. Dermatol. 38 (1998) 1010-1011.

[19] K.L. Grant, C.D. Schneider. Am. J. Health. Syst. Pharm. 57 (2000) 1121-1122.

[20] C.R. Ireson, D.J. Jones, S. Orr, M.W. Coughtrie, D.J. Boocock, M.L. Williams, Cancer Epidemiol. Biomarkers Prev. 11 (2002) 105-111.

[21] E.C. Van Os, B.J. Zins, W.J. Sandborn, D.C. Mays, W.J. Tremaine, D.W. Mahoney, A.R. Zinsmeister, J.J. Lipsky, Gut 39 (1996) 63-68.

[22] S. Trombino, S. Serini, F. Di Nicuolo, L. Celleno, S. Andò, N. Picci, G. Calviello, P. Palozza, J. Agric. Food Chem. 52 (2004) 2411-2420.

[23] R. Cassano, R. Dabrowski, J. Dziaduszek, N. Picci, G. Chidichimo, G. De Filpo, R. Muzzalupo, F. Puoci, Tetrah. Lett. 48 (2007) 1447–1450.

[24] R. Cassano, S. Trombino, E. Bloise, R. Muzzalupo, F. Iemma, G. Chidichimo N. Picci, J. Agr. Food Chem. 55 (2007) 9489-9495.

[25] Compound CA: orange powder, yield 17 g (43%). GC/MS: 294 (1%), 210 (30%), 110 (100%). FT-IR (KBr) ν in cm^{-1}: 3076, 3031, 2941, 2851, 1699, 1275, 1020, 973, 942. ^{1}H-NMR ($CDCl_3$) δ (ppm): 1.1 (m, 10H), 1.41 (m, 8H), 1.59–1.72 (m, 16H), 2.1 (m, 2H), 3.42 (t, 4H), 3.93 (t, 4H), 4.8 (m, 2H), 4.44 (s, 4H), 6.82 (m, 4H), 7.23 (m, 10H), 7.9 (m, 4H).

[26] B. van der Burg, G.R. Rutteman, M.A. Blankenstein, S.W de Laat, E.J. van Zoelen. J. Cell Physiol. 34 (1988) 101–108.

[27] M. Hansen, S. Nielsen, K. Berg, J. Immunol. Methods 119 (1989) 203-210.

[28] R. Cassano, S. Trombino, R. Muzzalupo, L. Tavano, N. Picci, Eur. J. Pharm. Biopharm. 72 (2009) 232-238.

[29] S. Trombino, R. Cassano, E. Bloise, R. Muzzalupo, S. Leta, F. Puoci, N. Picci Macromol. Biosci. 8 (2008) 86-95.

[30] S. Trombino, R. Cassano, E. Bloise, R. Muzzalupo, L. Tavano, N. Picci, Carbohydr. Polym. 75 (2009) 184-188.

[31] F. Iemma, U.G. Spizzirri, F. Puoci, R. Muzzalupo, S. Trombino, R. Cassano , S. Leta, N. Picci, Int. J. Pharm. 312 (2006) 151–157.

Figure Captions

Fig. 1. MTT assay. Cells, serum starved, were exposed to vehicle (-), or different concentrations of curcumin or CA in medium containing 1% dextran charcoal-stripped FBS for 4d (treatments were renewed every 2d). Results indicate mean of three independent experiments done in triplicate; bars SD.

Fig. 2. Graphs showing the inhibition of *tert*-BOOH induced MDA formation in rat microsomal membranes. The microsomal membranes were incubated with 0.25 10^{-3} M *tert*-BOOH at 37 °C under air and in the dark. The results represent the mean standard deviation (SDM) of three separate experiments. Results indicate mean of three independent experiments done in triplicate; bars SD.

Fig. 3. FT-IR spectra of: a) curcumin; b) acrylated curcumin (CA); c) microparticles curcumin based.

Fig. 4. (a) Optical micrograph and (b) scanning electron image of microparticles.

Fig. 5. Graph of azathioprine release from curcumin acrylated-based microspheres. Results indicate mean of three independent experiments done in triplicate; bars SD.

Table Captions

Table 1. Copolymerization of CA with EBA.

Table 2: Microspheres swelling behavior.

Scheme Captions

Scheme 1. Synthetic route to CA and microspheres preparation.

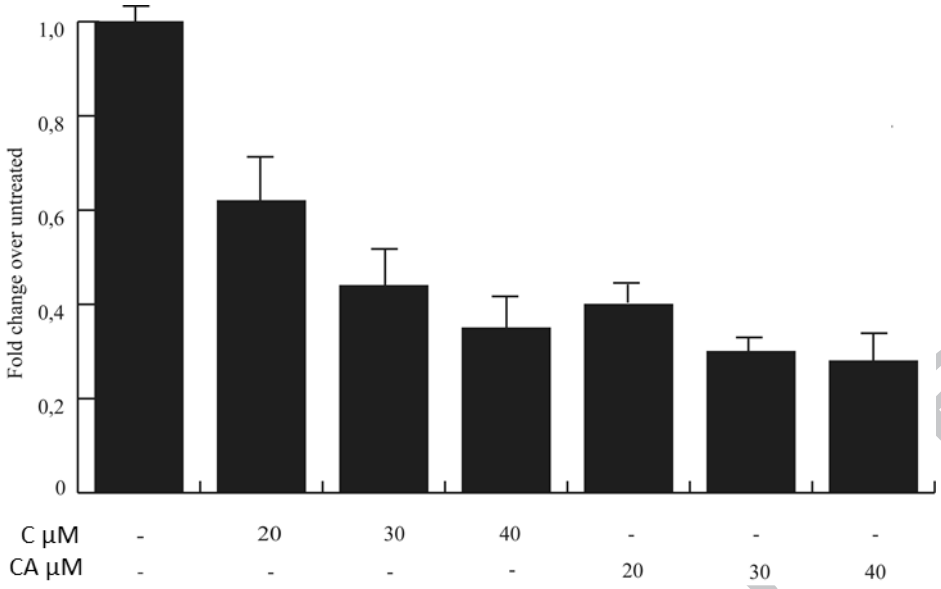

Fig. 1

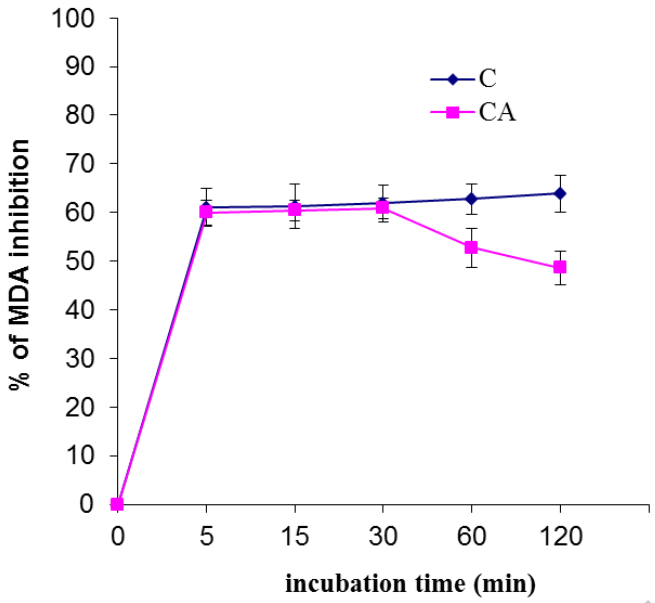

Fig. 2

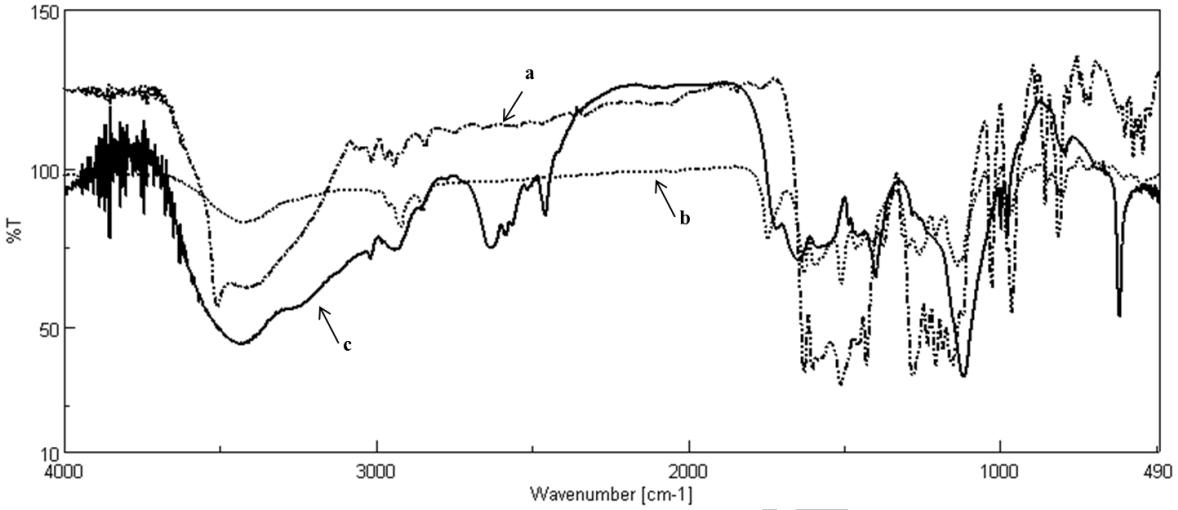

Fig. 3

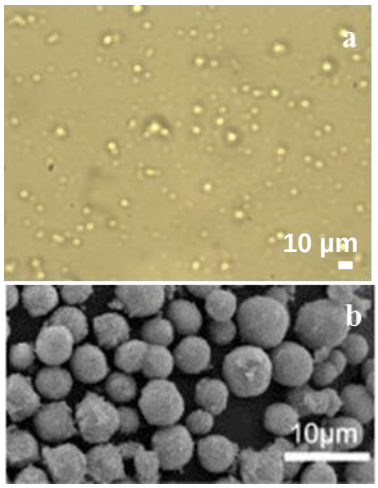

Fig. 4

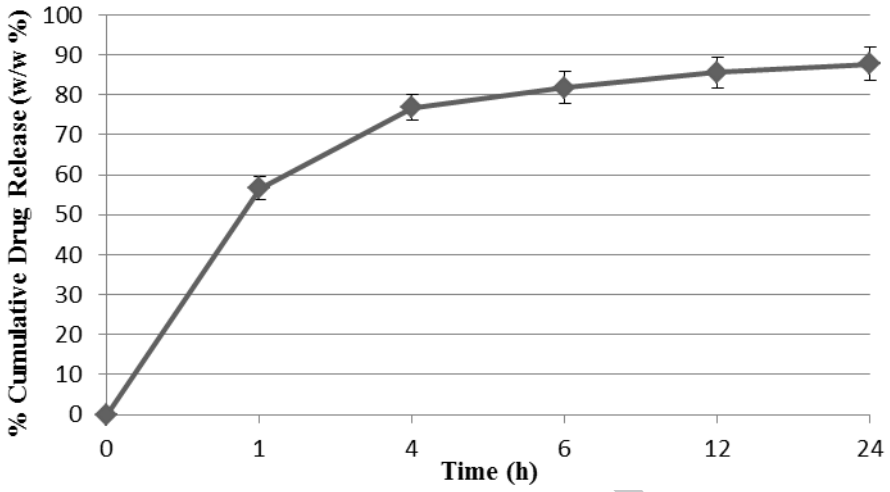

Fig. 5

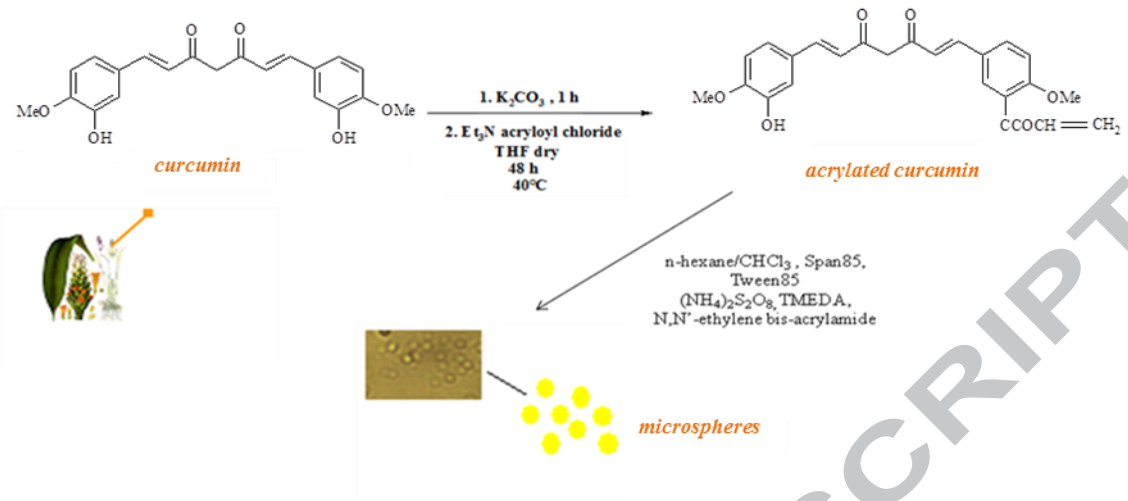

Scheme 1

Aqueous dispersed phase *Reagents (mg)*	Organic continuous phase *$CHCl_3$/hexane (ml/ml)*	Microspheres *mg (conv. %)*
CA($1.2 \cdot 10^3$ mg) EBA (440 mg)	18/20	$1 \cdot 10^3$ mg(83%)

For polymerization, the amount of aqueous phase is 3 ml; initiator system is $(NH_4)_2S_2O_8$/TMEDA (150 mg/150 µl); surfactants are Span 85/Tween 85 (100 µl /50 µl).

Table 1

Time	**Swelling (α %)**		
	pH 1.2	pH 6.8	pH 7.4
1h	*13*	*120*	*66*
6h	*21*	*135*	*83*
12h	*25*	*149*	*85*
24h	*27*	*151*	*86*

Table 2

RESEARCH ARTICLE

Epigallocatechin gallate affects survival and metabolism of human sperm

Francesca De Amicis[1,2], Marta Santoro[1,3], Carmela Guido[1], Alessandra Russo[1] and Saveria Aquila[1,2]

[1] Centro Sanitario, University of Calabria, Arcavacata di Rende (CS), Italy
[2] Department of Pharmaco-Biology, University of Calabria, Arcavacata di Rende (CS), Italy
[3] Post-graduate School in Clinical Pathology, University of Calabria, Arcavacata di Rende (CS), Italy

Received: April 3, 2012
Revised: August 1, 2012
Accepted: August 13, 2012

Scope: Green tea and its major constituent epigallocatechin gallate (EGCG) have been extensively studied as potential treatment for a variety of diseases. We assessed the influence of EGCG on male fertilizing potential by analyzing different features of human sperm involved in capacitation process.

Methods and results: Using human normozoospermic samples, we evaluated the effect of EGCG (2 μM, 20 μM, 60 μM) on sperm activities. Our results showed that lower doses of EGCG (from 2 to 20 μM) increased cholesterol efflux and tyrosine phosphorylation through the estrogen receptor (ER), since ICI 182,780, a specific ER antagonist, abrogated 20 μM EGCG effects. Besides, we evidenced that EGCG at similar concentrations, increased sperm motility, viability, and phosphorylation of proteins controlling cell survival such as Bcl2, Akt, and Src, via ER. Furthermore, we observed reduction of triglycerides content, induction of lipase, as well as the G6PDH activity. These results address to an increase in energy expenditure. On the contrary, treatment of 60 μM EGCG produced opposite effects that still appear after ICI cotreatment.

Conclusion: These results provide a novel mechanism involving ERs through which low doses of EGCG exerted benefits to sperm physiology, also detected data evidence the adverse action of high EGCG concentrations probably related to its prooxidant and antiestrogenic potential.

Keywords:
Epigallocatechin / Green tea / Reproduction / Sperm / Metabolism

1 Introduction

An expanding body of preclinical evidences suggests that epigallocatechin gallate (EGCG), the major catechin found in green tea, has the potential to impact a variety of human diseases. EGCG depending on concentrations, functions as a powerful antioxidant, preventing oxidative damage in healthy cells, but also as an antiangiogenic and antitumor agent with chemopreventative properties [1].

The green tea extracts (GTEs) show protection of cardiovascular system [2], reduction of blood glucose and cholesterol [3], and anti-inflammatory [4] effects. Besides in vitro research using human cancerous cell lines has shown EGCG to inhibit cell proliferation [5–7], to alter progression through the cell cycle [8, 9], to induce apoptosis [8–11], and to promote telomere shortening [12].

Moreover, catechins oral administration in rats has been reported many endocrinological actions. Among others, Divi and Doerge [13] demonstrated that catechin inhibits thyroid peroxidase (TPO), though in vivo long-term effect on thyroid functions has not been reported. Administration to rats of Polyphenone-60 (P-60), which are water extracts of green tea leaves, at high dose induced goiters and decreased weights of the testis and prostate gland in F344 rats [14]. However, the effect of catechins on endocrine system especially related to male fertility was seldom studied [15]. There was evidence that green tea polyphenols inhibited testosterone production in rat Leydig cells (LCs) in vitro by inhibitions of the PKA/PKC pathways, P450 side chain cleavage enzyme (P450scc), and 17b-hydroxysteroid dehydrogenase (17b-HSD) [16]. It is worth of notice that EGCG, via its gallate group, may act on the Estogen Receptor (ER-α and ER-β), thereby mimicking the

Correspondence: Professor Saveria Aquila, Centro Sanitario, University of Calabria, Arcavacata di Rende (CS) 87036, Italy
E-mail: aquisav@libero.it
Fax: +39 0984 496204

Abbreviations: **Bcl2**, B cell lymphoma gene-2; **EGCG**, epigallocatechin-gallate; **E2**, 17-β-estradiol; **ER-α**, estrogen receptor alpha; **ER-β**, estrogen receptor beta; **G6PDH**, glucose-6-phosphate dehydrogenase; **PI3K**, phosphoinositide 3-kinase; **PR**, progesterone receptor

7α-position of 17β-estradiol (E2) [17]. In target cells, it exerts opposite effects, eliciting antiestrogenic action and cytotoxicity [18, 19] at higher doses (100–150 μM), while coestrogenic for ER-α at lower doses (≤5 μM).

ER-α and ER-β are detected in germ cells from spermatogonia to spermatozoa [20, 21]. In human sperm, ERs were found differently located since both receptors are in the midpiece, while ER-β also in the flagellum. Sperm are able to synthesize estrogen [22] and in ejaculated sperm, E2/ERs activate the PI3K/Akt pathway, stimulates various sperm functions including motility, longevity, capacitation, and acrosome reaction [23, 24].

Immediately after ejaculation, human spermatozoa do not possess the ability to fertilize an oocyte, but they acquire this ability in the female reproductive tract. This process is known as capacitation [25–27]. Capacitation enables the sperm to bind to the zona pellucida (ZP) and undergo the acrosome reaction, to facilitate the penetration of the ZP and, subsequently, to aid the oocyte–sperm fusion process [25].

Despite the data supporting the beneficial effects of a diet rich in green tea polyphenols, few studies have shown their safety and potential toxicity when administered at high doses, as highly concentrated or nearly pure compounds [28].

Hence, by analyzing several biochemical changes of capacitation, we assessed the influence of different concentrations of EGCG on male fertilizing potential. Since the tyrosine kinase Src is a key player in the signal transduction cascade occurring during sperm capacitation [26] while Akt and Bcl2 in survival, we assessed their expression. In addition, as there is a close link between energy balance and reproduction [29], and we recently reported that sperm cells are able to modulate their own metabolism independently of systemic regulation [30], we evaluated the action of EGCG on lipid and glucose metabolism in human sperm.

2 Materials and methods

2.1 Chemicals

Percoll (colloidal PVP-coated silica for cell separation), sodium bicarbonate, sodium lactate, sodium pyruvate, DMSO, Earle's balanced salt solution, and (−)-EGCG from green tea were purchased from Sigma-Aldrich (# E4143) (Milan, Italy). ICI 182,780 (ICI, ER antagonist), and RU486 (PR antagonist) were purchased from Zeneca Pharmaceuticals (Cheshire, UK). Both are used to test the specific action of EGCG through ER but not through PR. Acrylamide bisacrylamide was from Labtek Eurobio (Milan, Italy). Triton X-100, Eosin Y was from Farmitalia Carlo Erba (Milan, Italy). ECL Plus Western blotting detection system, Hybond™ ECL™, Hepes Sodium Salt were from Amersham Pharmacia Biotech (Buckinghamshire, UK). Abs p-Src (Tyr139), p-Bcl2, p-Akt, total Src, total Bcl2, total Akt were from Santa Cruz Biotechnology (Heidelberg, Germany). Antiphosphotyrosine was from Calbiochem (Canada, US). EGCG was dissolved in water. ICI and RU486 were dissolved in ethanol (0.02% final concentration in culture). Ethanol was used as solvent control.

2.2 Semen samples and spermatozoa preparations

Human semen was collected, according to the World Health Organization [31] recommendations, by masturbation from healthy volunteer donors. Spermatozoa preparations were performed as previously described [22]. Each sperm sample was obtained by pooling the ejaculates of three different normozoospermic healthy donors. In our experience, this was necessary to obtain enough cells to perform all the tests [32, 33]. Final sperm concentration of resuspended samples during treatments was 20×10^6/mL.

After liquefaction, the normal ejaculates were pooled and subjected to centrifugation (800×g) for 5′ on a discontinuous Percoll density gradient (80:40% v:v) [31]. The 80% Percoll fraction was examined using an optical microscope at 100× magnification to ensure that a pure sample of sperm was obtained. Percoll-purified sperm was washed with uncapacitating medium (Earle's balanced salt solution medium) (t0), and incubated for 30 min at 37°C and 5% CO_2, without (−) or with the indicated concentrations of EGCG. Also, all the parameters were assessed at time 0 (t0). When combined treatments were performed, the cells were pretreated for 15 min with the ER antagonist ICI (1 μM) or RU486 (1 μM).

Each assay was performed using six different sperm samples. Histograms represent mean ± SD of six independent experiments each in duplicate. The study was approved by the local medical ethical committees, and all participants gave their informed consent.

2.3 Evaluation of sperm motility and viability

Sperm motility was assessed as previously described [33]. Viability was assessed by red eosin exclusion test using eosin Y [32].

2.4 Measurement of cholesterol in the sperm culture medium

Cholesterol was measured in duplicate in the incubation medium from human spermatozoa by a cholesterol oxidase–peroxidase (CHOD–POD) enzymatic colorimetric method accordingly to the manufacturer's instructions (Inter-Medical Biogemina, Naples, Italy). For each sperm, sample culture media were recovered by centrifugation, lyophilized, and subsequently dissolved in 1 mL of reaction buffer. The samples were incubated for 10 min at room temperature, then the cholesterol content was measured spectrophotometrically at 505 nm. The cholesterol standard used was 2 g L^{-1}. The limit of sensitivity for the assay was 0.005 mg L^{-1}. Inter- and intra-assay variations were 0.04 and 0.03%, respectively. Cholesterol results are shown as mg per 10^7 spermatozoa.

2.5 Western blot analysis of sperm proteins

Each sperm sample treated as indicated was centrifuged for 5 min at 5000 × *g*. The pellet was resuspended in lysis buffer [22]. An equal amount of protein (80 μg) was boiled for 5 min and processed as previously described [33].

2.6 Triglyceride assay

Triglycerides were measured in duplicate as previously described [33] by a glycerol-3- phosphate oxidase–POD enzymatic colorimetric method according to the manufacturer's instructions (Inter-Medical). Data are presented as $\mu g/10^6$ spermatozoa.

2.7 Lipase activity assay

Lipase activity (Inter-Medical) was evaluated by the method of Panteghini et al. [34] based on the use of 1,2-*o*-dilauryl-rac-glycero-3-glutaric acid-(6′-methylresorufin) ester (DGGR) as substrate [33].

2.8 G6PDH activity

The G6PDH activity (Inter-Medical) was performed as previously described [32]. Data are expressed in nmol $min^{-1}/10^6$ spermatozoa. The enzymatic activity was determined with three control media: without glucose-6-phosphate as substrate, or without the coenzyme ($NADP^+$) and the third without either substrate or coenzyme (data not shown).

2.9 Measurement of glucose in the sperm culture medium

Glucose was measured in duplicate in the incubation medium from human spermatozoa by oxidase-POD reaction with a chromogen accordingly to the manufacturer's instructions (Inter-Medical). Ten microliters of the lysate were added to 1 mL of the buffer reaction and incubated for 10 min at room temperature. Then, the glucose content was measured at 500 nm using a spectrophotometer. Data are presented as $\mu g/10^6$ spermatozoa.

2.10 Statistical analysis

All data are presented as means ± SD for six experiments of six separate samples. Data were analyzed by two-way ANOVA test, using the GraphPAD Prism4 software (GraphPad Software, USA). Differences were considered statistically significant at $p < 0.05$.

3 Results

3.1 Effect of EGCG on human sperm motility and viability

We first determined flagellar sperm motility upon increasing concentrations of EGCG (2 μM, 20 μM, 60 μM) in human normozoospermic samples. Our data indicated that sperm motility was increased by EGCG at 2 and 20 μM (Fig. 1A), but not at higher concentration (60 μM). Similar results were obtained when we analyzed the effects of the same concentrations of EGCG on sperm viability (Fig. 1B).

It is reported that ECGC [35] is able to elicit antiestrogenic action [18, 19] at higher doses or coestrogenic for ER-α at lower doses. Since our previous studies [21] demonstrated that human sperm expresses the ERs mediating E2-induced capacitation and acrosome reaction in human sperm and aromatase, we hypothesized that both the "classical" ERs could be able to mediate EGCG action in sperm. Therefore, we pretreated the cells with ICI. This cotreatment abrogated the 20 μM EGCG effects either on sperm motility or viability (Fig. 1A and B) while no change was evidenced on 60 μM EGCG. Also, RU486 had no effect.

3.2 Double effects of EGCG on cholesterol efflux and protein tyrosine phosphorylation in human spermatozoa

We then investigated the influence of different concentrations of EGCG on sperm membrane cholesterol efflux and protein tyrosine phosphorylation [26, 27] in human normozoospermic samples. Our results showed that lower EGCG treatment (from 2 to 20 μM EGCG) increased the cholesterol efflux compared with untreated samples as shown in Fig. 2A, and ICI, but not RU486, abrogated 20 μM EGCG effect. No change was observed upon 60 μM EGCG also after ICI or RU 486.

It was reported that cholesterol efflux initiates signaling events leading to tyrosine phosphorylation of sperm proteins [26, 27]. In our study, it appears that an increase in the protein tyrosine phosphorylation was obtained upon EGCG, from 2 to 20 μM (Fig. 2B) and the combination of ICI markedly reduced the 20 μM EGCG action. On the contrary, treatment with higher EGCG dose produced a significant decrease of tyrosine phosphorylation compared with the untreated cells as indicated by densitometric evaluation.

3.3 EGCG modulates Src, Akt, and Bcl2 phoshorylation in human spermatozoa

We then evaluated the impact of EGCG on Src activity, evaluating the levels of tyrosine phosphorylation at position 139. The results of this study clearly showed that 2–20 μM EGCG significantly induced Src phosphorylation.

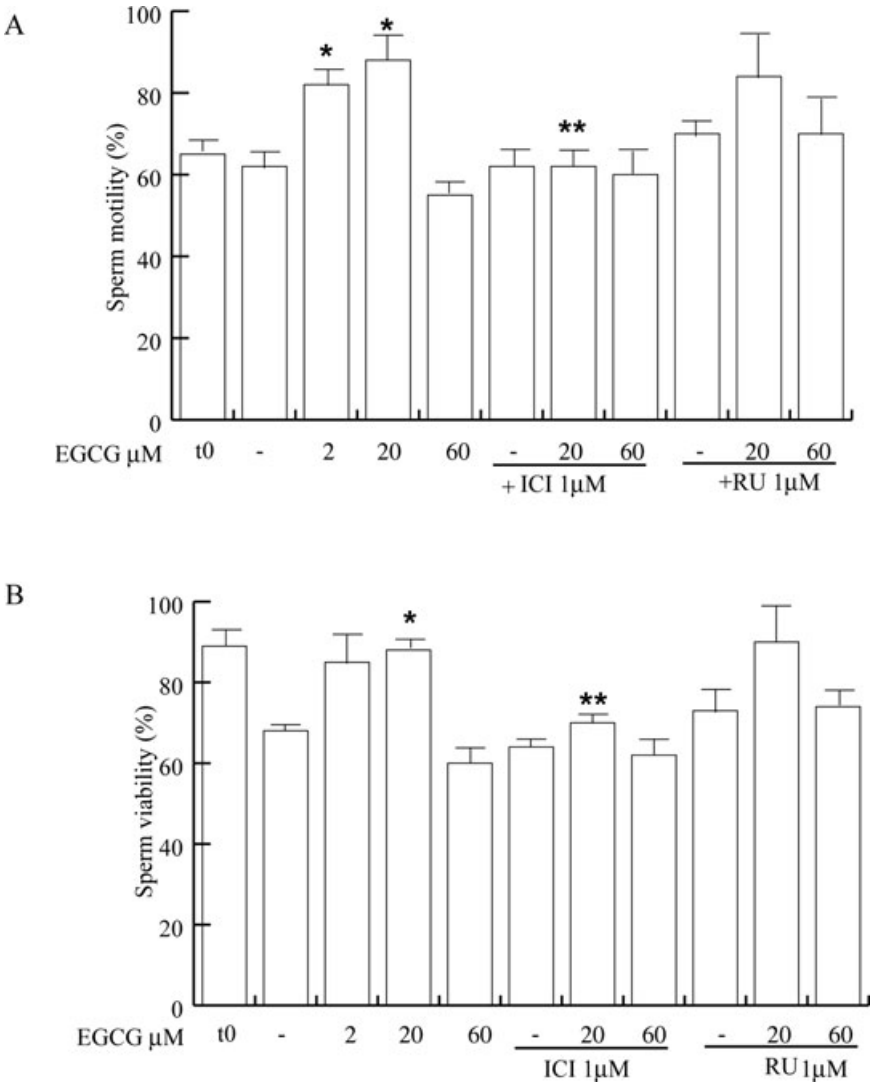

Figure 1. EGCG affects sperm motility and viability. Spermatozoa were incubated in unsupplemented Earle's medium (uncapacitating medium) for 30 min at 37°C and 5% CO_2, in the absence (−) or in the presence of increasing concentrations of EGCG, and/or ICI (1 μM) or RU486 (1 μM). Sperm motility (A) and viability (B) were assessed also at t0. *$p < 0.05$ versus untreated (−); **$p < 0.05$ versus 20 μM EGCG.

While RU486 cotreatment had no significant effect, the combination with ICI attenuated the 20 μM EGCG-induced effects (Fig. 3). At the opposite, high dose of EGCG reduced p-Src expression levels.

In order to provide further insights on the molecular action of EGCG, we also evaluated phosphorylation levels of key proteins controlling cell survival such as Akt and Bcl-2. Our findings indicate (Fig. 3) that EGCG at the concentration of 2–20 μM induced Akt protein phosphorylation and this disappear upon ICI cotreatment. At the concentration of 60 μM EGCG, Akt phoshorylation levels were reduced.

Furthermore, low concentrations of EGCG exposure enhanced Bcl-2 phosphorylation at Serine 70, which is a physiologically relevant phosphorylation site, necessary for a full and potent antiapoptotic function. This effect was greatly inhibited in the presence of ICI. All these results suggest that low concentrations of EGCG through ERs ameliorate survival in human sperm.

Although phosphorylation levels of the above-mentioned proteins were influenced by EGCG stimulus, the expression of total Akt and total Bcl-2 remains unchanged.

3.4 EGCG influences both lipid and glucose metabolism in human sperm

We investigated the effects of increasing stimuli of EGCG in the intracellular levels of triglycerides and lipase activity. A significant decrease in sperm triglycerides levels was observed (Fig. 4A) at the concentrations of 20 μM and ICI, but not RU486, reverted the effect. On the contrary, 60 μM EGCG did not influence tryglicerides levels either in the ICI or RU.

These results well correlate with data obtained on lipase activity that was significantly enhanced by 20 μM EGCG (Fig. 4B).

To gain more insight on sperm energy management, we evaluated the EGCG action on glucose metabolism. As shown

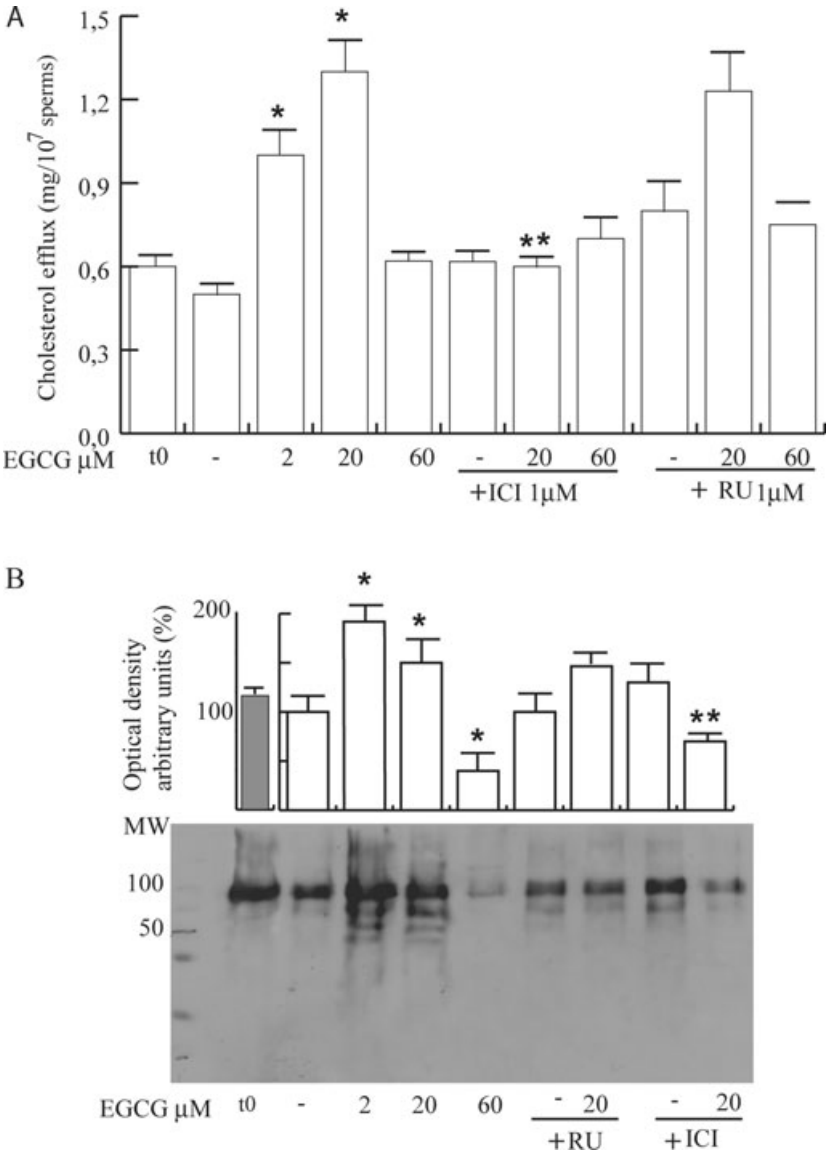

Figure 2. EGCG affects cholesterol efflux and protein tyrosine phoshorylation. Sperm cells were incubated in unsupplemented Earle's medium for 30 min at 37°C and 5% CO_2, in the absence (−) or in the presence of increasing concentrations of EGCG, and/or ICI (1 μM) or RU 486 (1 μM). Cholesterol efflux (A) was measured also at t0. $*p < 0.05$ versus untreated (−); $**p < 0.05$ versus 20 μM EGCG. (B) Sperm lysates were used for Western blot analysis performed to determine protein tyrosine phosphorylation. Representative Western blots of tyrosine phosphorylation are shown. Sperm cells were incubated in unsupplemented Earle's medium for 30 min at 37°C and 5% CO_2, in the absence (−) or in the presence of increasing concentrations of EGCG, and/or ICI (1 μM) or RU 486 (1 μM). Time 0 (t0). Densitometric analysis (mean ± SD) of the 95 kDa band/actin of six independent experiments performed. $*p < 0.05$ versus untreated (−),$**p < 0.05$ versus 20 μM EGCG. Autoradiograph presented is a representative example. MW, molecular weight marker.

in Fig. 5A, EGCG at low concentrations was effective to increase the enzymatic activity while at the high concentration (60 μM) did not produced significant change compared with the untreated samples. ICI cotreatment partially counteracted the above-described results obtained by 20 μM EGCG suggesting that other signaling pathways could be also involved in the regulation of sperm metabolism by EGCG.

These results were confirmed by the data obtained by evaluating the glucose levels (Fig. 5B).

4 Discussion

Although the bioactive component of green tea, EGCG, has received considerable attention [1–4] particularly as antiangiogenic and antitumor agent with chemopreventative properties, the effects on male fertilizing capacity are seldom studied. EGCG could offer a protective role against cell oxidative damage involved in the pathogenesis of male infertility [36] but besides to studies promoting the health benefits of green tea consumption [37], it is also known that EGCG has prooxidant potential [28, 38].

Hastak et al. [39] and Weinreb et al. [40] noted that low concentrations of EGCG induced an antiapoptotic pattern of gene expression thereby modulating cell survival. Whereas high concentrations of EGCG induced a proapoptotic pattern thereby modulating cell death in different cell models.

Numerous molecules are proposed to be the target of EGCG action and several studies demonstrated that green tea catechins can bind and downregulate ER-α and ER-β [35, 41], which are expressed from spermatogonia to spermatozoa [20, 21]. ERs mediate mammalian sperm capacitation,

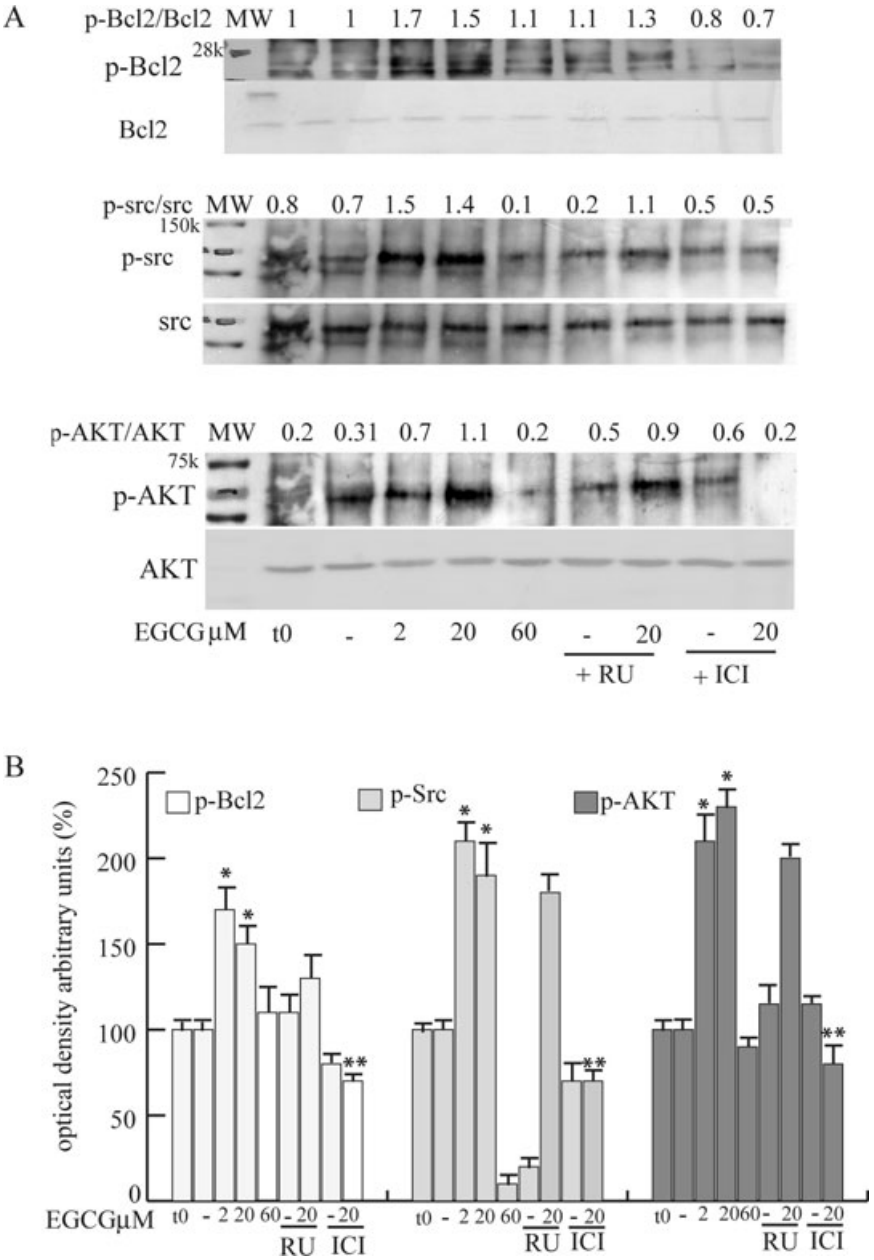

Figure 3. EGCG influences Src, Akt, and Bcl2 phosphorylation in sperm cells. Washed spermatozoa were incubated in uncapacitating medium for 30 min at 37°C and 5% CO_2, in the absence (−) or in the presence of increasing concentrations of EGCG, and/or ICI (1 μM) or RU 486 (1 μM). (A) Representative Western blots of p-Akt (p-Akt) and p-Bcl2 (pBcl2) and p-Src are shown. (B) Densitometric analysis (mean ± SD) of six independent experiments are reported as pSrc/Src, pAkt/Akt, and pBcl2/Bcl2 relative intensity. $*p < 0.05$ versus untreated (−); $**p < 0.05$ versus EGCG 20 μM.

acrosome reactions, and fertilizing ability stimulated by E2 and environmental estrogens, with the environmental estrogens being much more potent than E2 [23], suggesting our hypothesis that EGCG could influence sperm capacitation through ERs.

It is reported that EGCG, depending on concentrations, can exert estrogenic or antiestrogenic activities.

Particularly in HeLa cells expressing ectopic ER-α or ER-β, EGCG resulted in significant decreases in the E2-/ER-α-mediated signal while, at concentrations lower than 5 μM, resulted in an increase. On the other hand, catechins enhanced the E2-/ER-β-mediated luc activity at either of the concentrations tested [18, 19].

Further studies reported that relatively low concentration of EGCG could induce a pronounced ER-α re-expression in ER-α-negative breast cancer cells, suggesting that EGCG can reactivate the estrogen signal pathways via ER-α [42].

All these findings sustaining estrogenic and antiestrogenic dual properties of EGCG, support the results observed in the present study, in which we evidence the different effects of the catechin on the most relevant human spermatozoa functions for a successful fertilization. Specifically, we demonstrate for the first time that low concentrations of EGCG (2 and 20 μM) through ER increased motility, viability, and known hallmarks of sperm capacitation while high doses exert opposite actions. Our data are in agreement with

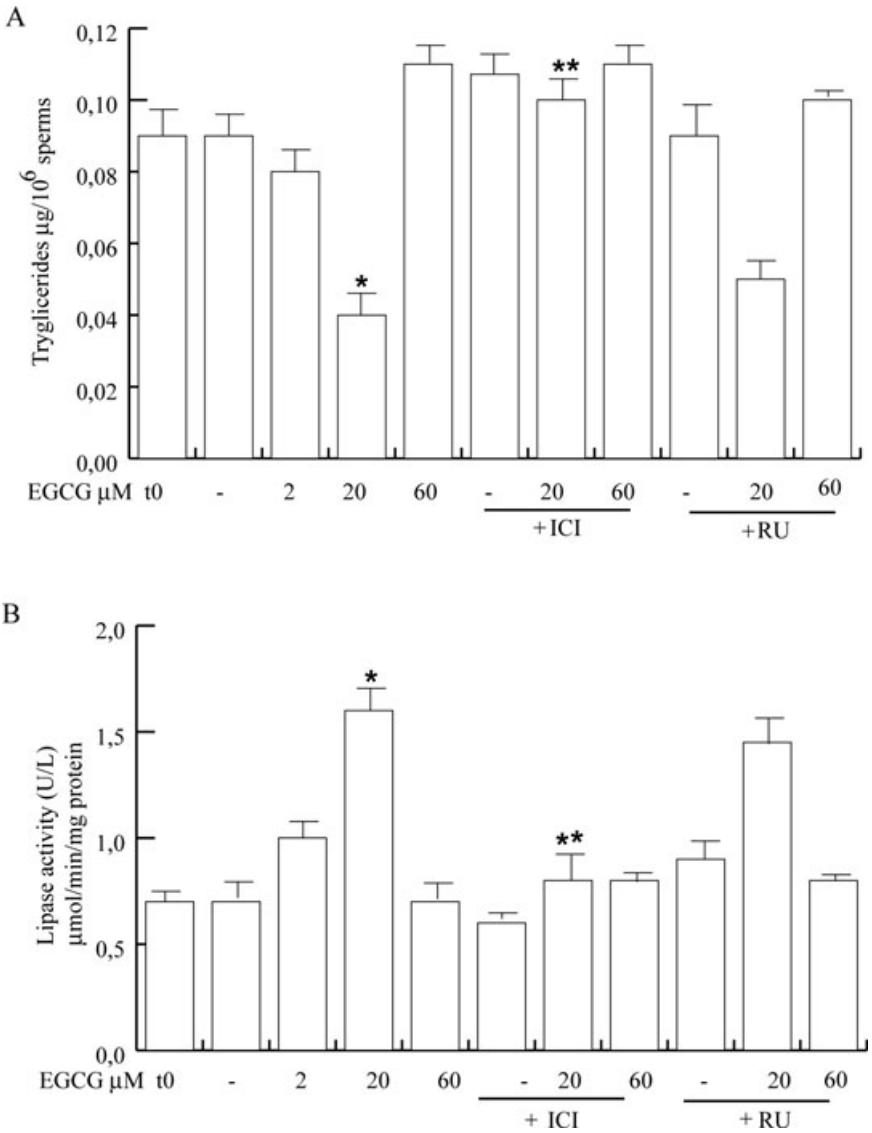

Figure 4. EGCG effects on lipid metabolism in human sperm. Washed spermatozoa were incubated in uncapacitating medium for 30 min at 37°C and 5% CO_2, in the absence (−) or in the presence of increasing concentrations of EGCG, and/or ICI (1 μM) or RU 486 (1 μM). Triglyceride content (A) and lipase activity (B) were determined also at t0. *$p < 0.05$ versus untreated (−); **$p < 0.05$ versus EGCG 20 μM.

previous report [38], although we also defined the molecular mechanisms.

During its life, mammalian spermatozoa goes through two different physiological conditions: uncapacitated condition, during which spermatozoa maturation occurs in a resting state accumulating and/or economizing energy substrates and the capacitated condition, which allows spermatozoa to achieve the final competence to fertilize the oocyte.

The process of sperm maturation, capacitation, and fertilization occurs in different molecular milieu provided by epididymis and female reproductive tract including oviduct. Specifically, sperm are exposed to estrogens within the male and female tract particularly in tubal fluid following follicle rupture and when in close vicinity to ovulated oocytes. A body of evidences reports that E2 and environmental estrogens induce both capacitation and acrosin activity in normal sperm [21, 23]. Our results demonstrate that 20 μM EGCG, mimicking a coestrogenic action, induces cholesterol efflux and this effect was abrogated by ICI cotreatment. Sixty micromolar EGCG exerted opposite action probably inducing oxidative cellular damage due to antiestrogenic performance. It has been suggested that similar compounds at high concentrations may be responsible for a variety of reproductive disturbances in men, including possible declines in sperm concentration [43, 44].

Proteins phosphorylation provides cells with a "switch" that can turn on or turn off the function of various proteins. Several studies have correlated the degree of tyrosine phosphorylation with the capacitative state of spermatozoa. Visconti et al. [26] observed a time-dependent increase in protein tyrosine phosphorylation of a set of specific proteins in the molecular range of 40–120 kDa, which was correlated with the capacitation state of spermatozoa [21]. Later studies reported that the protein tyrosine phosphorylation increases in spermatozoa during capacitation in various species [45].

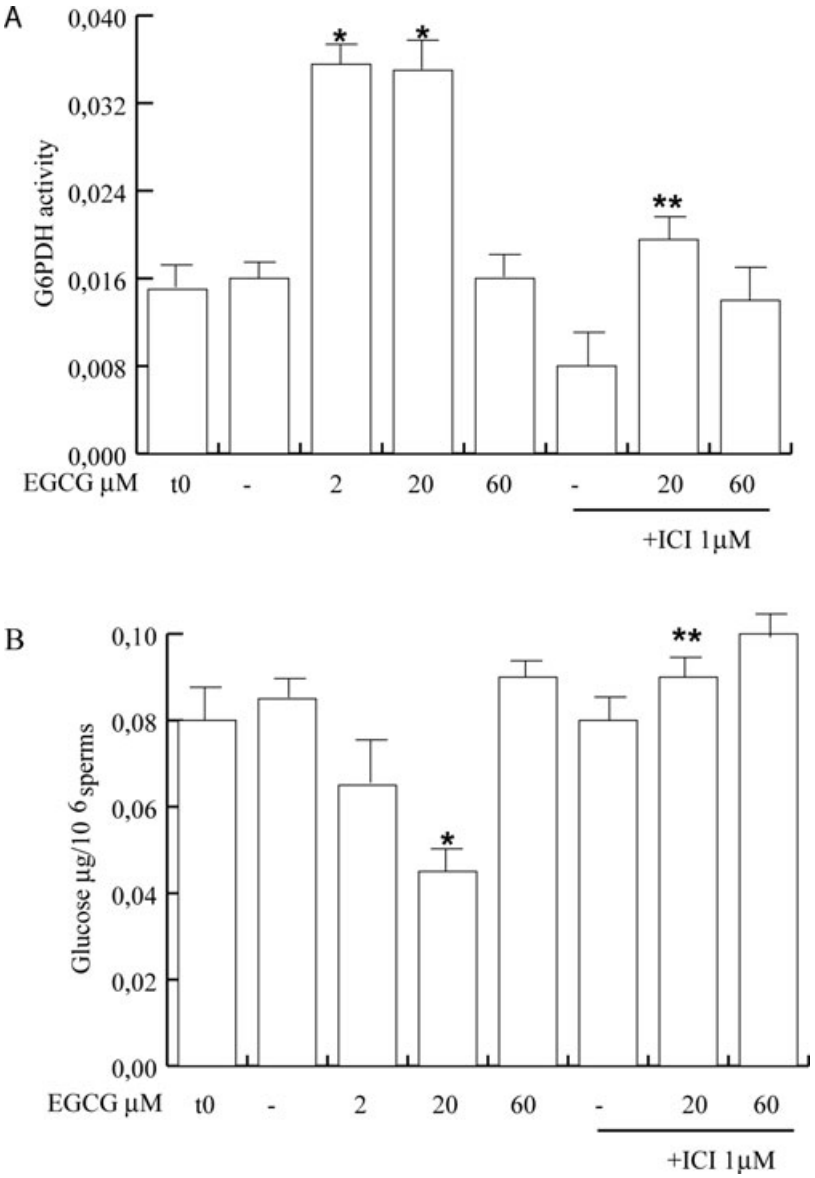

Figure 5. EGCG action on glucose metabolism in human sperm. Sperm samples, washed twice with an uncapacitating medium, were incubated in the same medium for 30 min at 37°C and 5% CO_2, and treated in the absence (−) or in the presence of increasing concentrations of EGCG, and/or ICI (1 μM). (A) The conversion of $NADP^+$ to NADPH catalyzed by G6PDH was measured by the increase of absorbance at 340 nm every 20 s for 1.5 min. The assay was performed also at t0. Data are expressed in nmol·min−1/10^6 spermatozoa, and represent mean ± SD. *$p < 0.05$ versus untreated (−); **$p < 0.05$ versus EGCG 20 μM. (B) Glucose content was determined also at t0, and data shown represent mean ± SD of six independent experiments each in duplicate. *$p < 0.05$ versus untreated (−); **$p < 0.05$ versus EGCG 20 μM.

We show that low concentrations of EGCG induced protein tyrosine phosphorylation indicating a stimulation of the adenylate cyclase/cAMP/PKA signaling, which plays a crucial role in capacitation [22]. Furthermore, treatment with both 20 μM EGCG and ICI, but not RU486, reversed the effect demonstrating that EGCG action is specifically mediated by ERs. This is not surprising since we previously demonstrated that ER activation induces tyrosine phosphorylation in human sperm [21]. At the opposite, after 60 μM EGCG exposure, we evidenced inhibition of tyrosine phoshorylation pattern, probably also related with cytotoxic effects due to the higher concentrations. The biphasic effects observed in our phoshorylation studies may be partly explained by the dual properties of EGCG evidenced in several studies demonstrating that EGCG, starting from concentrations of 50 μM [46] binds strongly to many molecules and affects a variety of enzyme activities via inhibition of protein phosphoylation thus inducing cell death.

In somatic cells, EGCG influences Src and AKT activity and these two kinases play an important role in capacitation, whereas Akt in survival [21, 47]. From our data, given the activation of Src and Akt by low concentrations of EGCG we may support, in part, beneficial effects of green tea consumption. Indeed, drinking 8–10 cups of green tea is sufficient to increase serum levels of EGCG into the low micromolar range investigated in our study, thus exerting increase of sperm motility and viability [48] necessary in female genital tract. The high concentrations of EGCG produced the drastic reduction of p-Src and p-Akt probably due to the generation of H_2O_2 in culture medium causing inhibition of phosphorylation of these proteins [46].

The interaction between energy balance and reproduction is subject of intensive investigations [29]. Capacitated sperm displays an increased metabolic rate and overall energy expenditure, presumably to affect the changes in sperm signaling and function during capacitation. For example a successful gamete fusion requires glucose to produce NADPH through the pentose phosphate pathway (PPP) [49]. From this point of view, we investigated whether the double action produced by the different concentration of EGCG on capacitated status, survival, and motility could involve specific changes in glucose and lipid metabolism.

EGCG has been shown to increase the expression of genes related to fat oxidation in the skeletal muscle [50] but data evidencing an influence on sperm metabolism are still lacking.

We found that low doses of the compound induced human sperm energy expenditure, by stimulating lipase activities, with a concomitant reduction of triglycerides levels. As for glucose metabolism, we observed an enhanced G6PDH activity at 2 and 20 μM EGCG, also addressing to an induction of energy consumption via ERs. These results well correlate with our previous data demonstrating that E2/ERs induce insulin secretion closely related with GDPDH activity [51].

Taken together all our data acquire more emphasis corroborating previous findings indicating that, at medium dosages, EGCG increases the number of porcine sperms that bind to ZP [38, 51]. We defined the molecular mechanisms of EGCG action on male fertilizing potential thus suggesting that EGCG may be an effective supplement for improvement in human ART.

In conclusion, in the present study, we demonstrate for the first time that tightly depending on the used concentration, EGCG/ERs are able to improve fertilization potential of the human male gamete, evidencing the specific effects on motility, viability, and energy expenditure in human sperm. This could be explained by the coestrogenic action upon low concentration of EGCG required for capacitation and the acrosome reaction. Paradoxically, the use of elevated concentrations of the antioxidant EGCG might instead has a negative effect on fertility due to antiestrogenic potential at high concentrations. Therefore, it cannot be totally excluded that excessive EGCG concentrations seem to be harmful for parameters related to reproduction.

This work was supported by MIUR Ex 60% – 2011.

The authors have declared no conflict of interest.

5 References

[1] Singh, B. N., Shankar, S., Srivastava, R. K., Green tea catechin, epigallocatechin-3-gallate (EGCG): mechanisms, perspectives and clinical applications. *Biochem. Pharmacol.* 2011, *82*, 1807–1821.

[2] Basu, A., Lucas, E. A., Mechanisms and effects of green tea on cardiovascular health. *Nutr. Rev.* 2007, *65*, 361–375.

[3] Hara, Y., Physiological functions of tea polyphenols: part 2. *Am. Biotechnol. Lab.* 1994, *12*, 18.

[4] Shapiro, H., Lev, S., Cohen, J., Singer, P., Polyphenols in the prevention and treatment of sepsis syndromes: rationale and pre-clinical evidence. *Nutrition* 2009, *25*, 981–997.

[5] Mukhtar, H., Ahmad, N., Green tea in chemoprevention of cancer. *Toxicol. Sci.* 1999, *52*, 111–117.

[6] Uesato, S., Kitagawa, Y., Kamishimoto, M., Kumagai, A. et al., Inhibition of green tea catechins against the growth of cancerous human colon and hepatic epithelial cells. *Cancer Lett.* 2001, *170*, 41–44.

[7] Takada, M., Nakamura, Y., Koizumi, T., Toyama, H. et al., Suppression of human pancreatic carcinoma cell growth and invasion by epigallocatechin-3-gallate. *Pancreas* 2002, *25*, 45–48.

[8] Ahmad, N., Feyes, D. K., Nieminen, A. L., Agarwal, R. et al., Green tea constituent epigallocatechin-3-gallate and induction of apoptosis and cell cycle arrest in human carcinoma cells. *J. Natl. Cancer Inst.* 1997, *89*, 1881–1886.

[9] Salucci, M., Stivala, L. A., Maiani, G., Bugianesi, R. et al., Flavonoids uptake and their effect on cell cycle of human colon adenocarcinoma cells (Caco2). *Br. J. Cancer* 2002, *86*, 1645–1651.

[10] Chen, C., Shen, G., Hebbar, V., Hu, R. et al., Epigallocatechin-3-gallate-induced stress signals in HT-29 human colon adenocarcinoma cells. *Carcinogenesis* 2003, *24*, 1369–1378.

[11] Hsu, S., Yu, F. X., Huang, Q., Lewis, J. et al., A mechanism-based in vitro anticancer drug screening approach for phenolic phytochemicals. *Assay Drug Dev. Technol.* 2003, *1*, 611–618.

[12] Naasani, I., Oh-Hashi, F., Oh-Hara, T., Feng, W. Y. et al., Blocking telomerase by dietary polyphenols is a major mechanism for limiting the growth of human cancer cells in vitro and in vivo. *Cancer Res.* 2003, *63*, 824–830.

[13] Divi, R. L., Doerge, D. R., Inhibition of thyroid peroxidase by dietary flavonoids. *Chem. Res. Toxicol.* 1996, *9*, 16–23.

[14] Sakamoto, Y., Mikuriya, H., Tayama, K., Takahashi, H. et al., Goitrogenic effects of green tea extract catechins by dietary administration in rats. *Arch. Toxicol.* 2001, *75*, 591–596.

[15] Kao, Y. H., Hiipakka, R. A., Liao, S., Modulation of endocrine systems and food intake by green tea epigallocatechin gallate. *Endocrinology* 2000, *141*, 980–987.

[16] Figueiroa, M. S., César Vieira, J. S., Leite, D. S., Filho, R. C. et al., Green tea polyphenols inhibit testosterone production in rat Leydig cells. *Asian J. Androl.* 2009, *11*, 362–370.

[17] Fang, H., Tong, W., Shi, L. M., Blair, R. et al., Structure-activity relationships for a large diverse set of natural, synthetic, and environmental estrogens. *Chem. Res. Toxicol.* 2001, *14*, 280–294.

[18] Belguise, K., Guo, S., Sonenshein, G. E., Activation of FOXO3a by the green tea polyphenol epigallocatechin-3-gallate induces estrogen receptor alpha expression reversing invasive phenotype of breast cancer cells. *Cancer Res.* 2007, *67*, 5763–5770.

[19] Farabegoli, F., Barbi, C., Lambertini, E., Piva, R., (−)-Epigallocatechin-3-gallate downregulates estrogen receptor alpha function in MCF-7 breast carcinoma cells. *Cancer Detect. Prev.* 2007, *31*, 499–504.

[20] Hess, R. A., Bunick, D., Bahr, J. M., Sperm, a source of estrogen. *Environ. Health Perspect.* 1995, *103*, 59–62.

[21] Aquila, S., Sisci, D., Gentile, M., Middea, E. et al., Estrogen receptor (ER) alpha and ER beta are both expressed in human ejaculated spermatozoa: evidence of their direct interaction with phosphatidylinositol-3-OH kinase/Akt pathway. *J. Clin. Endocrinol. Metab.* 2004, *89*, 1443–1451.

[22] Aquila, S., Sisci, D., Gentile, M., Middea, E. et al., Human ejaculated spermatozoa contain active P450 aromatase. *J. Clin. Endocrinol. Metab.* 2002, *87*, 3385–3390.

[23] Adeoya-Osiguwa, S. A., Markoulaki, S., Pocock, V., Milligan, S. R. et al., 17beta-Estradiol and environmental estrogens significantly affect mammalian sperm function. *Hum. Reprod.* 2003, *18*, 100–107.

[24] Aquila, S., Sisci, D., Gentile, M., Carpino, A. et al., Towards a physiological role for cytochrome P450 aromatase in ejaculated human sperm. *Hum. Reprod.* 2003, *8*, 1650–1659.

[25] Suarez, S. S., Control of hyperactivation in sperm. *Hum. Reprod.* 2008, *14*, 647–657.

[26] Visconti, P. E., Westbrook, V. A., Chertihin, O., Demarco, I. et al., Novel signaling pathways involved in sperm acquisition of fertilizing capacity. *J. Reprod. Immunol.* 2002, *53*, 133–150.

[27] Travis, A. J., Kopf, G. S., The role of cholesterol efflux in regulating the fertilization potential of mammalian spermatozoa. *J. Clin. Invest.* 2002, *110*, 731–736.

[28] Isbrucker, R. A., Edwards, J. A., Wolz, E., Davidovich, A. et al., Safety studies on epigallocatechin gallate (EGCG) preparations. Part 3: teratogenicity and reproductive toxicity studies in rats. *Food Chem. Toxicol.* 2006, *44*, 651–661.

[29] Chehab, F. F., Leptin as a regulator of adipose mass and reproduction. *Trends Pharmacol. Sci.* 2000, *21*, 309–314.

[30] Andò, S., Aquila, S., Arguments raised by the recent discovery that insulin and leptin are expressed in and secreted by human ejaculated spermatozoa. *Mol. Cell. Endocrinol.* 2005, *256*, 49.

[31] World Health Organization, *WHO Laboratory Manual for the Examination and Processing of Human Semen*, 5th edn. Cambridge University Press, Cambridge, UK 2010.

[32] Aquila, S., Gentile, M., Middea, E., Catalano, S. et al., Autocrine regulation of insulin secretion in human ejaculated spermatozoa. *Endocrinology* 2005, *146*, 552–557.

[33] Aquila, S., Guido, C., Laezza, C., Santoro, A. et al., A new role of anandamide in human sperm: focus on metabolism. *J. Cell. Physiol.* 2009, *221*, 147–153.

[34] Panteghini M., Bonora R., Pagani F, Measurement of pancreatic lipase activity in serum by a kinetic colorimetric assay using a new chromogenic substrate. *Ann. Clin. Biochem.* 2001, *38*, 365–370.

[35] Goodin, M. G., Fertuck, K. C., Zacharewski, T. R., Rosengren, R. J., Estrogen receptor-mediated actions of polyphenolic catechins in vivo and in vitro. *Toxicol. Sci.* 2002, *69*, 354–361.

[36] Lombardo F., Sansone A., Romanelli F., Paoli D. et al., The role of antioxidant therapy in the treatment of male infertility: an overview. *Asian J. Androl.* 2011, *13*, 690–697.

[37] Webb, T., Green tea experiments in lab, clinic yield mixed results. *J. Natl. Cancer Inst.* 2000, *92*, 1038–1039.

[38] Spinaci M., Volpe S., De Ambrogi M., Tamanini C., Galeati G., Effects of epigallocatechin-3-gallate (EGCG) on in vitro maturation and fertilization of porcine oocytes. *Theriogenology* 2008, *69*, 877–885.

[39] Hastak, K., Gupta, S., Ahmad, N., Agarwal, M. K. et al., Role of p53 and NF-kappaB in epigallocatechin-3-gallate-induced apoptosis of LNCaP cells. *Oncogene* 2003, *22*, 4851–4859.

[40] Weinreb, O., Mandel, S., Youdim, M. B., Gene and protein expression profiles of anti- and pro-apoptotic actions of dopamine, R-apomorphine, green tea polyphenol (−)-epigallocatechine-3-gallate, and melatonin. *Ann. NY Acad. Sci.* 2003, *993*, 351–361.

[41] Kuruto-Niwa, R., Inoue, S., Ogawa, S., Maramatsu, M. et al., Effect of tea catechins on the ERE-regulated estrogenic activity. *J. Agric. Food Chem.* 2000, *48*, 6355–6361.

[42] Li, Y., Yuan, Y. Y., Meeran, S. M., Tollefsbol, T. O.. Synergistic epigenetic reactivation of estrogen receptor-α (ER-α) by combined green tea polyphenol and histone deacetylase inhibitor in ER-α-negative breast cancer cells. *Mol. Cancer* 2010 *14*, 274.

[43] Sharpe, R. M., Hormones and testis development and the possible adverse effects of environmental chemicals. *Toxicol. Lett.* 2001, *120*, 221–232.

[44] Skakkebaek, N. E., Rajpert-De Meyts, E., Main, K. M., Testicular dysgenesis syndrome: an increasingly common developmental disorder with environmental aspects. *Hum. Reprod.* 2001, *16*, 972–978.

[45] Bragado, M. J., Gil, M. C., Martin-Hidalgo, D., Hurtado de Llera, A. et al., Src family tyrosine kinase regulates acrosome reaction but not motility in porcine spermatozoa. *Reproduction.* 2012, *144*, 67–75.

[46] Fujiki, H., Suganuma, M., Okabe, S., Sueoka, N. et al., Cancer inhibition by green tea. *Mutat. Res.* 1998, *402*, 307–310.

[47] Aquila, S., Middea, E., Catalano, S., Marsico, S. et al., Human sperm express a functional androgen receptor: effects on PI3K/AKT pathway. *Hum. Reprod.* 2007, *22*, 2594–2605.

[48] Lee, M. J., Maliakal, P., Chen, L., Meng, X. et al., Pharmacokinetics of tea catechins after ingestion of green tea and (−)-epigallocatechin-3-gallate by humans: formation of different metabolites and individual variability. *Cancer Epidemiol. Biomarkers Prev.* 2002, *11*, 1025–1032.

[49] Urner, F., Sakkas, D., Characterization of glycolysis and pentose phosphate pathway activity during sperm entry into the mouse oocyte. *Biol. Reprod.* 1999, *60*, 973–978.

[50] Sae-tan, S., Grove, K. A., Kennett, M. J., Lambert, J. D., (−)-Epigallocatechin-3-gallate increases the expression of genes related to fat oxidation in the skeletal muscle of high fat-fed mice. *Food Funct.* 2011, *2*, 111–116.

[51] Guido, C., Perrotta, I., Panza, S., Middea, E. et al., Human sperm physiology: estrogen receptor alpha (ER-α) and estrogen receptor beta (ER-β) influence sperm metabolism and may be involved in the pathophysiology of varicocele-associated male infertility. *J. Cell Physiol.* 2011, *226*, 3403–3412.

RESEARCH ARTICLE

In vitro mechanism for downregulation of ER-α expression by epigallocatechin gallate in ER+/PR+ human breast cancer cells

Francesca De Amicis[1,2], Alessandra Russo[1], Paola Avena[1], Marta Santoro[1], Adele Vivacqua[2], Daniela Bonofiglio[1,2], Loredana Mauro[3], Saveria Aquila[1,2], Donatella Tramontano[4], Suzanne AW Fuqua[5] and Sebastiano Andò[1,2,3]

[1] Centro Sanitario, University of Calabria, Arcavacata di Rende (CS), Italy
[2] Department of Pharmaco-Biology, University of Calabria, Arcavacata di Rende (CS), Italy
[3] Department of Cellular Biology, University of Calabria, Arcavacata di Rende (CS), Italy
[4] Department of Cellular and Molecular Pathology "L. Califano", University of Naples "Federico II", Italy
[5] Lester and Sue Smith Breast Center, Baylor College of Medicine, Houston, TX, USA

Received: August 20, 2012
Revised: October 24, 2012
Accepted: December 5, 2012

Scope: Exposure of the breast to estrogens and other sex hormones is an important cancer risk factor and estrogen receptor downregulators are attracting significant clinical interest. Epigallocatechin gallate (EGCG), a polyphenolic compound found in green tea, has gained considerable attention for its antitumor properties. Here we aimed to investigate the molecular mechanisms through which EGCG regulates ER-α expression in ER+ PR+ breast cancer cells.
Material and methods: Western blotting analysis, real-time PCR, and transient transfections of deletion fragments of the ER-α gene promoter show that EGCG downregulates ER-α protein, mRNA, and gene promoter activity with a concomitant reduction of ER-α genomic and nongenomic signal. These events occur through $p38^{MAPK}$/CK2 activation, causing the release from Hsp90 of progesterone receptor B (PR-B) and its consequent nuclear translocation as evidenced by immunofluorescence studies. EMSA, and ChIP assay reveal that, upon EGCG treatment, PR-B is recruited at the half-PRE site on ER-α promoter. This is concomitant with the formation of a corepressor complex containing NCoR and HDAC1 while RNA polymerase II is displaced. The events are crucially mediated by PR-B isoform, since they are abrogated with PR-B siRNA.
Conclusion: Our data provide evidence for a mechanism by which EGCG downregulates ER-α and explains the inhibitory action of EGCG on the proliferation of ER+ PR+ cancer cells tested. We suggest that the EGCG/PR-B signaling should be further exploited for clinical approach.

Keywords:
Estrogen receptor / Hsp90 / p38MAPK / Progesterone receptor

1 Introduction

Breast cancer risk factors, such as early age at menarche, late age at menopause, postmenopausal hormone therapy, and high BMI are thought to affect breast carcinogenesis by increasing the lifetime exposure of the breast to estrogens and other sex hormones [1]. Estrogens particularly are mitogenic to breast epithelial cells, and since the effects of estrogens are mediated by both estrogen receptors (ER-α and ER-β), the magnitude of their effects may be determined by the individual levels of ERs expressed in the breast.

Upregulated ER-α expression in mice produces ductal hyperplasia, lobular hyperplasia, and ductal carcinoma in situ, demonstrating the consequences of unregulated ER-α levels at all stages of breast cancer development [2]; in contrast ER-βs act to regulate the degree of estrogen action by negatively modulating ER-α, and the estrogen-independent transcriptional activity of ER-β isoforms is inhibited by ER-α [3]. Further evidence shows that ER-α levels in both hyperplastic lesions and ER-positive tumors are greatly elevated as compared with adjacent normal tissue [4]. Therefore, it is

Correspondence: Professor Sebastiano Andò, Centro Sanitario-University of Calabria, Arcavacata di Rende (CS) 87030, Italy
E-mail: sebastiano.ando@unical.it
Fax: +39-0984-496203

Abbreviations: CDKs, cyclin dependent kinases; **CS**, charcoal-stripped; **EGCG**, Epigallocatechin gallate; **FBS**, fetal bovine serum; **HDACs**, histone deacetylases; **IP**, immunoprecipitation; **ISK**, Ishikawa endometrial cancer cells; **MAPKs**, mitogen-activated protein kinases; **PR-B**, progesterone receptor B; **WB**, Western blotting

not surprising that elevated levels of ER-α in benign breast epithelium is, itself, considered a risk factor for progression to invasive breast disease [5].

The strong correlation between ER-α expression, breast disease pathophysiology, and therapeutic response has justified the use of estrogen receptor downregulators as attractive intervention, with significant clinical interest in their use. In this regard, many naturally occurring compounds, commonly present in the diet have gained considerable attention as well [6, 7]. In recent years, epigallocatechin gallate (EGCG), a polyphenolic compound found in green tea, has demonstrated chemopreventative and antitumor properties [8].

Epidemiological studies have suggested that green tea consumption is linked to a decrease in the incidence and recurrence of breast cancer [9]. Additionally, treatment with EGCG (50 mg/kg/day, 14 days) reduced the growth of MCF-7 implanted breast tumors in athymic nude mice by 40% [10], and it has been reported that catechin inhibited the proliferation of human breast cancer cells in vitro [11]. This is partly attributable to its effects on modulating the activity of mitogen-activated protein kinases (MAPKs), IGF/IGF-1 receptor, AKT, NF-κB, and CDKs [12, 13]. EGCG also inhibits growth factor receptor extracellular signaling, the proteasome, mitochondrial depolarization, and fatty acid synthase [14–16].

Recent studies report that the antitumor activity of EGCG is mediated by targeting HSP70 and HSP90 in vitro and in vivo, through a mechanism that involves direct binding of EGCG to the *C*-terminal region of HSP90 [17], a chaperone protein that is constitutively expressed at high levels in many cancer cells. HSP90 is assembled into heterocomplexes with unliganded steroid receptors, such as GR and PR, thus influencing their cellular distribution and activity [18].

Particularly recent studies on breast cancer models have implicated EGCG in the regulation of ER-α. Since the catechin family is structurally similar to isoflavones, it has been shown that catechins, such as EGCG, were co-estrogenic for ER-α at lower doses (<5 μM) but antiestrogenic at higher doses (100–150 μM) and eliciting a concomitant massive cell death at the higher levels [11, 19].

In the present study, we report that EGCG produces a significant inhibition of ER+ PR+ breast cancer cell proliferation and we define the molecular mechanisms associated with this growth effect. Concomitant with nuclear localization of PR, EGCG treatment causes a downregulation of ER-α protein, mRNA, and gene promoter activity. We demonstrate that these effects are crucially mediated by progesterone receptor B (PR-B) via its recruitment to the ER-α proximal promoter.

2 Materials and methods

2.1 Materials

Epigallocatechin 3 gallate (EGCG), aprotinin, leupeptin, phenylmethylsulfonyl fluoride, and sodium orthovanadate were from Sigma (Milan, Italy). PD 169316 and TBB from Calbiochem (Darmstadt, Germany). ICI 182 780 (ICI, ER antagonist) was purchased from Zeneca Pharmaceuticals (Cheshire, UK). Antibodies used in this study were GAPDH, laminin B, NCoR, RNA Pol II, HDAC1, total p38, phosphorylated p38, ER-α, PR-B, EGFR, Raf1, Her2, Hsp90, CK2 from Santa Cruz Biotechnology (Santa Cruz, CA, USA); progesterone receptors (PR-B, PR-A), total MAPK, total AKT, phosphorylated p42/44 MAPK (Thr202/Tyr 204), and pAKT (Ser437), from Cell Signaling Technology (Beverly, MA, USA).

2.2 Cell Culture

Cells utilized in the studies were obtained from American Type Culture Collection (Manassas, VA, USA). MCF-7 and T47D, were cultured as described [20]. Ishikawa endometrial cancer cells (ISK) were maintained in DMEM without phenol red supplemented with 10% fetal bovine serum (FBS). SkBr3 cells were cultured in RPMI1640 with 10% FBS. Treatments were performed, after 48 h of serum starvation, in 1% dextran charcoal stripped (CS) FBS to reduce steroid concentration [20].

2.3 MTT assay

Cells (3×10^4 cells/mL) were plated in 24-well plates and serum-starved for 48 h before the addition of treatment for 4 days. The MTT assay was performed as the following: 100 μL of MTT (2 mg/mL) (Sigma Aldrich, Milan, Italy) were added to each well, and the plates were incubated for 2 h at 37°C. Then, 500 μL of DMSO were added. The absorbance was measured with the Ultrospec 2100 Prospectrophotometer (Amersham-Biosciences, Milan, Italy) at a test wavelength of 570 nm.

2.4 Anchorage-independent growth assays

T47D cells (5000/well) were plated in 4 mL of 0.35% agarose with 5% CS FBS in phenol red free media, on a 0.7% agarose base in 6-well plates. Two days after plating, media containing control vehicle or hormonal treatments was added to the top layer, and the appropriate media was replaced every 2 days. After 14 days, 150 μL of MTT was added to each well and allowed to incubate at 37°C for 4 h. Plates were then placed in 4°C overnight and colonies ≥50 μm diameter from triplicate assays were counted. Data are the mean colony number of three plates and representative of two independent experiments analyzed for statistical significance ($p < 0.05$) using a two-tailed student's test, performed by Graph Pad Prism 5 (GraphPad Software, San Diego, CA, USA). SDs are shown.

2.5 Plasmids

XETL [21], the wild-type human ER-α (HEGO) [22], the full-length PR-B consisting of the full-length PR-B cDNA fused with the SV40 early promoter (a gift from Dr. D. Picard, University of Geneve, Switzerland) [20], the PR DNA-binding mutant C587A (mDBD PR) previously described by Faivre et al. [23] (gift from Dr. C. Lange, University of Minnesota Cancer Center, Minneapolis, MN, USA), the full-length PR-A [24], and the deletion fragments of the ER-α gene promoter [25]. The Renilla luciferase expression vector pRL-TK (Promega, Milan, Italy) was used as a transfection standard.

2.6 Reverse transcription and real-time PCR

Cells (6×10^6) were treated as indicated and processed as described [26]. cDNA diluted were analyzed in triplicates by real-time PCR in an iCycler iQ Detection System (Bio-Rad, USA). The primers were: (ER-α forward) 5′-AGAGGGCATGGTGGAGATCTT-3′; (ER-α reverse) 5′-CAAACTCCTCTCCCTGCAGATT -3′; (pS2 forward) 5′-TTCTATCCTAATACCATCGACG-3′; (pS2 reverse) 5′-TTTGAGTAGTCAAAGTCAGAGC-3′; (IRS1 forward) 5′-AGGATATTTAATTTGCCTCGG-3′; (IRS1 reverse) 5′-AAGCGTTTGTGCATGCTCTTG-3′; (CD1 forward) 5′-TCTAAGATGAAGGAGACCATC-3′; (CD1 reverse) 5′-GCGGTAGTAGGACAGGAAGTTGTT-3′; (18S forward) 5′-GGCGTCCCCCAACTTCTTA-3′ (18S reverse) 5′-GGGCATCACAGACCTGTTATT-3′.

2.7 Western blotting (WB) and immunoprecipitation

Protein expression or complex formation were assessed as described [27] by Western blotting (WB) or immunoprecipitation (IP) followed by WB, using total protein lysates, cytoplasmic, or nuclear protein lysates, where appropriate. Cells (6×10^6) were harvested to be analyzed using 500 μL of lysis buffer containing 50 mmol/L HEPES (pH 7.5), 150 mmol/L NaCl, 1%b Triton X-100, 1.5 mmol/L MgCl2, 10 mmol/L EGTA (pH 7.5), 10% glycerol, and inhibitors (0.1 mmol/L Na3VO4, 1% PMSF, and 2.0 mg/mL aprotinin) to obtain cytoplasmic proteins. After the collection using a scraper, incubation of 30′ on ice, we lysed the nuclei for 15′ at 4°C using 250 μL of nuclear buffer containing 20 mmol/L HEPES (pH 8), 0.1 mmol/L EDTA, 5 mmol/L MgCl2, 0.5 mol/L NaCl, 20% glycerol, 1% NP-40, and inhibitors (1.7 mg/mL aprotinin, 1 mg/mL leupeptin 200 mmol/L PMSF, 200 mmol/L sodium orthovanadate, and 100 mmol/L sodium fluoride). Then lysates were collected and centrifuged at 10 000 × *g* for 10′ at 4°C.

For total protein extracts, 500 μL RIPA buffer (50 mM Tris-HCl, pH 7.4, 150 mM NaCl, 1% NP-40, 0.25% Na deoxycholate, plus inhibitors 1.7 mg/mL aprotinin, 1 mg/mL leupeptin 200 mmol/L PMSF, 200 mmol/L sodium orthovanadate, and 100 mmol/L sodium fluoride) was added to the 100 mL cell culture plate for 15′ at 4°C. Then lysates were collected and centrifuged at 10 000 × *g* for 10′ at 4°C. The protein content was determined using Bradford dye reagent (Bio-Rad). For WB, 50 μg of total, cytoplasmic or nuclear lysates were separated on an 11% polyacrylamide denaturing gel (SDS-PAGE) and transferred to nitrocellulose membranes. Proteins of interest were detected with specific Abs, recognized by peroxidase-coupled secondary Abs, and developed using the ECL Plus Western Blotting detection system (Amersham Pharmacia Biotech, UK). For IP, 500 μg of protein of cytoplasmic or nuclear lysates were precleared for 1 h with protein A/G-agarose (Santa Cruz), incubated with primary Abs at 4°C for 18 h in HNTG buffer (20 mmol/L HEPES, pH 7.5, 150 mmol/L NaCl, 0.1% Triton X-100, 10% glycerol, and 0.1 mmol/L Na3VO4), and then the antigen–Ab complexes were precipitated with protein A/G agarose for 2 h in HNTG buffer. The immunoprecipitated proteins were washed three times with HNTG buffer, separated on SDS-PAGE, and processed by WB. The images were acquired by using an Epson Perfection scanner (Epson, Japan) using Photoshop software (Adobe). The optical densities of the spots were analyzed by using ImageJ software (NIH; http://rsb.info.nih.gov/IJ). Images are representative of three different experiments.

2.8 Immunofluorescence

T47D cells seeded on glass cover-lips were treated with 40 μM EGCG for 12 h, washed with PBS, and then fixed with 4% paraformaldehyde in PBS for 20 min at room temperature. Next, cells were permeabilized with 0.2% Triton X-100 in PBS for 5 min, blocked with 5% BSA for 30 min, and incubated with anti-PR-B antibody (1:50) in PBS overnight at 4°C. The day after the cells were washed three times with PBS and incubated with the secondary antibody anti-rabbit IgG-FITC (1:200) for 1 h at room temperature. To check the specificity of immunolabeling, the primary antibody was replaced by normal rabbit serum (negative control). The blue-fluorescent DAPI was used for nuclear stain. Immunofluorescence analysis was carried out on an OLYMPUS BX51 microscope using a ×40 objective. Images are representative of three different experiments.

2.9 Transfections and luciferase assays

Transfections were done as described [20] using Fugene 6 reagent (Roche Diagnostics, Milan, Italy). Luciferase activity was measured with the Dual Luciferase kit (Promega, Milan, Italy). Results represent mean of luciferase activities observed in three independent experiments done in triplicate.

2.10 Site-directed mutagenesis

Mutagenesis was performed on Fragment D of the ER-α promoter using the QuikChange mutagenesis kit (Stratagene, La Jolla, CA, USA) following the manufacturer's

instructions. The sequence for the sense primer was: 5′-AGCAGGGAGATGAGGATTGCTGAAGTCCATGGGGGT ATGT-3′. The plasmids were then sequenced to confirm the mutation of the desired site.

2.11 Lipid-mediated transfection of siRNA duplexes

Custom-synthesized siRNA (Invitrogen) annealed duplexes (25-bp double-stranded RNA) were used for effective depletion of PR-B. A nonspecific siRNA (NS) (Invitrogen) that lacked identity with known gene targets was used as a control for nonsequence-specific effects. Cells were transfected using Lipofectamine 2000 reagent (Invitrogen, Paisley, UK) according to the manufacturer's instructions and then treated as indicated.

2.12 Electrophoretic mobility shift assay (EMSA)

EMSA was carried out as previously described [25], with a few modifications. Cells were treated for 6 h before harvesting for the assay. The sequence of ER-α-half-PRE oligonucleotide used as probe or the unlabeled competitor was 5′- AGGATTGTGTTCTCCATGGG -3′, mutated 5′-AGGATTGTTAAGTCCATGGG-3′. To test specific binding, nuclear extracts were pre-incubated with rabbit polyclonal PR antibody or normal rabbit IgG. The reactions were separated on 6% polyacrylamide gel in 0.25× Tris borate–EDTA for 3 h at 150 V. Images are representative of three different experiments.

2.13 Chromatin immunoprecipitation (ChIP) assays

Cells were treated for 12 h before harvesting for the assay performed as described [28]. ER-α promoter primers used for PCR: forward, 5′-ACGTTCTTGATCCAGCAGGGTA-3′ and reverse, 5′-ACCTGCCAAATTATATGCAAATGGCAG-3′ containing the half-PRE site; and forward, 5′-GTGGCCATTGTTGACCTACAG- 3′ and reverse, 5′-CTGTAGGTCAACAATGGCCAC-3′ upstream the half-PRE site. Images are representative of three different experiments.

2.14 Statistical analysis

Each datum point represents the mean ± SD of three different experiments. Data were analyzed by Student's *t*-test using the GraphPad Prism 4 software program. $p < 0.05$ was considered as statistically significant.

3 Results

3.1 EGCG treatment decreases ER+ PR+ cancer cell proliferation

We first investigated whether EGCG affects cancer cell proliferation following extended treatments with low doses of the catechin. We tested ER+ PR+ breast cancer cell lines, including T47D cells, which are known to express ER-α and elevated levels of endogenous PRs [20], MCF-7 cells that express ER-α and low levels of PR, and a well-differentiated ER+ PR+ human endometrial adenocarcinoma cell line (Ishikawa cells). Proliferating cells were exposed to different nontoxic concentrations of EGCG (10 μM; 20 μM; 40 μM) and then analyzed in MTT growth assays (Fig. 1A). After 4-day treatment, 10 μM EGCG inhibited basal cell proliferation of both T47D (50%), and MCF-7 (20%). With increasing doses of EGCG (20 and 40 μM), T47D cell number was further reduced by 52 to 67%, respectively. MCF-7 (25–50%) and ISK (55–68%) cells growth was also significantly decreased. EGCG inhibitory action was still present after pre-treatment with 1 μM ICI 182 780, a potent and specific antagonist with excellent growth inhibitory effects in several cell and animal models of human breast cancer, which induce ER-α degradation through ubiquitin-mediated mechanism [29]. This suggests that growth inhibition was not mediated by binding of EGCG to ER.

Of note is that the antiproliferative effects produced by EGCG occur earlier in T47D cells with respect of those observed in MCF-7 and ISK. Consistent with MTT assay results, 40 μM EGCG treatment also markedly reduced basal and E2-induced colony formation of T47D cells growing in soft agar (Fig. 1B).

3.2 EGCG downregulates ER-α expression and transcriptional activity

It is well known that increased expression of ER-α is an early event in breast carcinogenesis, driving breast cancer cell proliferation. We thus hypothesized that EGCG's effects in ER-α-positive breast cancer cells could involve the regulation of ER-α itself. As shown in Fig. 2A, ER-α protein expression levels were decreased after 24 h of increasing EGCG concentrations, in MCF-7 and T47D. E2 treatment was used as control for downregulation of ER-α.

To investigate the functional effects of downregulation of ER-α by EGCG, we next analyzed ER-α genomic activity after treatment. To this aim, a luciferase reporter plasmid containing a consensus estrogen-responsive element (XETL) was transiently transfected into MCF-7 cells. EGCG treatment caused a significant decrease of basal, and with more intensity of E2-induced luciferase activity (sevenfold) (Fig. 2B). To confirm these results, we also evaluated mRNA levels of known estrogen-regulated genes, such as IRS1, pS2, and cyclin D1 (CD1). As assessed by real-time PCR, EGCG at 40 μM significantly decreased basal and E2-induced levels (Fig. 2C) of IRSI, pS2, and cyclin D1 in T47D and MCF-7 cells.

Stemming from our evidence that EGCG inhibited ER-α levels, we hypothesized that it could also influence E2/ER-α nongenomic rapid effects within seconds to minutes [30]. Therefore to demonstrate the effects of EGCG on E2-induced nongenomic activity, we pretreated T47D cells with EGCG for

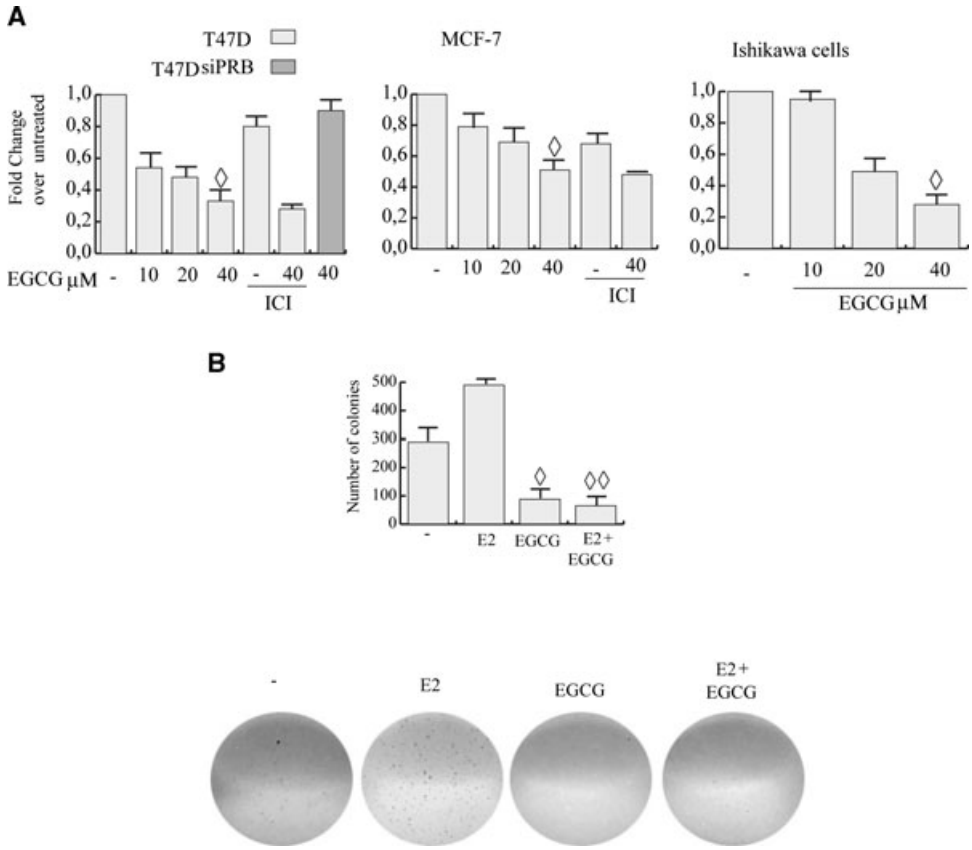

Figure 1. EGCG inhibits ER+ PR+ cancer cell proliferation (A) MTT assay. Cells, serum starved, were exposed to vehicle (−), or 1 μM ICI and/or different concentrations of EGCG in medium containing 1% dextran charcoal-stripped FBS for 4 days (treatments were renewed every 2 days). Results indicate mean of three independent experiments done in triplicate; *bars* SD; ◊ $p < 0.05$ compared with untreated cells. (B) EGCG blocks E2-induced anchorage independent growth of T47D. Soft agar colony formation assay was performed in control conditions (−), or in the presence of 10 nM estrogen (E2) and/or 40 μM EGCG. Cells were allowed to grow for 14 days and the number of colonies ≥50 μm were quantified. *bars* SD; ◊ $p < 0.05$ compared with untreated cells; ◊◊ $p < 0.05$ compared with E2-treated cells. Pictures at the bottom show typical well for each condition.

24 h causing ER-α levels to decrease, and subsequently we treated the same cells with short exposures to E2. As shown in Fig. 2D, EGCG treatment blocked E2-induced phosphorylation of MAPK and AKT. Five percent CS treatments were used as positive controls for activation of downstream signaling.

The ERK/MAPK and PI3K/AKT signaling pathways that are rapidly activated by the ER-α–E2 complex, also have critical roles in estrogen action as survival agents. In fact, these pathways enhance the expression of the anti-apoptotic protein Bcl-2 and block the activation of p38 kinase [31]. Western blot analysis in MCF-7 cells revealed that p38MAPK phosphorylation was significantly upregulated in EGCG-exposed cells, effectively opposing estrogen's effect (Fig. 2D). These results suggest that EGCG-induced ER-α downregulation can affect nongenomic events in the E2/ER-α signaling cascade.

3.3 EGCG downregulates ER-α mRNA via a region between −2769 and −1000 bp of its promoter

To further investigate the molecular basis for regulation of ER-α expression by EGCG, we examined its effects on ER-α mRNA levels in T47D and MCF-7, treated for 24 h. EGCG (20 μM and 40 μM) significantly downregulated ER-α as assessed by real-time-PCR (Fig. 2E). Since EGCG downregulated ER-α mRNA, we next evaluated whether it could act at the level of gene transcription through regulatory regions within the ER-α promoter. Therefore, we examined the ER-α promoter region covered from −4100 bp to +212 bp first with a bioinformatics approach using the NCBI Genome database (www.ncbi.nlm.nih.gov). The region examined in this study contains multiple regulatory elements, including binding sites for AP-1, NF-κB, Oct-1, Sp1, CCAAT-binding proteins, CREB-2, USF1, half PRE [20, 25]. Five overlapping ER-α promoter deletion constructs, −245 bp to +212 bp (A), −735 bp to +212 bp (B), −1000 bp to +212 bp (C), −2769 bp to +212 bp (D), and −4100 bp to +212 bp (E), all relative to the first transcriptional ATG start site (depicted in Fig. 3A) and previously described [25], were transiently transfected into T47D and MCF-7 cells and the data are shown as relative promoter activity in luciferase units (Fig. 3B). We found that 40 μM EGCG had no effect on the promoter activity of fragments A, B, or C. In contrast, it reduced the activity of fragments D and E by 44% and 40%, respectively, indicating that the region between −2769 and −1000 bp may be responsible for downregulation of ER-α promoter activity after EGCG treatment.

Precisely within this region of ER-α promoter, we also previously reported the presence of a functional half-PRE site responsible for transcriptional repression of ER-α mediated by the B isoform of the PR [20]. Green tea polyphenols have

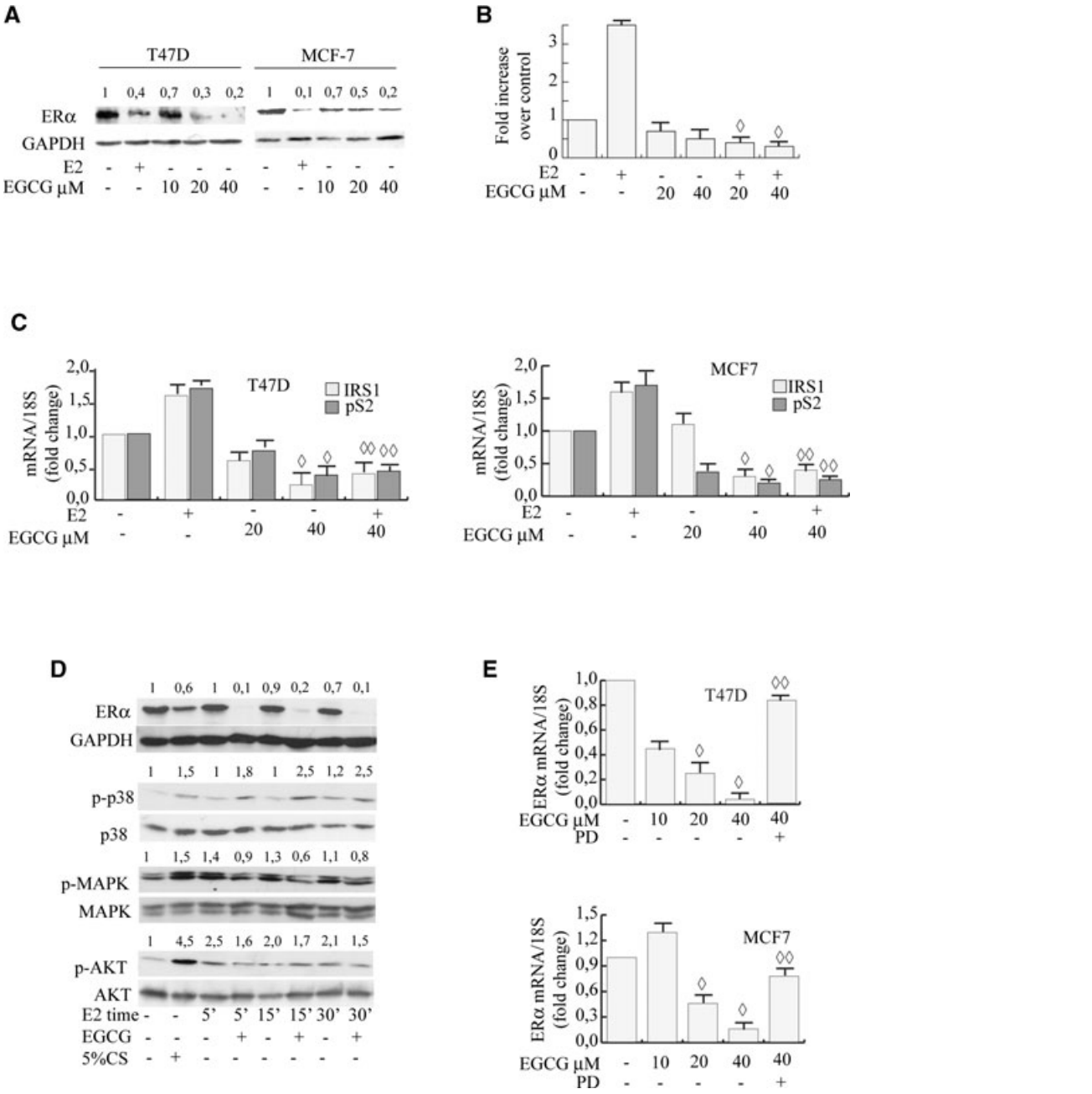

Figure 2. EGCG downregulates ER-α expression, genomic and nongenomic signal (A) Immunoblot analysis. Cells were treated with different concentrations of EGCG for 24 h. The whole-cell lysates obtained were then collected and analyzed by WB using specific Abs. Numbers represent the average fold change in ER-α and GAPDH levels. (B) ERE luciferase reporter assay. XETL was transiently transfected into MCF-7 cells treated with vehicle (−) or 10 nM E2 and/or different concentrations of EGCG. Cells were then harvested, and luciferase activities were determined; *Columns,* mean of relative luciferase units (RLU); *bars* SD; ◊, $p < 0.05$ compared with E2. (C) Real-time PCR assay. mRNA expression of pS2, IRS1, and CD1 in T47D and MCF-7 cells treated with vehicle (−) or 10 nM E2 and/or different concentrations of EGCG for 24 h; 18S was determined as a control. Graphs are the mean of three independent experiments run in triplicate; *bars* SD;◊ $p < 0.05$ compared with untreated cells; ◊◊ $p < 0.05$ compared with E2-treated cells. (D) Immunoblot analysis. T47-D cells pretreated with 40 μM EGCG for 24 h were then treated with 10 nM E2 for different times as indicated or with 5% CS for 24-h treatment. The whole-cell lysates obtained were then collected and analyzed by WB using specific Abs. Numbers represent the average fold change in ER-α and GAPDH, p-p38 and p38, p-MAPK and MAPK, p-AKT, and AKT levels E, Real-time PCR assay. mRNA expression of ER-α. Cells were treated with vehicle (−), different concentrations of EGCG for 24 h as indicated in presence or absence of PD. *Columns* mean of three independent experiments; *bars*, SD. ◊, $p < 0.05$ compared with untreated cells, ◊◊, $p < 0.05$ compared with 40 μM EGCG.

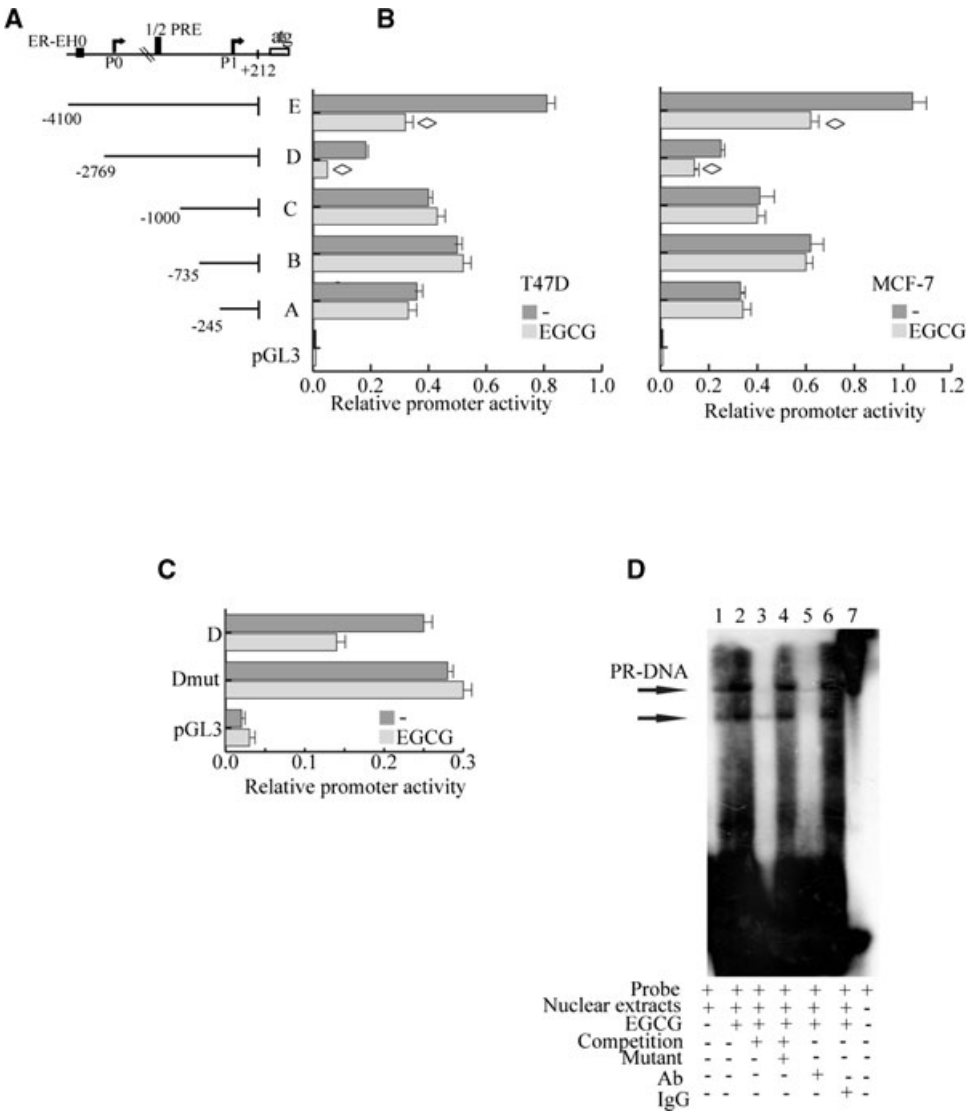

Figure 3. EGCG downregulates ER-α promoter activity through a half-PRE site. (A) Schematic representation of deletion fragments of the ER-α gene promoter. Fragments coordinates are expressed relative to the primary transcription start site. (B) Promoter activity of the ER-α 5′−flanking region. Constructs depicted in panel A were transiently transfected in T47D and MCF-7 cells, treated with vehicle (−) or 40 μM EGCG. After 24 h, cells were harvested and luciferase activities were determined; *bars*, SD; ◇, $p < 0.05$ compared with untreated cells. (C) Site-directed mutagenesis of the half-PRE site present in D fragment. Fragment D and fragment D mut promoter constructs were cotransfected into MCF-7 cells, and promoter activity was assessed in the absence or presence of 40 μM EGCG; *bars*, SD. (D) EMSA assay. Nuclear extracts from T47-D cells treated with vehicle (-, lane 1) or 40 μM EGCG (lanes 2–6) were incubated with an ER-α promoter/half-PRE annealed probe (lane 2) or, for competition analysis, 100-fold excess unlabeled annealed probe (lane 3), or mutated in half-PRE site (lane 4). EGCG-treated nuclear extracts were also incubated with anti-PR-Bffibf (lane 5), IgG (lane 6), or probe alone (lane 7). Picture is representative of three independent experiments.

been reported to exert their biological effects through steroid receptors [15]; therefore, we hypothesized that EGCG downregulatory effects on ER-α gene transcription might involve this potential half-PRE site. To test this hypothesis, we next used site-directed mutagenesis to alter this site. Mutation of 3 bp of the half-PRE site of the ER-α promoter D fragment resulted in the loss of EGCG-responsiveness, suggesting that this half-PRE site could be an effector of EGCG signaling (Fig. 3C).

To investigate DNA–protein interactions induced by EGCG within this promoter region, we next performed EMSA, using oligonucleotide from the ER-α promoter sequence bearing the half-PRE site (Fig. 3D). Cell extracts prepared in the absence of ligand (lane 1) generated double retarded bands corresponding to half-PRE complexes that were enhanced in EGCG-treated extracts (lane 2), and whose appearance was effectively competed by a 100-fold molar excess of unlabeled probe (lane 3), thus demonstrating the specificity of the DNA-binding complexes. This inhibition was no longer observed using a mutated half-PRE oligonucleotide as competitor (lane 4). A rabbit antibody to PR also completely disrupted the DNA-protein complexed bands (lane 5) while normal rabbit IgG addition did not affect protein–DNA complex formation (lane 6).

3.4 EGCG inhibits Hsp90 client proteins and promotes PR-B translocation into the nucleus

The functions of PR are modulated by Hsp90 and its inhibition can be measured via the degradation of its many client proteins (such as c-Raf and Her2) [32]. As shown in Fig. 4A, we observed depletion of Hsp90 client proteins EGFR, Raf-1, and Her 2 after EGCG treatment.

Thus, we characterized the effects of EGCG on protein interaction between PR and Hsp90, performing co-IP assay

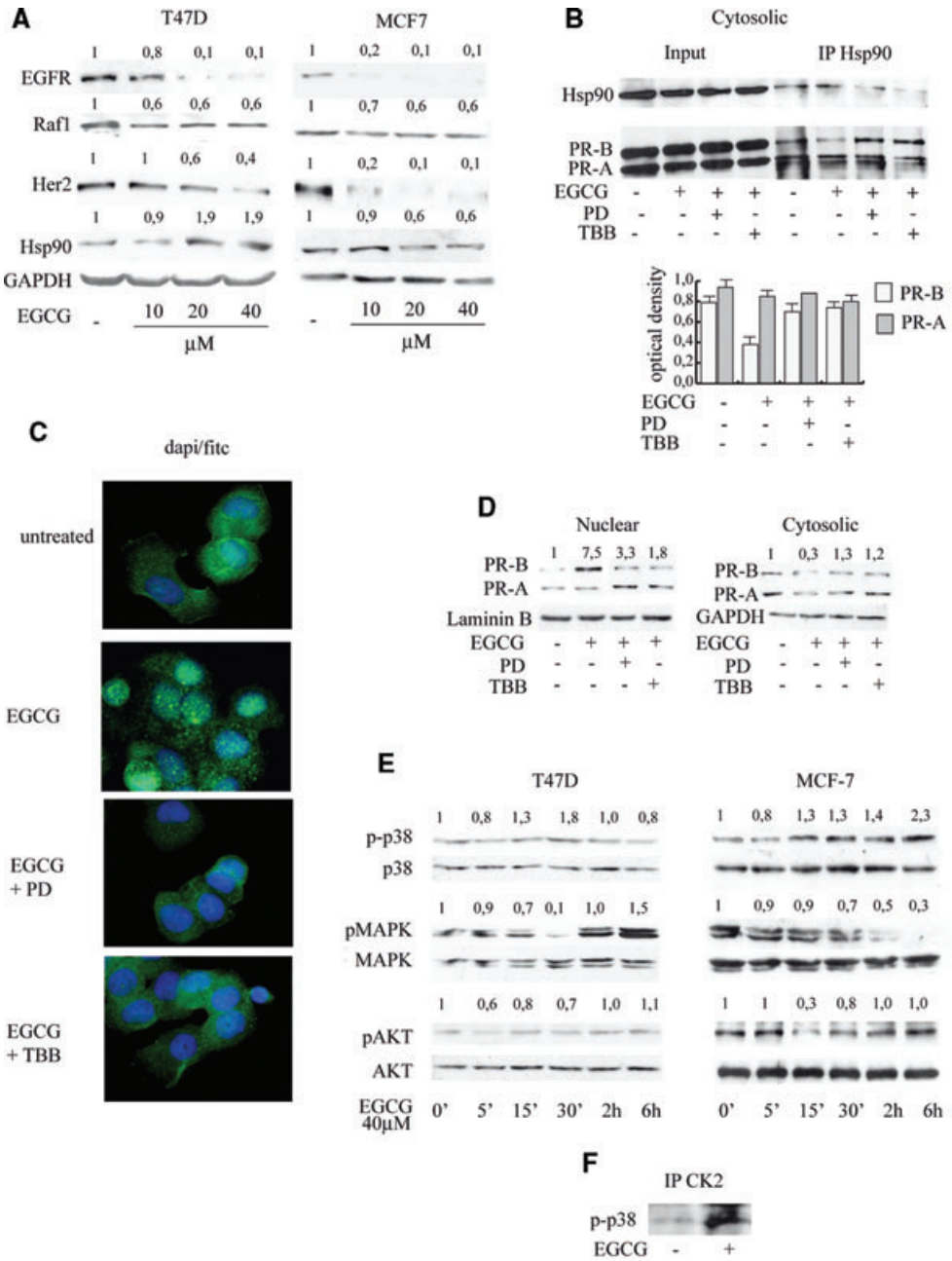

Figure 4. EGCG inhibits Hsp90 client proteins and promotes PR translocation into the nucleus *via* p38MAPK activation (A) Immunoblot analysis. Cells were treated with different concentrations of EGCG for 24 h. The whole-cell lysates obtained were then collected and analyzed. Numbers represent the average fold change in EGFR or Raf1 or Her2 or Hsp90 and GAPDH levels (B) Co-immunoprecipitation assay. T47-D cells were treated for 24 h with vehicle (−) or 40 μM EGCG in presence or absence of PD or TBB. Cytosolic cell lysates were immunoprecipitated using anti-Hsp90 and then blotted with anti-Hsp90 or anti-PR antibody. *Columns*, mean of three independent experiments in which band intensities were evaluated in terms of optical density arbitrary units and expressed as IP/input; *bars*, SD;◇ $p < 0.05$ compared with untreated cells. (C) Immunofluorescence with anti-PR-B antibody. T47-D cells were treated for 12 h with vehicle (−) or 40 μM EGCG in presence or absence of PD or TBB, then were stained (DAPI/FITC merge is presented). Immunofluorescent receptor is cytoplasmic in absence of treatment but shifted into the nucleus after EGCG administration. Pictures are representative of three independent experiments (D) Immunoblot analysis. Cells were treated with 40 μM of EGCG for 12 h in presence or absence of PD or TBB, then nuclear and cytoplasmic protein extracts were analyzed. Numbers represent the average fold change in PR-B and Laminin B or GAPDH levels. (E) Immunoblot analysis. Cells were treated with vehicle (−) or 40 μM EGCG at different times as indicated. The whole-cell lysates obtained were then collected and analyzed. Numbers represent the average fold change in p-p38 and p38, p-MAPK and MAPK, p-AKT, and AKT levels. (F) Co-immunoprecipitation assay. Cells were treated for 24 h with vehicle (−) or 40 μM EGCG. Cell lysates were immunoprecipitated using anti-CK2 and then blotted with anti-p-p38.

from T47D cells cytosolic extracts. EGCG reduced the specific interactions between PR-B isoform and Hsp90 (Fig. 4B), while it did not affect PR-A/Hsp90 complex. We also investigated the influence of EGCG treatment on PR-B cellular localization by immunofluorescence microscopy experiments using a specific antibody. As shown in Fig. 4C, PR-B showed both a light nuclear and a stronger cytoplasmic distribution in untreated T47D cells. Interestingly, when cells were exposed to 40 μM EGCG, there was a remarkable redistribution of the PR-B from the cytosol to the nucleus. Results confirmed, by WB analysis of isolated cellular compartments (Fig. 4D), that the PR-B nuclear isoform was specifically influenced by EGCG (7.5-fold nuclear versus 0.3-fold cytoplasmic).

Therefore, we next examined the effects of a short treatment of EGCG on the activation of kinase cascades. As shown in Fig. 4E, 40 μM EGCG at different times modulated basal levels of p42/p44 MAPK and pAKT depending upon the cell type. At 15′, in both cell types, EGCG induced p38MAPK phosphorylation, which remained activated in MCF-7 cells even after 24 h of treatment (data not shown). An important effector of p38MAPK is CK2 [33]. IP assays revealed that EGCG treatment enhanced a physical interaction between CK2 and p-p38 (Fig. 4F).

Stemming from these results, we next investigated the relevance of activated p38 in triggering the effects of EGCG treatment, by using a p38 inhibitor PD169316, known to block the p38 kinase activity [34]. Pretreatment with PD or with the CK2 inhibitor TBB, strongly restored the specific interaction between Hsp90 and PR-B (Fig. 4B) indicating that activation of p38/CK2 signaling by ECGC modulates Hsp90/PR-B interaction.

Moreover, PD and TBB clearly changed the cellular localization of PR-B produced by EGCG (Fig. 4C and D) demonstrating that EGCG via p38/CK2 allows PR nuclear translocation; furthermore, PD attenuated ER-α mRNA downregulation by EGCG (Fig. 2E).

3.5 Downregulation of ER-α expression by EGCG is dependent on PR-B

We next investigated the role of the PR-B isoform in mediating EGCG effects on ER-α. We co-transfected equal amounts of expression plasmids encoding PR-B or PR-A into the ER-PR-negative SKBR3 cell line, along with the ER-α promoter reporter fragments. Only PR-B reduced ER-α promoter activity (51%) with EGCG treatment (Fig. 5A). Co-transfection of equal amounts of expression plasmids encoding either the PR-A isoform or the PR mutant with a disrupted DNA-binding domain (Cys587 to Ala, called mDBD PR) did not affect ER-α promoter activity either in presence or absence of EGCG, strongly suggesting that PR-B was responsible for EGCG downregulatory effects on ER-α, which occur at the transcriptional level.

We also performed PR-B siRNA knockdown experiments during EGCG treatment of T47D cells. Addition of a PR-B-targeting siRNA resulted in a remarkable decrease in PR-B protein levels (Fig. 5B) that greatly blocked ER-α downregulation by EGCG treatment. PR-B knockdown also blocked the growth inhibitory effect of EGCG in MTT assays (Fig. 1A). Altogether these data strongly support the hypothesis that PR-B through the half-PRE site within the ER-α promoter mediates EGCG effects on transcriptional regulation of ER-α.

3.6 The NCoR co-repressor is recruited with PR-B brk to the ER-α promoter upon EGCG treatment

To demonstrate the recruitment of PR to the ER-α gene promoter, we also used ChIP assays. T47D and MCF-7 cells were exposed to either control vehicle or 40 μM EGCG, after which chromatin was cross-linked with formaldehyde, and protein–DNA complexes were immunoprecipitated with antibodies directed against PR, RNA polymerase II, or the co-repressors NCoR, DAX-1, and SMRT. Results obtained demonstrate an enhanced recruitment of PR to the ER-α promoter with EGCG treatment (Fig. 5C); as a control we did not see recruitment to an unrelated ER-α promoter region located upstream of the half-PRE site (data not shown). Specific knockdown of PR-B also confirmed the recruitment of this isoform to the ER-α promoter (Fig. 5C).

Concomitant with the increased recruitment of PR-B to the ER-α promoter after EGCG treatment, we saw the similar molecular events we described previously [20]: displacement of RNA polymerase II, indicating that the chromatin in this region is probably in a less permissive environment for gene transcription, recruitment of NCoR in T47D and MCF7 cells (Fig. 5C). Since it is known that different co-repressor complexes contain one or more HDACs, as candidate mediators of PR action [35] we looked for histone deacetylases, in particular the class I HDAC-1 and HDAC-3. Our results show that HDAC-1 was the most strongly recruited following EGCG treatment. These data indicate PR-B binds to the ER-α promoter at half-PRE site and this results in enhancement of the tripartite complex containing NCoR and HDAC1 with EGCG treatment and a concomitant release of RNAPol II, thereby inhibiting ER-α transcription. Thus the catechin may acquire pharmacological significance acting as an estrogen receptor downregulator in breast cancer cells.

To further address the interaction between PR-B, HDAC1, and NCoR, we performed co-IP assays from nuclear extracts of T47D cells. EGCG induced the complex formation between PR-B, NCoR, and HDAC1 (Fig. 5D) via p-38/CK2, since pretreatment with PD or TBB prevented the interaction upon EGCG.

4 Discussion

Epidemiological studies have shown that breast cancer incidence rates are lowest among Asians, suggesting that Asian

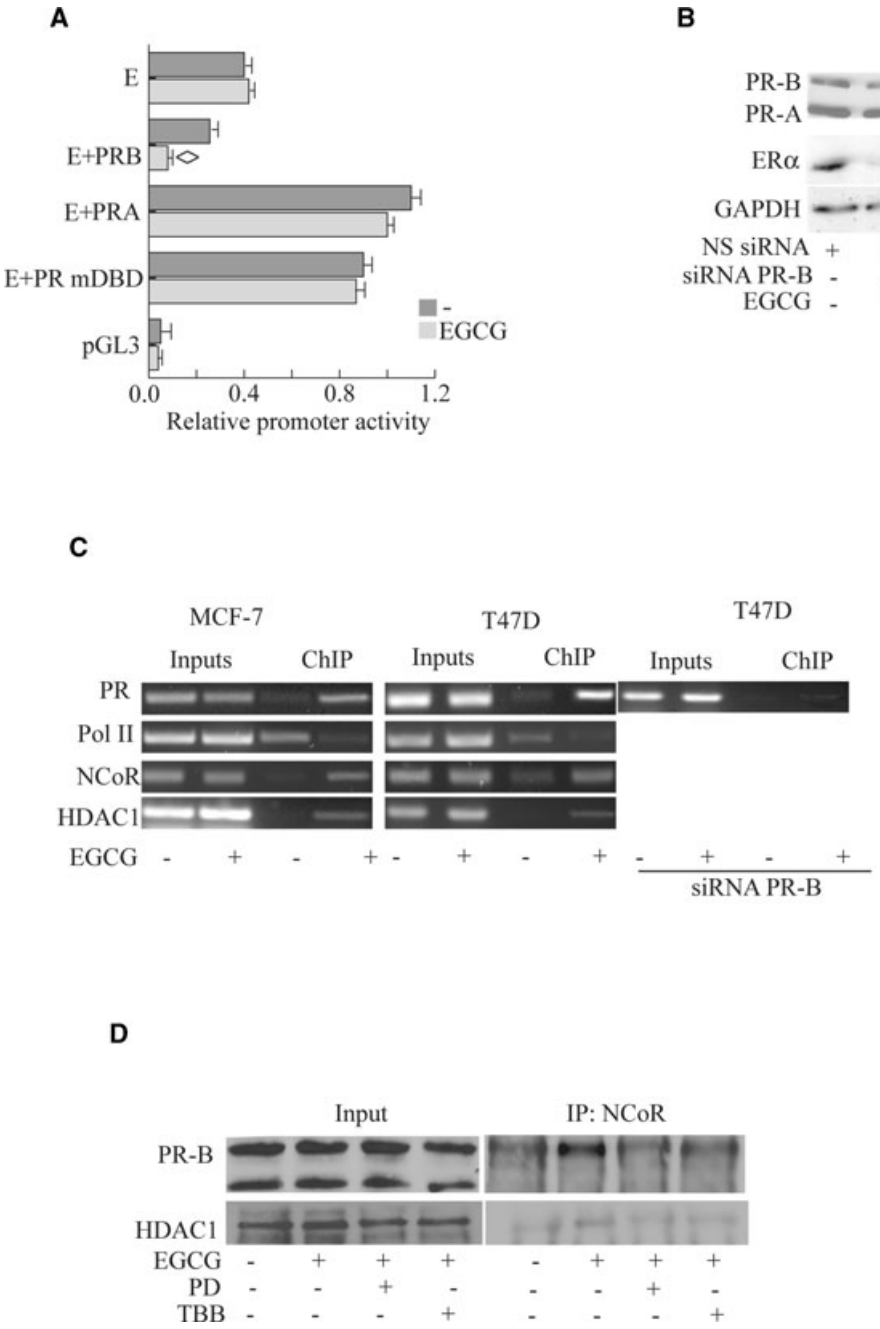

Figure 5. PR-B mediates the EGCG effects on ER-α promoter and recruits an NCoR corepressor complex A, Promoter activity of the ER-α 5′−flanking region. Fragment E was transiently transfected into Skbr3 cells in the presence or absence of full-length PR-B, or PR-A, or mDBD PR expression plasmid, then treated with 40 μM EGCG or left untreated. After 24 h, cells were harvested, and luciferase activities were determined; *bars,* SD $p < 0.05$ compared with untreated cells (B) Immunoblot analysis.T47-D cells were transfected with NS siRNA or targeted against PR-B and treated with vehicle (−) or 40 μM EGCG. (C) ChIP assay. Cells were treated for 12 h with vehicle (−) or 40 μM EGCG and then harvested. Antibodies used to immunoprecipitate the protein–DNA complex are indicated on the left. PCR primers encompass half-PRE site within the ER-α promoter. Results are representative of three independent experiments. (D) Coimmunoprecipitation assay. T47-D cells were treated with vehicle (−) or 40 μM EGCG in presence or absence of PD or TBB. Nuclear cell lysates were immunoprecipitated using anti-NCoR and then blotted with anti-PR or anti-HDAC1 antibody.

diets may contain phytochemicals with antibreast cancer activities. Accumulating clinical evidence indicates the protective effects of polyphenols derived from green tea in ER+/PR+/HER2− breast tumor patients [36], while recent in vitro studies demonstrate their specific cytotoxicity toward breast cancer cells regardless of their ER status [37]. This could be due to the use of high doses of phytochemicals that may produce misleading results with regard to DNA damage and in several other respects. Specifically it was reported that dietary chemopreventive compounds can increase oxidative stress and cause DNA damage at high concentrations [38], whereas they act as antioxidants to reduce DNA damage at dietary or pharmacologic concentrations [39]. Often, the doses utilized in these studies are not achievable in vivo; therefore, whether phytochemicals might exert translational promises and benefits in clinical settings and prevention of breast cancer remain unclear.

In this study, we tested EGCG doses considerably lower than the dose of 100–120 μM used for most in vitro studies and thus are closer to levels with physiological relevance [40].

We demonstrate that at doses of 10, 20, 40 μM EGCG effectively inhibits the growth of ER+ PR+ cancer cells (Fig. 1), and it exerts its effects through multiple mechanisms of action including (i) modulation of Hsp90 chaperone activity (Fig. 4A and B) and (ii) activation of p38MAPK /CK2 signaling (Fig. 4E and F), influencing the redistribution of the PR (Fig. 4C) from the cytosol to the nucleus, (iii) recruitment of PR-B onto the ER-α promoter (Fig. 5C) leading to transcriptional inhibition of ER-α (Fig. 3B) thus reducing its expression (Fig. 2A) and E2/ER-α genomic (Fig. 2B and C) and nongenomic activity (Fig. 2D). We herein indicate that EGCG via modulation of ER-α blocks cancer cell proliferation. These studies provide a better understanding of the specific factors that can mediate ER-α downregulation in breast cancer cells, which may be critical for future therapeutic strategies attempting to reduce its expression.

A body of evidences obtained by in vivo studies demonstrate the consequences of unregulated ER-α levels at all stages of breast cancer development. For instance, transgenic mice with elevated ER-α levels can develop ductal hyperplasias, lobular hyperplasias, and ductal carcinoma in situ [2]. Furthermore, it is shown that *ESR1* is amplified in subsets of breast cancers and in precancerous breast diseases [41]. Therefore, it is reasonable to consider ER-α downregulators of significant clinical interest. In this concern, we show that EGCG treatment decreased both ER-α genomic and rapid nongenomic activity as a consequence of ER-α content depletion that occurs through PR-B nuclear translocation. These novel findings corroborate our previous studies [20] indicating that inhibition of ER-α by PR-B is a critical regulatory pathway in ER-α-positive breast cancer cells, and highlight the protective role of PR-B as determinant of EGCG downregulatory effects, since PR-B knockdown attenuated the inhibition of ER-α levels after EGCG stimulus.

Steroid receptors such as PR in the absence of ligand, interact with Hsp90 [42]. Previous studies demonstrated that EGCG interferes with Hsp90 chaperone activity for PR, by binding to Hsp90 at or near a *C*-terminal ATP-binding site [43]. We demonstrate that EGCG acts at both ER-α mRNA and protein level via Hsp90/p-38MAPK signaling to PR-B in T47D and MCF-7 cells. We also define the molecular mechanisms through which EGCG interferes with ER-α gene transcription. Our functional experiments using five deletion constructs of the ER-α promoter showed that EGCG's downregulatory effects occur through a region between −2769 and −1000 bp of the promoter (Fig. 3A) which contains a known half-PRE site that is required for repression of the ER-α promoter by PR-B [20]. Our data support previous clinical and in vitro studies [20, 44] illustrating the protective role of PR-B expression in breast cancer. This concept is further reinforced by studies showing that HER-2/neu signaling, is also inversely associated with PR levels [45].

EGCG specifically reduced the expression of HSP70 and HSP90 [43] with overproduction instead, resulting in the increased incidence of cell transformation [46]. Our results correlate with these data since EGCG decreased Hsp90 client proteins expression levels (Fig. 4A) with a concomitant reduction of cell proliferation and estradiol-induced colony formation of MCF-7 and T47D (Fig. 1B). Hsp90 inhibition is known to impact cellular client protein homeostasis via different mechanisms [32, 47]. For example, Hsp90 inhibition can arrest maturation of Hsp90-bound client proteins without disrupting the cochaperone complex, can block the release of the refolded protein, leading to ubiquitin-dependent degradation or can prevent the binding of the target client protein to Hsp90. Our results confirm that EGCG acts as an inhibitor of Hsp90 chaperone function in ER+ PR+ breast cancer cell types examined, since it produced a drastic reduction of Her 2, EGFR, raf1 levels in a dose-dependent manner (Fig. 4A).

Hsp90 functions in part as a cytoplasmic retention factor for steroid receptors [42], and our results suggest a role of Hsp90 as mediator of EGCG action in the modulation of the subcellular localization of PR-B isoforms. The nucleocytoplasmic distribution of PR-B in T47D cells was affected by EGCG treatment (Fig. 4C). Unliganded receptors mainly localize to the cytoplasm. However, EGCG treatment leads to more PR-B nuclear localization, concomitant to a reduced cytoplasmic retention due to inhibition of the PR-B–Hsp90 interaction (Fig. 4B). EGCG treatment via p38/CK2 activation indeed resulted in destabilization of Hsp90–PR-B complexes. We also demonstrated the specific involvement of the PR-B isoform in mediating EGCG action using the isoform-specific siRNA experiments (Fig. 5B and C).

Our results are consistent with previous studies [48] showing that disruption of the chaperone function of Hsp90 by treatment with different drugs increased polyubiquitylation and depletion of ER-α levels and transcriptional activity resulting in growth arrest and apoptosis [49, 50].

EGCG may indirectly affect steroid receptors nuclear translocation influencing their ability to interact with Hsp90 clients via MAP kinase superfamily. It has been reported that PR-A and PR-B stability and transcriptional activities is selectively regulated by p38 and p42/44 MAPK through specific phosphorylation sites [51] and MAPKs are known to play important roles in PR subcellular trafficking via Ser294 phosphorylation [52]. A significant finding in our study is that sustained p38 and CK2 activation by EGCG influenced Hsp90–PR-B interactions, and played a critical role in the nuclear localization of PR-B as demonstrated with specific inhibitors of p38 and CK2 (Fig. 4C and D). Dissociation of PR with its chaperones and receptor dimerization, leads to its binding to PREs in the promoters of target genes and the recruitment of specific co-regulators and general transcription factors, resulting in the modulation of transcription of those genes [53]. Recent studies in the human endometrium have demonstrated that PR-A and PR-B are distributed either evenly throughout the nucleus or into discrete nuclear foci, and that there is a link between the subnuclear distribution of PR and its transcriptional activity [53]. These data collectively indicate that these nuclear foci contain multiple activated PR-co-regulator complexes that can influence the basic transcriptional machinery. Our ChIP assays (Fig. 5C) of

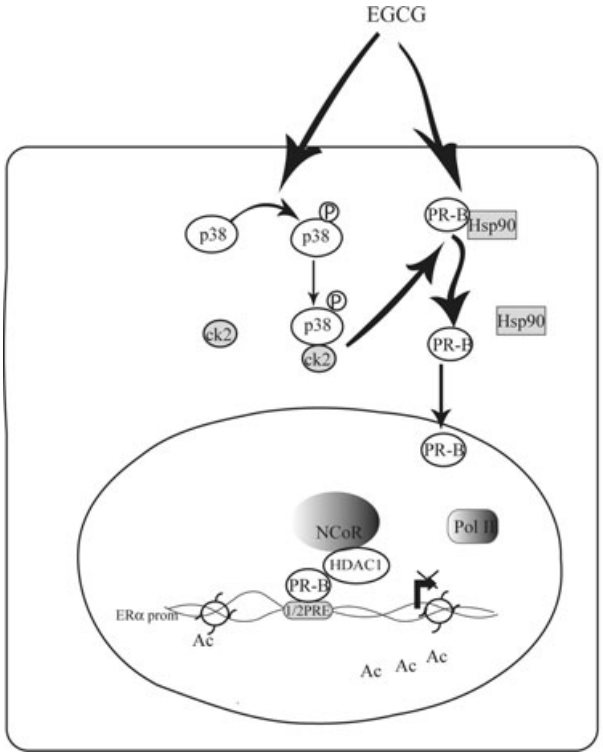

Figure 6. A proposed model for EGCG-induced repression of ER-α promoter in ER+ breast cancer cells. For details, see the text. Ac, acetylation.

the ER-α promoter correlate well with these previous reports and also show a release of RNAPol II. This is concomitant to the enhancement of the tripartite co-repressor complex PR-B/NCoR/HDAC1 (Fig. 5C) due to PR-B nuclear localization via p38/CK2 activation.

Our results support the molecular mechanism that EGCG's inhibition of ER-α gene transcription is mediated by a physical recruitment to the promoter of PR-B, which then exerts a repressive effect on chromatin by maintaining interactions between the co-repressor NCoR and HDAC1 with the ER-α gene (Fig. 5C). Thus, PR-B recruitment after EGCG treatment is to the PRE half-sites in the ER-α promoter. We also show that EGCG induces PR-B binding directly to this PRE half-site. Results from transient cell transfection assays, with ER-α reporter gene containing point mutations in the half PRE (Fig. 3C), further confirm the importance of PR DNA binding and the PRE half-site for a functional inhibitory response to EGCG. Furthermore, siRNA knockdown of PR-B confirmed that recruitment of the PR-B isoform to the half-PRE site within the ER-α gene promoter is a prerequisite in mediating EGCG downregulatory effects on ER-α expression in breast cancer cells.

We propose a novel model (Fig. 6) for the inhibitory action of EGCGs on the proliferation of ER+ PR+ breast cancer cells, through regulation of ER-α gene transcription. The p38/CK2 activation by EGCG provides a mechanism for the downregulation of Hsp90–PR-B interactions, as well as PR-B nuclear localization which is necessary for its recruitment to the half-PRE site within the ER-α promoter. The formation of a tripartite complex, containing PR-B, HDAC1, and NCoR that interacts with the half PRE, induces those alterations in chromatin structure such as deacetylation which then blocks promoter accessibility to the transcriptional machinery such as RNAPol II.

In conclusion, we discovered that EGCG can function as ER-α downregulator thus inhibiting ER+/PR+ breast cancer cell growth. Our results suggest that potentiating EGCG/PR-B signaling should be further exploited for clinical approach.

This work was supported by PRIN–MIUR and Ex 60% 2011- and NIH/NCI R01 CA72038 to SAWF. Authors declare that the experiments comply with the current laws of the country in which they were performed.

The authors have declared no conflict of interest.

5 References

[1] Herynk, M. H., Fuqua, S. A., Estrogen receptor mutations in human disease. *Endocr. Rev.* 2004, *25*, 869–898.

[2] Frech, M. S., Halama, E. D., Tilli, M. T., Singh, B. et al., Deregulated estrogen receptor alpha expression in mammary epithelial cells of transgenic mice results in the development of ductal carcinoma in situ. *Cancer Res.* 2005, *65*, 681–685.

[3] Poola, I., Abraham, J., Baldwin, K., Saunders, A. et al. Estrogen receptor h4 and h5 are ligand independent transcription factors and negative modulators of ER-α: cloning from human ovary and functional characterization. *Endocrine* 2005, *27*, 227–238.

[4] van Agthoven, T., Timmermans, M., Dorssers, L. C., Henzen-Logmans, S. C., Expression of estrogen, progesterone and epidermal growth factor receptors in primary and metastatic breast cancer. *Int. J. Cancer.* 1995, *63*, 790–793.

[5] Khan, S. A., Rogers, M. A., Obando, J. A., Tamsen, A., Estrogen receptor expression of benign breast epithelium and its association with breast cancer. *Cancer Res.* 1994, *54*, 993–997.

[6] Hong, W. K., Sporn, M. B., Recent advances in chemoprevention of cancer. *Science* 1997, *278*, 1073–1077.

[7] De Amicis, F., Giordano, F., Vivacqua, A., Pellegrino, M. et al., Resveratrol, through NF-Y/p53/Sin3/HDAC1 complex phosphorylation, inhibits estrogen receptor {alpha} gene expression via p38MAPK/CK2 signaling in human breast cancer cells. *FASEB J.* 2011, *25*, 3695–3707.

[8] Mukhtar, H., Wang, Z. Y., Katiyar, S. K., Agarwal, R., Tea components: antimutagenic and anticarcinogenic effects. *Prev. Med.* 1992, *21*, 351–360.

[9] Nakachi, K., Suemasu, K., Suga, K., Takeo, T. et al., Influence of drinking green tea on breast cancer malignancy among Japanese patients. *Jpn. J. Cancer. Res.* 1998, *89*, 254–261.

[10] Liao, S., Umekita, Y., Guo, J., Kokontis, J. M. et al., Growth inhibition and regression of human prostate and breast

tumors in athymic mice by tea epigallocatechin gallate. *Cancer Lett.* 1995, *96*, 239–243.

[11] Belguise, K., Guo, S., Sonenshein, G. E., Activation of FOXO3a by the green tea polyphenol epigallocatechin-3-gallate induces estrogen receptor alpha expression reversing invasive phenotype of breast cancer cells. *Cancer Res.* 2007, *67*, 5763–5770.

[12] Sah, J. F., Balasubramanian, S., Eckert, R. L., Rorke, E. A., Epigallocatechin-3-gallate inhibits epidermal growth factor receptor signaling pathway. Evidence for direct inhibition of ERK1/2 and AKT kinases. *J. Biol. Chem.* 2004, *279*, 12755–12762.

[13] Gupta, S., Hastak, K., Ahmad, N., Lewin, J. S. et al., Inhibition of prostate carcinogenesis in TRAMP mice by oral infusion of green tea polyphenols. *Proc. Natl. Acad. Sci. USA* 2001, *98*, 10350–10355.

[14] Liang, Y. C., Lin-shiau, S. Y., Chen, C. F., Lin, J. K., Suppression of extracellular signals and cell proliferation through EGF receptor binding by (−)-epigallocatechin gallate in human A431 epidermoid carcinoma cells. *J. Cell. Biochem.* 1997, *67*, 55–65.

[15] Siddiqui, I. A., Asim, M., Hafeez, B. B., Adhami, V. M. et al., Green tea polyphenol EGCG blunts androgen receptor function in prostate cancer. *FASEB J.* 2011, *25*, 1198–1207.

[16] Qanungo, S., Das, M., Haldar, S., Basu, A., Epigallocatechin-3-gallate induces mitochondrial membrane depolarization and caspase-dependent apoptosis in pancreatic cancer cells. *Carcinogenesis* 2005, *26*, 958–967.

[17] Tran, P. L., Kim, S. A., Choi, H. S., Yoon, J. H. et al., Epigallocatechin-3-gallate suppresses the expression of HSP70 and HSP90 and exhibits anti-tumor activity in vitro and in vivo. *BMC Cancer* 2010, *10*, 276. doi:10.1186/1471-2407-10-276.

[18] Carson-Jurica, M. A., Schrader, W. T., O'Malley, B. W., Steroid receptor family: structure and functions. *Endocr. Rev.* 1990, *11*, 201–220.

[19] Farabegoli, F., Barbi, C., Lambertini, E., Piva, R., (-)-Epigallocatechin-3-gallate downregulates estrogen receptor alpha function in MCF-7 breast carcinoma cells. *Cancer Detect. Prev.* 2007, *31*, 499–504.

[20] De Amicis, F., Zupo, S., Panno, M. L., Malivindi, R. et al., Progesterone receptor B recruits a repressor complex to a half-PRE site of the estrogen receptor alpha gene promoter. *Mol. Endocrinol.* 2009, *23*, 454–465.

[21] Bunone, G., Briand, P. A., Miksicek, R. J., Picard, D., Activation of the unliganded estrogen receptor by EGF involves the MAP kinase pathway and direct phosphorylation. *EMBO J.* 1996, *15*, 2174–2183.

[22] Tora, L., Mullick, A., Metzger, D., Ponglikitmongkol, M. et al., The cloned human oestrogen receptor contains a mutation which alters its hormone binding properties. *EMBO J.* 1989, *8*, 1981–1986.

[23] Faivre, E. J., Lange, C. A., Progesterone receptors upregulate Wnt-1 to induce epidermal growth factor receptor transactivation and c-Src-dependent sustained activation of Erk1/2 mitogen-activated protein kinase in breast cancer cells. *Mol. Cell. Biol.* 2007, *27*, 466–480.

[24] Kastner, P., Krust, A., Turcotte, B., Stropp, U. et al., Two distinct estrogen-regulated promoters generate transcripts encoding the two functionally different human progesterone receptor forms A and B. *EMBO J.* 1990, *9*, 1603–1614.

[25] deGraffenried, L. A., Hilsenbeck, S. G., Fuqua, S. A., Sp1 is essential for estrogen receptor α gene transcription. *J. Steroid Biochem. Mol. Biol.* 2002, *82*, 7–18.

[26] Vivacqua, A., Lappano, R., De Marco, P., Sisci, D. et al., G protein-coupled receptor 30 expression is up-regulated by EGF and TGF alpha in estrogen receptor alpha-positive cancer cells. *Mol. Endocrinol.* 2009, *23*, 1815–1826.

[27] De Amicis, F., Thirugnansampanthan, J., Cui, Y., Selever, J. et al., Androgen receptor overexpression induces tamoxifen resistance in human breast cancer cells. *Breast Cancer Res. Treat.* 2010, *121*, 1–11.

[28] Guido, C., Panza, S., Santoro, M., Avena, P. et al., Estrogen receptor beta (ER-β) produces autophagy and necroptosis in human seminoma cell line through the binding of the Sp1 on the phosphatase and tensin homolog deleted from chromosome 10 (PTEN) promoter gene. *Cell Cycle* 2012, *11*, 2911–2921.

[29] Hu, X. F., Veroni, M., De Luise, M., Wakeling, A. et al., Circumvention of tamoxifen resistance by the pure anti-estrogen ICI 182,780. *Int. J. Cancer* 1993, *55*, 873–876.

[30] Castoria, G., Migliaccio, A., Bilancio, A., Di Domenico, M. et al., PI3-kinase in concert with Src promotes the S-phase entry of oestradiol-stimulated MCF-7 cells. *EMBO J.* 2001, *20*, 6050–6059.

[31] Acconcia, F., Totta, P., Ogawa, S., Cardillo, I. et al., Survival versus apoptotic 17b-estradiol effect: role of ER-α and ER-β activated nongenomic signalling. *J. Cell. Physiol.* 2005, *203*, 193–201.

[32] Tillotson, B., Slocum, K., Coco, J., Whitebread, N. et al., Hsp90 (heat shock protein 90) inhibitor occupancy is a direct determinant of client protein degradation and tumor growth arrest in vivo. *J. Biol. Chem.* 2010, *285*, 39835–39843.

[33] Hildesheim, J., Salvador, J. M., Hollander, M. C., Fornace, A. J. Jr., Casein kinase 2- and protein kinase A-regulated adenomatous polyposis coli and beta-catenin cellular localization is dependent on p38 MAPK. *J. Biol. Chem.* 2005, *280*, 17221–17226.

[34] Duval, D., Malaisé, M., Reinhardt, B., Kedinger, C., Boeuf, H., A p38 inhibitor allows to dissociate differentiation and apoptotic processes triggered upon LIF withdrawal in mouse embryonic stem cells. *Cell Death Differ.* 2004, *11*, 331–341.

[35] Jepsen, K., Rosenfeld, M. G., Biological roles and mechanistic actions of co-repressor complexes. *J. Cell. Sci.* 2006, *115*, 689–698.

[36] Ogunleye, A. A., Xue, F., Michels, K. B., Green tea consumption and breast cancer risk or recurrence: a meta-analysis. *Breast Cancer Res. Treat.* 2010, *119*, 477–484.

[37] Thangapazham, R. L., Passi, N., Maheshwari, R. K., Green tea polyphenol and epigallocatechin gallate induce apoptosis and inhibit invasion in human breast cancer cells. *Cancer Biol. Ther.* 2007, *6*, 1938–1943.

[38] De Amicis, F., Santoro, M., Guido, C., Russo, A. et al., Epigallocatechin gallate affects survival and metabolism of human sperm. *Mol. Nutr. Food. Res.* 2012, *56*, 1655–1664.

[39] Moiseeva, E. P., Almeida, G. M., Jones, G. D., Manson, M. M., Extended treatment with physiologic concentrations of dietary phytochemicals results in altered gene expression, reduced growth, and apoptosis of cancer cells. *Mol. Cancer Ther.* 2007, *6*, 3071–3079.

[40] Hsieh, T. C., Wu, J. M., Suppression of cell proliferation and gene expression by combinatorial synergy of EGCG, resveratrol and gamma-tocotrienol in estrogen receptor-positive MCF-7 breast cancer cells. *Int. J. Oncol.* 2008, *33*, 851–859.

[41] Holst, F., Stahl, P. R., Ruiz, C., Hellwinkel, O. et al., Estrogen receptor alpha (*ESR1*) gene amplification is frequent in breast cancer. *Nat. Genet.* 2007, *39*, 655–660.

[42] Schowalter, D. B., Sullivan, W. P., Maihle, N. J., Dobson, A. D. et al., Characterization of progesterone receptor binding to the 90- and 70-kDa heat shock proteins. *J. Biol. Chem.* 1991, *266*, 21165–21173 .

[43] Yin, Z., Henry, E. C., Gasiewicz, T. A., Epigallocatechin-3-gallate is a novel Hsp90 inhibitor. *Biochemistry* 2009, *48*, 336–345.

[44] Hopp, T. A., Weiss, H. L., Hilsenbeck, S. G., Cui, Y. et al., Breast cancer patients with progesterone receptor PR-A-rich tumors have poorer disease-free survival rates. *Clin. Cancer Res.* 2004, *10*, 2751–2760.

[45] Huang, H. J., Neven, P., Drijkoningen, M., Paridaens, R. et al., Association between HER-2/neu and the progesterone receptor in oestrogen-dependent breast cancer is age-related. *Breast Cancer Res. Treat.* 2005, *91*, 81–87.

[46] Ciocca, D. R., Calderwood, S. K., Heat shock proteins in cancer: diagnostic, prognostic, predictive, and treatment implications. *Cell Stress Chaperones* 2005, *10*, 86–103.

[47] Basso, A. D., Solit, D. B., Chiosis, G., Giri, B. et al., Akt forms an intracellular complex with heat shock protein 90 (Hsp90) and Cdc37 and is destabilized by inhibitors of Hsp90 function. *J. Biol. Chem.* 2002, *277*, 39858–39866.

[48] Fiskus, W., Ren, Y., Mohapatra, A., Bali, P. et al., Hydroxamic acid analogue histone deacetylase inhibitors attenuate estrogen receptor-alpha levels and transcriptional activity: a result of hyperacetylation and inhibition of chaperone function of heat shock protein 90. *Clin. Cancer Res.* 2007, *13*, 4882–4890.

[49] Bagatell, R., Khan, O., Paine-Murrieta, G., Taylor C. W. et al., Destabilization of steroid receptors by heat shock protein 90-binding drugs: a ligand-independent approach to hormonal therapy of breast cancer. *Clin. Cancer Res.* 2001, *7*, 2076–2084.

[50] Lee, M., Kim, E., Kwon, H. J., Kim, Y. M. et al., Radicicol represses the transcriptional function of the estrogen receptor by suppressing the stabilization of the receptor by heat shock protein 90. *Mol. Cell. Endocrinol.* 2002, *188*, 47–54.

[51] Khan, J. A., Amazit, L., Bellance, C., Guiochon-Mantel, A. et al., p38 and p42/44 MAPKs differentially regulate progesterone receptor A and B isoform stabilization. *Mol. Endocrinol.* 2011, *25*, 1710–1724.

[52] Qiu, M., Olsen, A., Faivre, E., Horwitz, K. B. et al., Mitogen-activated protein kinase regulates nuclear association of human progesterone receptors. *Mol. Endocrinol.* 2003, *17*, 628–642.

[53] Arnett-Mansfield, R. L., Graham, J. D., Hanson, A. R., Mote, P. A. et al., Focal subnuclear distribution of progesterone receptor is ligand dependent and associated with transcriptional activity. *Mol. Endocrinol.* 2007, *21*, 14–29.

Original Research Article

Epigallocatechin gallate inhibits growth and Epithelial-to-Mesenchymal Transition in human thyroid carcinoma cell lines[†]

Francesca De Amicis[1,2*], Anna Perri[1-3*], Donatella Vizza[3], Alessandra Russo[1,2], Maria Luisa Panno[2], Daniela Bonofiglio[1,2], Cinzia Giordano[1], Loredana Mauro[2], Saveria Aquila[1,2], Donatella Tramontano[4] and Sebastiano Andò[1,2]

[1]Centro Sanitario, [2]Department of Pharmacy, Health and Nutrition Sciences, University of Calabria, Italy; [3]Research Center Kidney and Transplantation, Annunziata Hospital, Cosenza, Italy; [4]Department of Cellular and Molecular Pathology "L. Califano", University of Naples "Federico II", Italy

*De Amicis F: and Perri A. equally contributed to this work

Running title: **Epigallocatechin effect on thyroid carcinoma cells**

Corresponding address:
Sebastiano Andò, Centro Sanitario-University of Calabria, Arcavacata di Rende (CS) 87036, ITALY.
TEL: +39 0984 496201, FAX: +39 0984 496203, E-mail: sebastiano.ando@ unical.it

Note: Authors declare that the experiments comply with the current laws of the country in which they were performed. The authors declare that they have no conflict of interest.

This work was supported by PRIN – MIUR Ex 60 % 2011- and Epidemiologic Observatory Endemic Goiter and Iodine prophylaxis', Calabria Region, Centro Sanitario-Italy

Received 12 November 2012; Revised 7 March 2013; Accepted 20 March 2013
Journal of Cellular Physiology

DOI 10.1002/jcp.24372

Abstract

Well-differentiated papillary and follicular thyroid carcinoma are the most frequent types of thyroid cancer and the prognosis is generally favorable however, a number of patients develops recurrences. Epigallocatechin-3-gallate (EGCG), a major catechin in green tea, was shown to possess remarkable therapeutic potential against various types of human cancers, although data on thyroid cancer cells are still lacking. The aim of this study was to investigate the effect of EGCG on the proliferation and motility of human thyroid papillary (FB-2) and follicular (WRO) carcinoma cell lines.

Our results demonstrate that EGCG (10, 40, 60 μM) treatment inhibited the growth of FB-2 and WRO cells in a dose-dependent manner. These changes were associated with reduced cyclin D1, increased p21 and p53 expression. Furthermore, EGCG suppressed phosphorylation of AKT and ERK1/2. In addition EGCG treatment results in reduction of cell motility and migration. Changes in motility and migration in FB-2 were associated with modulation in the expression of several proteins involved in cell adhesion and reorganization of actin cytoskeleton. After 24h EGCG caused an increase of the E-cadherin expression and a concomitant decrease of SNAIL, ZEB and the basic helix–loop–helix transcription factor TWIST. Besides expression of Vimentin, N-cadherin and α5-integrin was down-regulated. These data well correlate with a reduction of MMP9 activity as evidenced by gelatin zymography.

Our findings support the inhibitory role of EGCG on thyroid cancer cell proliferation and motility with concomitant loss of epithelial-to-mesenchymal cell transition markers.

Key words: green tea, cancer, proliferation, motility

Introduction

Thyroid cancer is the most common malignancy of the endocrine system, representing approximately 1% of all malignancies in Western countries. The majority of thyroid cancers are well differentiated types which comprise follicular and papillary carcinomas. The prognosis of well differentiated thyroid carcinoma is generally favorable. However, a number of patients develop recurrences and metastases (Mazzaferri et al., 1999), therefore development of novel therapeutic or preventive strategies is desirable.

Some human epidemiologic studies show that naturally occurring dietary substances are capable of slowing or blocking the carcinogenic process without adverse effects (Surh et al., 2003; De Amicis et al., 2011). Of these substances, epigallocatechin gallate (EGCG), a polyphenolic compound found in green tea showed chemo-preventive effect on various tumor models (Katiyar & Mukhtar, 1996) and reduced the tumor incidence, the number of tumor masses and metastasis (Chung et al., 2003). It is well known that EGCG induces apoptosis in many human cell lines: prostate cancer cell lines (Paschka et al., 1998), human epidermoid carcinoma A431 cells (Gupta et al., 2004), breast carcinoma MCF-7 cells (Mittal et al., 2004) and pancreatic cancer cells, while the effects of EGCG on thyroid cells are seldom studied (Lim & Cha, 2011).

Many molecular mechanisms of action have been proposed. EGCG modulates the proteasome, mitochondrial depolarization, and fatty acid synthase (Yang et al., 2011). EGCG also inhibits growth factor receptor extracellular signaling such as IGF/IGF-1 receptor, Akt, NF-κB and mitogen-activated protein kinases (MAPKs) (Kanwar et al., 2012; Saeki et al., 2002).

Constitutive activation of MAP kinase effectors -the tyrosine receptor kinase RET and the intracellular signaling effectors RAS and BRAF- are essential for the pathogenesis of papillary thyroid carcinoma (Santoro et al., 2004). Many of the genetic alterations (Ras mutations, PTEN mutations, RET/PTC and PPARγ/Pax8 rearrangements) in thyroid cancer could potentially activate both the MAPK and PI3K/AKT pathways (Xing et al., 2010) which usually result in cancer progression and metastasis.

The extracellular matrix plays a fundamental role in the process of tumor invasion. Extensive studies in the last decade have revealed that matrix metalloproteases (MMPs) are frequently over-expressed in most forms of human tumor (Edwards & Murphy, 2002) and are implicated in the destruction of the extracellular matrix, thus facilitating tumor invasion (Yamamura et al., 2002). EGCG has inhibitory effects on MMP-2 and MT1-

MMP in glioblastoma cells (Annabi et al., 2002) reduces MT1-MMP activity in an invasive human fibrosarcoma cell line (Dell' Aica et al., 2002) and induces repression of MMP-9 expression in lung carcinoma cells (Yang et al., 2005). In 1993, Isemura et al. reported that EGCG inhibited the adhesion of cancer cells to endothelial cell layers.

In the present study we aimed to investigate the inhibitory role of EGCG on the growth and migratory capacities of human papillary and follicular thyroid cancer cell lines, FB-2 and WRO.

Materials and Methods

Materials – Epigallocatechin 3 gallate (EGCG), aprotinin, leupeptin, phenylmethylsulfonyl fluoride (PMFS), and sodium orthovanadate were from Sigma Aldrich (Milan, Italy). Antibodies used in this study were GAPDH, cyclin D1, p21, p53, E-cadherin, N-cadherin, MMP9, Vimentin, α5 integrin from Santa Cruz Biotechnology (Santa Cruz, CA); total MAPK (ERK1/2), total AKT, phosphorylated p42/44 MAPK (pERK1/2) (Thr202/Tyr 204) and pAKT (Ser473), from Cell Signaling Technology (Beverly, MA).

Cell Culture – FRTL5 cells clone 2, human thyroid papillary carcinoma (FB-2) and thyroid follicular carcinoma (WRO) cell lines were kindly provided by Dr. Basolo F. (Pisa, Italy) and cultured as described (Villone et al., 1997; Basolo et al., 2002). Treatments were performed, after 48h of serum starvation, in 1% dextran charcoal-stripped (CS) FBS to reduce steroid concentration (De Amicis et al., 2009).

MTT assay - Cells (3×10^4cells/mL) were plated in 24 well plates and serum-starved for 48h before the addition of treatment for 4 days (d). The MTT assay was performed as previously described (Vivacqua et al., 2009). The absorbance was measured with the Ultrospec 2100 Prospectrophotometer (Amersham-Biosciences, Milan, Italy) at a test wavelength of 570nm.

[^{3}H] thymidine incorporation- FB-2 and WRO cells, serum starved for 48h, were treated with 10, 40, and 60 μm EGCG for 18h. For the last 6h, [^{3}H]thymidine (1 μCi/ml) was added to the culture medium. After rinsing with PBS, the cells were washed once with 10% and three times with 5% trichloroacetic acid, lysed by adding 0.1N NaOH, and then incubated for 30 min at 37 °C. Thymidine incorporation was determined by scintillation counting.

DNA fragmentation - FB-2 cells, serum starved for 48h, were treated with 10, 40, and 60 μm EGCG for 24h Samples were collected, washed with PBS and pelleted at 1,800□rpm for 5□min and resuspended in

0.5 ml of extraction buffer (50 mmol/L Tris–HCl, pH 8; 10 mmol/L EDTA, 0.5% SDS) for 20 min in rotation at 4°C. DNA was extracted three times with phenol-chloroform and one time with chloroform. The aqueous phase was used to precipitate nucleic acids with 0.1 volumes of 3 M sodium acetate and 2.5 volumes cold ethanol overnight at −20°C. The DNA pellet was resuspended in 15 µl H_2O treated with RNase A for 30 min at 37°C. The extracted DNA was subjected to electrophoresis on 1.5% agarose gels, stained and then photographed.

Wound healing assay – Method was performed as previously described (De Amicis et al., 2006). Briefly, cells were grown to confluence in regular medium, and then were maintained in serum-free medium for 48h. The monolayers were scratched using a P200 pipette tip rinsed, photographed (t0) and treated as indicated. Then wound-healing was photographed again at 24h. Images are representative of three different experiments.

Motility assay - Cells synchronized in serum free media for 48h were dispersed with versene, washed twice, and processed as previously reported (De Amicis et al., 2006) using Boyden chambers. After 12h of incubation the upper chamber were removed. The migrated cells were counted using an inverted microscope.

Reverse transcription and real-time PCR - Cells were treated as indicated and processed as described (Guido et al., 2012). The primers were: (p53 forward) 5'-GTGGAAGGAAATTTGCGTGT-3'; (p53 reverse) 5'-CCAGTGTGATGATGGTGAGG-3'; (p21 forward) 5'-CTGTGCTCACTTCAGGGTCA-3'; (p21 reverse) 5'-CATAGTTAGTCACACCTCGT-3'; (SNAIL forward) 5'-CAGACCCACTCAGATGTCAA-3'; (SNAIL reverse) 5'-CATAGTTAGTCACACCTCGT -3'; (ZEB1 forward) 5'- GCACCTGAAGAGGACCAGAG -3'; (ZEB1 reverse) 5'-GTGTAACTGCACAGGGAGCA -3'; (ZEB2 forward) 5'- CGCTTGACATCACTGAAGGA -3'; (ZEB2 reverse) 5'- CTTGCCACACTCTGTGCATT- -3'; (TWIST forward) 5'-GGGAGTCCGCAGTCTTAC -3'; (TWIST reverse) 5'- CCTGTCTCGCTTTCTCTTT -3'; (18S forward) 5'-GGCGTCCCCCAACTTCTTA-3' (18S reverse) 5'-GGGCATCACAGACCTGTTATT-3' .

Gelatin zymography - Gelatinolytic activity and quantity in conditioned media were analyzed by gelatin zymography. In brief cells were cultured as indicated, and the conditioned medium was centrifuged to

remove cellular debris and then separated on sodium dodecyl sulfate–polyacrylamide gel electrophoresis gel containing 1 mg/ml gelatin. The gel was washed with buffer I (Tris–HCl [pH 7.5] and 2.5% Triton X-100), incubated overnight in buffer II (150 mM NaCl, 5 mM CaCl2, 50 mM Tris–HCl [pH 7.6]) at 37 °C and stained with Coomassie blue. The clear bands indicate where MMPs degraded gelatin.

Western blotting - Protein expression was assessed by Western blotting (WB). For total protein extracts, RIPA buffer was used (50 mM Tris-HCl, pH 7.4, 150 mM NaCl, 1% NP-40, 0.25% Na deoxycholate, plus inhibitors). The protein content was determined using Bradford dye reagent (Bio-Rad). 50 μg of lysates were separated on an 11% polyacrylamide denaturing gel (SDS-PAGE) and transferred to nitrocellulose membranes. Proteins of interest were detected with specific Abs, recognized by peroxidase-coupled secondary Abs, and developed using the ECL Plus Western Blotting detection system (Amersham Pharmacia Biotech, United Kingdom). The images were acquired by using an Epson Perfection scanner (Epson, Japan) using Photoshop software (Adobe). The optical densities of the spots were analyzed by using ImageJ software (NIH; http://rsb.info.nih.gov/IJ).

Statistical Analysis - Each datum point represents the mean ± S.D. of three different experiments. Data were analyzed by Student's t test using the GraphPad Prism 4 software program. $P<0.05$ was considered as statistically significant.

Results

EGCG treatment decreases FB-2 and WRO cell proliferation

We investigated first whether EGCG effects on FB-2 and WRO cell proliferation could be detected following extended treatments with low doses of the catechin. Proliferating cells were exposed to different nontoxic concentrations of EGCG (10μM; 40μM; 60μM) and then analyzed in MTT growth assay (Fig.1A). After 4 days treatment, 10μM EGCG inhibited basal cell proliferation (40% in FB-2 and 35% in WRO). With increasing doses of EGCG (40 and 60μM), cell number was further reduced by 68% to 73%, respectively in FB-2 and 55% to 70% in WRO. In contrast basal cell proliferation of a normal thyroid cell line FRTL5, was not affected after EGCG treatment.

We next determined the effect of EGCG on FB-2 cell growth by measuring changes in the rate of DNA synthesis (^{3}H thymidine incorporation). Consistently with MTT assays, after 18h treatment, EGCG reduced

basal ^{3}H Thymidine incorporation in a dose dependent manner reaching 78% inhibition at the concentration of 60μM (Fig.1B). Similar results were obtained in WRO cells.

To ascertain if these events were associated with cell death we determined whether EGCG treatment may induce changes in the inter-nucleosomal fragmentation profile of genomic DNA, a diagnostic hallmark of cells undergoing apoptosis. As shown in Fig. 1C, no DNA fragmentation was evidenced in FB-2 after EGCG exposure at all tested concentrations. Similar results were obtained in WRO cells (data not shown). We also evaluated expression levels of pro-apoptotic effectors such as Bax and Bad by immunoblotting analysis. We found a decrease in the levels of Bax and Bad expression compared to the control (Fig. 1D)

EGCG decreases cyclin D1 and up-regulates p21$^{WAF1/Cip1}$ and p53 expression in FB-2 cells

To characterize the molecular mechanism associated with the EGCG effects on FB-2 cell proliferation, we examined changes in the expression of genes involved in this process. Specifically cyclin D1 associates with selected cyclin-dependent kinases phosphorylating the retinoblastoma protein 1 (Rb1) inducing cell proliferation (Fu et al., 2004), therefore we assessed its expression.

FB-2 cells were incubated with different concentrations of EGCG (10μM; 40μM; 60μM) for 24hr prior to western blot analysis (Fig.2A). 10μM EGCG treatment caused a decrease in expression of cyclin D1 and treatment with higher concentrations of EGCG (40-60μM) produced stronger effects. The anti-proliferative response has been shown to be mediated by cyclin-dependent kinase inhibitors such as p21 (Gartel et al., 2005). We found that p21 protein and mRNA were markedly enhanced by EGCG at all tested concentrations, as evidenced by WB (Fig.2A) and real time PCR (Fig.2B).

The p53 tumor suppressor gene is considered to be a "master cellular regulator" which upon stress stimuli becomes activated and promotes cell cycle arrest and apoptosis (Laptenko et al., 2006), therefore we evaluated the effect of EGCG treatment on p53 expression. EGCG induced higher p53 levels in terms of protein (Fig. 2A) and mRNA levels (Fig.2B).

EGCG modulates AKT and MAPK signalling in FB-2 and WRO cells.

EGCG exerts its biological functions by modulation of multiple signaling pathways. To gain insight into the mechanism underlying the down-regulatory effect of EGCG on thyroid cancer cell proliferation, we examined the changes in signal transduction influenced by EGCG.

Cellular proteins were extracted from FB-2 and WRO cells treated with 40μM of EGCG at different times, and by WB analysis we determined the status of AKT phosphorylation. As shown in Fig.3A, EGCG within

5 min of treatment reduced by 50% phosphorylation level of AKT which remained significantly down-regulated until 24h treatment in FB-2 cells. In the follicular cell line a significant inhibition of p-AKT was reached after 60 min and was still maintained after EGCG prolonged exposure. We also exploited the phosphorylation level of p-MAPK (p-ERK1/2) in similar experimental conditions. We observed that 40μM EGCG produced a rapid and sustained, strong down-regulation of p-ERK1/2 levels in FB-2. In WRO cells, the early p-ERK1/2 down-regulation appears less evident after 6h but it is again significantly reduced after 24h EGCG exposure (Fig.3B).

EGCG inhibits motility in FB-2 and WRO cells

We then tested the effect of EGCG on cell motility by performing a wound-healing assay. Confluent cell monolayers were maintained in serum-free medium for 48h before scrape wounding and then stimulated with different concentrations of EGCG. After 24h, we found that EGCG greatly inhibited the wound closure (Fig. 4A) and it was able to reduce the number of WRO cells, elongated and morphologically more fibroblast like, compared to untreated.

Next we employed another approach to study the migratory capacity of FB-2 and WRO cells utilizing a modified Boyden chamber in the absence of extracellular matrix (ECM) proteins. Cells were serum starved for 48h, removed with versene (a non-proteolytic chelating agent), and seeded on poly-lysine coated Boyden chamber in the absence or presence of different concentration of EGCG. After 12h, treated cells showed a significant reduction of migration activity as compared to untreated cells (Fig. 4B).

EGCG treatment influences expression levels of cadherins in FB-2 cells

Cell motility is influenced by changes in the expression of specific proteins involved in cell adhesion among which cadherins play a central role (De Marzo et al., 1999). Thus, we evaluated specific expression levels in FB-2 cells after 24h treatment with different concentration of EGCG. We found that EGCG induced the expression of E-cadherin and reduced N-cadherin, Vimentin and α5-integrin consistently with the reduced cell motility (Fig.5A).

Increased expression of E-cadherin repressors such as SNAIL, ZEB and the basic helix–loop–helix transcription factor TWIST1 is related with loss of E-cadherin expression in thyroid cancer progression (Buehler et al., 2013). Accordingly, mRNA expression levels of SNAIL, ZEB1, ZEB2 and Twist were reduced over a period of 24h after stimulation with EGCG in FB-2 cells (Fig.5B).

EGCG treatment influences MMP9 activity in FB-2 cells

Degradation of extracellular matrix and vascular basement membrane is required for a cancer cell to invade and MMP9 and MMP2 are among the major proteinases that have such a role. As shown above, EGCG reduced cell motility, suggesting that MMP activity could be influenced by EGCG. The active form of MMP9 (the smaller band which is around 75KD) was significantly decreased upon EGCG treatments as evidenced by WB (Fig. 5A).

We next performed in-gel zymography to determine whether EGCG regulated the MMP9 activity. After 24 h of EGCG treatment, MMP9 activity clearly decreased with maximum effect at the concentration of 60 μM when almost completely disappeared (Fig.5C).

Discussion

Tea polyphenols, in particular (−)-epigallocatechin-3-gallate have gained considerable attention as potential treatment for a variety of diseases (Khan et al., 2009; De Amicis et al., 2012). A body of evidence show inhibition of enzyme activities and signal transduction pathways, resulting in the suppression of cell proliferation and enhancement of apoptosis, as well as the inhibition of cell invasion, angiogenesis and metastasis.

Cancer prevention by tea and tea components has been studied in many different animal models of carcinogenesis. Administration of tea polyphenols during the initiation or promotion stage of tumorigenesis inhibited 4-(N-methyl-N-nitrosamino)-l-(3-pyridyl)-l-butanone(NNK)-induced lung tumorigenesis in rats and mice tumours (von Pressentin et al.,. 2001; Shi et al., 1994).

The effects of tea consumption on the risk of human cancer have been investigated in many epidemiological studies, but the results are still under debate. 127 case–control studies and 90 cohort studies treat the relationship between tea consumption and the risk for colon, lung, stomach, breast, prostate, ovarian, pancreatic, kidney, bladder although data studies on thyroid cancer-preventive effect of tea are still lacking. (Yuan et al., 2011).

In this study we demonstrate that at doses of 10, 40, 60 μM EGCG effectively inhibits the growth and motility of FB-2 and WRO thyroid carcinoma cells, and it exerts its effects through multiple possible mechanisms of action including 1) modulation of cyclin D1, p21 and p53 expression 2) inhibition of MAPK and AKT signaling 3) decrease of metastatic markers, such as MMP9. The EGCG doses we used, are

considerably lower than the dose of 100-120 μM used for most in vitro studies and thus are closer to levels with physiological relevance (Moiseeva et al., 2007; Hsieh et al., 2008).

As first attempt, to provide new insight into the down-regulatory action exerted by EGCG on thyroid cell growth, we analyzed its effect on FB-2 and WRO cells and we found that the inhibitory effect of EGCG on cell proliferation and S-phase progression was significant, suggesting a G1 arrest. No substantial alteration was evidenced in FRTL5, a strain of normal and differentiated cells originally derived from adult rat thyroids. It is worth of notice that in our experimental conditions there is no evidence of apoptosis after EGCG exposure, as demonstrated by DNA laddering assay and by expression levels of pro-apoptotic proteins such as Bax and Bad .

Alterations of the mechanisms controlling proliferation and cell cycle progression play a central role in the pathogenesis of different human neoplasia. Particularly cell cycle is regulated by the coordinate action of cyclin-dependent kinases (cdk), specific cyclin proteins and cdk inhibitors. Cyclin D1 abnormalities may contribute to such malignant transformation (Fu et al., 2004). Altered expression of cyclin D1 may result from rearrangement, translocation, amplification and/or overexpression in head and neck, breast, squamous cell carcinomas, non-small cell lung cancer, colon and urinary bladder cancer. Of interest, we found that EGCG exposure down-regulates cyclin D1 protein levels at all the investigated concentrations. Our results are consistent with previous studies showing similar effects in human breast cancer cells (Chen et al., 2006), in colon cancer HT-29 cell line (Rouet-Benzineb et al., 2004) as well as in human hepatocarcinoma cells (Saxena et al., 2007).

Supporting these data it is a significant increase in p21 and p53. It is well accepted that p21 is a critical mediator of p53-dependent cell cycle arrest. EGCG treatment significantly increased p53 in terms of protein and mRNA levels.

Moreover, in our study, we demonstrated that EGCG influences ERK and AKT activation. As it emerges by western blotting observations, in FB-2 cells EGCG rapidly and strongly reduced the phosphorylation status of ERK1/2 as well as AKT and produced a sustained inactivation also in WRO cells which appear to endure the EGCG down-regulatory action. It is worth noting that our findings acquire more emphasis since previous reports indicate the involvement of PI3K-Akt/MAPK signaling in thyroid cancer oncogenesis and progression, due to oncogenic conversion of RET/RTK gene in thyroid cancer (Xing et al., 2010; Gschwind et al., 2004) activating both the MAPK and PI3K/Akt pathways which usually results in cancer progression

and metastasis. Besides the inhibitory roles of EGCG in papillary and follicular carcinoma cells suggest that such natural substances could be useful either alone or in combination with conventional therapeutics for the prevention of tumor progression and/or treatment of human malignancies (Sarkar et al., 2009; De Amicis et al., 2011).

Thyroid tumor progression is a complex process involving altered expression of many genes leading to metastatic disease. Distant metastasis represents one of the most lethal characteristics of thyroid cancer, and there are currently no effective therapeutic options for these patients. Metastasis is the result of a multi-stage course; initial local invasion, depends on both cell to cell adhesion and receptor-mediated adhesion to components of the ECM (Donald et al., 2001; Engl et al., 2005). In our study we found that EGCG treatment at all tested concentrations induces alteration of motility and adhesion in thyroid carcinoma cell lines tested. Our studies also show the variation of the expression levels of such motility-related factors. Particularly after EGCG treatment, FB-2 and WRO cells, showed a drastic decreased motility and a reduced migratory response. We found that this phenotype is associated with an increased expression of E-cadherin due to the reduced levels of several epithelial–mesenchymal transition (EMT) inducers such as the E-cadherin repressors SNAIL, ZEB and the basic helix–loop–helix transcription factor TWIST1. We also show the inverse association between the expression of α5 integrin and E-cadherin which emphasizes the modulatory action of EGCG for the adhesion of thyroid cancer cells as previously demonstrated in ovarian cancer (Thiery et al., 2009; Sawada et al., 2008).

It was reported that thyroid cancer cells are characterized by a mesenchymal phenotype, as revealed by spindle-shaped cells and absent or reduced levels of E-cadherin. Down-regulation of the expression of E-cadherin (Peinado et al., 2004) is an hallmark of epithelial-to-mesenchymal transition during embryonic development and contributes to important aspects of cancer development and progression (Batlle et al., 2000). It is worth of notice that E-cadherin appears clearly down-regulated in untreated FB-2 cells as demonstrated by our western blotting assay. Therefore EGCG can function to restore E-cadherin expression levels in thyroid cancer cells.

While E-cadherin functions as an invasion suppressor and is down-regulated in most carcinomas, N-cadherin, as an invasion promoter, is frequently up-regulated. Expression of N-cadherin in epithelial cells induces changes in morphology to a fibroblastic phenotype, rendering the cells more motile and invasive

(Cavallaro et al., 2004; Derycke et al., 2004). We evidence that EGCG was able to decrease N-cadherin expression after 24h of treatment and this well correlate with our cell motility studies.

Furthermore, recently the E-cadherin(low)/vimentin(high) expression profile was significantly correlated with shorter disease-free survival compared to E-cadherin(high)/vimentin(low) in hepatocellular carcinoma (Mima et al., 2013). Our study suggests that EGCG may counteract the invasive and metastatic phenotype and the process of EMT in thyroid cancer cells through overexpression of E-cadherin concomitant with the loss of vimentin.

The most common solid tumors metastasize preferentially to bone (Tantivejkul et al., 2004) and among these also thyroid cancer have an incidence of bone metastases of 7–20% (Wexler et al., 2011) and there are many factors that lead certain malignancies to have a predisposition to developing metastases. Among these factor, integrin receptors have been associated with cancer progression (Banyard & Zetter, 1999). Our study provides evidence that EGCG treatment in FB-2 thyroid cells down-regulates expression of the α5-integrin subunit, which mediates adhesion to fibronectin.

Important metastasis contributors are matrix metallo-proteinases (MMP2, MMP3 and MMP9) which function targeting the extracellular matrix (Noel et al., 2001). Activation of MMPs has been detected in almost all type of human cancer and closely correlated with advanced tumor stage, increased invasion and metastasis, and shortened survival time. Inhibition of MMP9 expression by a ribozyme could reduce the number of metastatic nodules formed in the lungs of mice (Pongracz et al., 2006). Our results demonstrate that after 24h EGCG treatment reduced the activity of MMP9 .Therefore, we indicate another mechanism of EGCG action, associated with increase of cell-cell adhesion by inhibition of MMP activity in digesting the extracellular matrix ingredients, thus blocking tumor cells to migrate to the adjacent tissues.

In summary, this study provided novel evidences that EGCG regulates the expression of specific set of genes and consequently can function as down-regulator of cell proliferation and cell motility in FB-2 and WRO thyroid cells. Our results suggest that potentiating EGCG signaling should be further exploited for clinical approach in papillary and follicular thyroid cancer.

References

[1] Annabi, B., Lachambre, M.P., Bousquet-Gagnon, N., Page, M., Gingras, D., Beliveau, R. (2002). Green tea polyphenol (-)-epigallocatechin 3-gallate inhibits MMP-2 secretion and MT1-MMP-driven migration in glioblastoma cells. *Biochimica et Biophysica Acta, 1542,* 209-220.

[2] Baker, A.H., Edwards, D.R., Murphy, G. (2002). Metalloproteinase inhibitors: biological actions and therapeutic opportunities. *Journal of Cell Science, 115,* 3719-3727.

[3] Banyard, J., Zetter, B.R. (1999). The role of cell motility in prostate cancer. *Cancer Metastasis Reviews, 17*, 449-458.

[4] Basolo, F., Giannini, R., Toniolo, A., Casalone, R., Nikiforova, M., Pacini, F., Elisei, R., Miccoli, P., Berti, P., Faviana, P., Fiore, L., Monaco, C., Pierantoni, G.M., Fedele, M., Nikiforov, Y.E., Santoro, M., Fusco A. (2002). Establishment of a non-tumorigenic papillary thyroid cell line (FB-2) carrying the RET/PTC1 rearrangement. *International Journal of Cancer, 97*, 608-614.

[5] Batlle, E., Sancho, E., Francí, C., Domínguez, D., Monfar, M., Baulida, J., García De Herreros, A. (2000). The transcription factor snail is a repressor of E-cadherin gene expression in epithelial tumour cells. *Nature Cell Biology, 2*, 84-89.

[6] Buehler D, Hardin H, Shan W, Montemayor-Garcia C, Rush PS, Asioli S, Chen H, Lloyd RV. Expression of epithelial-mesenchymal transition regulators SNAI2 and TWIST1 in thyroid carcinomas. Mod Pathol. 2013 Jan;26(1):54-61

[7] Cavallaro, U. (2004). N-cadherin as an invasion promoter: a novel target for antitumor therapy? *Current Opinion Investigational Drugs, 5*, 1274-1278.

[8] Chen, C., Chang, Y.C., Liu, C.L., Chang, K.J., Guo, I.C. (2006). Leptin-induced growth of human ZR-75-1 breast cancer cells is associated with up-regulation of cyclin D1 and c-Myc and down-regulation of tumor suppressor p53 and p21(WAF1/CIP1). *Breast Cancer Research and Treatment, 98,* 121–132.

[9] Chung, F.L., Schwartz, J., Herzog, C.R., Yang, Y.M. (2003). Tea and cancer prevention: studies in animals and humans. *The Journal of nutrition, 133,* 3268-3274.

[10] De Amicis, F., Lanzino, M., Kisslinger, A., Calì, G., Chieffi, P., Andò, S., Mancini, F.P., Tramontano, D. (2006). Loss of proline-rich tyrosine kinase 2 function induces spreading and motility of epithelial prostate cells. *Journal of Cellular Physiology , 209*, 74-80

[11] De Amicis, F., Zupo, S., Panno, M.L., Malivindi, R., Giordano, F., Barone, I., Mauro, L., Fuqua, S.A., Andò, S. (2009). Progesterone receptor B recruits a repressor complex to a half-PRE site of the estrogen receptor alpha gene promoter. *Molecular Endocrinology, 23,* 454-465.

[12] De Amicis, F., Giordano, F., Vivacqua, A., Pellegrino, M., Panno, M.L., Tramontano, D., Fuqua, S.A., Andò, S. (2011). Resveratrol, through NF-Y/p53/Sin3/HDAC1 complex phosphorylation, inhibits estrogen receptor alpha gene expression via p38MAPK/CK2 signaling in human breast cancer cells. *FASEB Journal, 25*, 3695-3707.

[13] De Amicis, F., Santoro, M., Guido, C., Avena P., Russo A. and Aquila S. (2013) Epigallocatechin-gallate affects survival and metabolism of human sperm. Mol Nutr Food Res. doi: 10.1002/mnfr.201200560.

[14] Dell'Aica, I., Dona, M., Sartor, L., Pezzato, E., Garbisa, S. (2002). (-)Epigallocatechin- 3-gallate directly inhibits MT1-MMP activity, leading to accumulation of nonactivated MMP-2 at the cell surface. *Laboratory Investigation; a journal of technical methods and pathology, 2002, 82,* 1685-1693.

[15] Derycke, L.D., Bracke, M.E. (2004). N-cadherin in the spotlight of cell-cell adhesion, differentiation, embryogenesis, invasion and signalling. *The International Journal of Developmental Biology , 48*, 463-476.

[16] Donald, C.D., Cooper, C.R., Harris-Hooker, S., Emmett, N., Scanlon, M., Cooke, D.B. (2001). Cytoskeletal organization and cell motility correlates with metastatic potential and state of differentiation in prostate cancer. *Cellular and Molecular Biology , 47*, 1033-1038.

[17] Engl, T., Relja, B., Blumenberg, C., Müller, I., Ringel, E.M., Beecken, W.D., Jonas, D., Blaheta, R.A. (2006). Prostate tumor CXC-chemokine profile correlates with cell adhesion to endothelium and extracellular matrix. *Life Sciences , 78*, 1784-1793.

[18] Fu, M., Wang, C., Li, Z., Sakamaki, T., Pestell, R.G. (2004). Minireview: Cyclin D1: normal and abnormal functions. *Endocrinology, 145*, 5439-47.

[19] Gschwind, A., Fischer, O.M., Ullrich, A. (2004). The discovery of receptor tyrosine kinases: targets for cancer therapy. *Nature Reviews. Cancer., 4*, 361–370.

[20] Guido, C., Panza, S., Santoro, M., Avena, P., Panno, M.L., Perrotta, I., Giordano, F., Casaburi, I., Catalano, S., De Amicis, F., Sotgia, F., Lisanti, M.P., Andò, S., Aquila, S. (2012). Estrogen receptor beta (ERβ) produces autophagy and necroptosis in human seminoma cell line through the binding of the Sp1 on

the phosphatase and tensin homolog deleted from chromosome 10 (PTEN) promoter gene. *Cell Cycle, 11*, 2911-2921.

[21] Gupta, S., Hastak, K., Afaq, F., Ahmad, N., Mukhtar, H. (2004). Essential role of caspases in epigallocatechin-3-gallate-mediated inhibition of nuclear factor kappa B and induction of apoptosis. *Oncogene, 23,* 2507-2522.

[22] Hsieh, T.C., Wu, J.M. (2008). Suppression of cell proliferation and gene expression by combinatorial synergy of EGCG, resveratrol and gamma-tocotrienol in estrogen receptor-positive MCF-7 breast cancer cells. *International Journal of Oncology, 33*, 851-859.

[23] Isemura, M., Suzuki, Y., Satoh, K., Narumi, K., Motomiya, M. (1993). Effects of catechins on the mouse lung carcinoma cell adhesion to the endothelial cells. *Cell Biology International, 17,* 5595-5564.

[24] Kanwar, J., Taskeen, M., Mohammad, I., Huo, C., Chan, T.H., Dou, Q.P. (2012). Recent advances on tea polyphenols. *Frontiers Bioscience, 4,* 111-131.

[25] Katiyar, S.K., Mukhtar, H. (1996). Tea in chemoprevention of cancer: Epidemiologic and experimental studies. *International Journal of Oncology, 8,* 221–238.

[26] Khan, N., Adhami, V.M., Mukhtar, H. (2009). Review: green tea polyphenols in chemoprevention of prostate cancer: preclinical and clinical studies. *Nutrition and Cancer, 61*, 836-841.

[27] Laptenko, O., Prives, C. (2006) Transcriptional regulation by p53: one protein, many possibilities. *Cell Death Differ.*, 13,951-61

[28] Lim, Y.C., Cha, Y.Y. (2011). Epigallocatechin-3-gallate Induces Growth Inhibition and Apoptosis of Human Anaplastic Thyroid Carcinoma Cells Through Suppression of EGFR/ERK Pathway and Cyclin B1/CDK1 Complex. *Journal of Surgical Oncology, 104,* 776–780.

[29] Mazzaferri, E.L. (1999). An overview of the management of papillary and follicular thyroid carcinoma. *Thyroid:Official Journal of the American Thyroid Association*, *9,* 421–427.

[30] Mima, K., Hayashi, H., Kuroki, H., Nakagawa, S., Okabe, H., Chikamoto, A., Watanabe, M., Beppu, T., Baba, H. (2013) Epithelial-mesenchymal transition expression profiles as a prognostic factor for disease-free survival in hepatocellular carcinoma: Clinical significance of transforming growth factor-β signaling. *Oncol Lett,* 5, 149-154.

[31] Mittal, A., Pate, M.S., Wylie, R.C., Tollefsbol, T.O., Katiyar, S.K. (2004). EGCG down-regulates telomerase in human breast carcinoma MCF-7 cells, leading to suppression of cell viability and induction of apoptosis. *International Journal of Oncology*, *24,* 703-710.

[32] Moiseeva, E.P., Almeida, G.M., Jones, G.D., Manson, M.M. (2007). Extended treatment with physiologic concentrations of dietary phytochemicals results in altered gene expression, reduced growth, and apoptosis of cancer cells. *Molecular Cancer Therapeutics, 6,* 3071-3079.

[33] Nagakawa, O., Akashi, T., Hayakawa, Y., Junicho, A., Koizumi, K., Fujiuchi, Y., Furuya, Y., Matsuda, T., Fuse, H., Saiki I. (2004). Differential expression of integrin subunits in DU-145/AR prostate cancer cells. *Oncology Reports, 12*, 837-841.

[34] Noel, A., Albert, V., Bajou, K., Bisson, C., Devy, L., Frankenne, F., Maquoi, E., Masson, V., Sounni, N.E., Foidart, J.M. (2001). New functions of stromal proteases and their inhibitors in tumor progression. *Surgical Oncology Clinics of North America,10*, 417-432.

[35] Paschka, A.G., Butler, R., Young, C.Y. (1998). Induction of apoptosis in prostate cancer cell lines by the green tea component, (-)-epigallocatechin-3-gallate. *Cancer Letters, 130,* 1-7.

[36] Peinado, H., Portillo, F., Cano, A. (2004). Transcriptional regulation of cadherins during development and carcinogenesis. *The International Journal of Developmental Biology, 48*, 365-375.

[37] Pongracz, J.E., Stockley, R.A. (2006). Wnt signalling in lung development and diseases. *Respiratory Research, 7*, 15.

[38] Rhoden, K.J., Unger, K., Salvatore, G., Yilmaz, Y., Vovk, V., Chiappetta, G., Qumsiyeh, M.B., Rothstein, J.L., Fusco, A., Santoro, M., Zitzelsberger, H., Tallini, G. (2006). RET/papillary thyroid cancer rearrangement in nonneoplastic thyrocytes: follicular cells of Hashimoto's thyroiditis share low-level recombination events with a subset of papillary carcinoma. *The Journal of Clinical Endocrinology and Metabolism, 91*, 2414-2423.

[39] Rouet-Benzineb, P., Aparicio, T., Guilmeau, S., Pouzet, C., Descatoire, V., Buyse, M., Bado, A. (2004). Leptin counteracts sodium butyrate-induced apoptosis in human colon cancer HT-29 cells via NF-kappaB signaling. *The Journal of Biological Chemistry , 279*, 16495-16502.

[40] Saeki, K., Kobayashi, N., Inazawa, Y., Zhang, H., Nishitoh, H., Ichijo, H., Saeki, K., Isemura M., Yuo, A. (2002). Oxidation-triggered c-Jun N-terminal kinase (JNK) and p38 mitogen-activated protein (MAP) kinase pathways for apoptosis in human leukaemic cells stimulated by epigallocatechin-3-gallate (EGCG): a

distinct pathway from those of chemically induced and receptor-mediated apoptosis. *The Biochemical Journal, 368,* 705–720.

[41] Sarkar, F.H., Li, Y., Wang, Z., Kong, D. (2009). Cellular signaling perturbation by natural products. *Cellular Signalling, 21*, 1541-1547.

[42] Saxena, N.K., Sharma, D., Ding, X., Lin, S., Marra, F., Merlin, D., Anania, F.A. (2007). Concomitant activation of the JAK/STAT, PI3K/AKT, and ERK signaling is involved in leptin-mediated promotion of invasion and migration of hepatocellular carcinoma cells. *Cancer Research, 67*, 2497-2507.

[43] Sawada, K., Mitra, A.K., Radjabi, A.R., Bhaskar, V., Kistner, E.O., Tretiakova, M., Jagadeeswaran, S., Montag, A., Becker, A., Kenny, H.A., Peter, M.E., Ramakrishnan, V., Yamada, S.D., Lengyel E. (2008) Loss of E-cadherin promotes ovarian cancer metastasis via alpha 5-integrin, which is a therapeutic target. *Cancer Research,68*, 2329-39

[44]] Shi, S.T., Wang, Z.Y., Smith, T.J., Hong, J.Y., Chen, W.F., Ho, C.T., Yang, C.S. (1994). Effects of green tea and black tea on 4-(methylnitrosamino)-1-(3-pyridyl)-1-butanone bioactivation, DNA methylation, and lung tumorigenesis in A/J mice. *Cancer Research, 54*, 4641-4647

[45 Surh, Y.J. (2003). Cancer chemoprevention with dietary phytochemicals. *Nature Reviews. Cancer, 3,* 768–780.

[46] Thiery, J.P., Acloque, H., Huang, R.Y. *et al*. (2009) Epithelial-mesenchymal transitions in development and disease. *Cell* ;*139*, 871–890.

[47] Villone, G., De Amicis, F., Veneziani, B.M., Salzano, S., Di Carlo, A., Tramontano, D 1997. Sustained versus transient cyclic AMP intracellular levels: effect on thyrotropin-dependent growth of thyroid cells. *Cell Growth Differ.*, *8*, 1181-8.

[48] Vivacqua, A., Lappano, R., De Marco, P., Sisci, D., Aquila, S., De Amicis, F., Fuqua, S.A., Andò, S., Maggiolini, M. (2009). G protein-coupled receptor 30 expression is up-regulated by EGF and TGF alpha in estrogen receptor alpha-positive cancer cells. *Molecular Endocrinology, 23,* 1815-1826.

[49] Von Pressentin, M.M., Chen, M., Guttenplan, J.B. (2001). Mutagenesis induced by 4-(methylnitrosamino)-1-(3-pyridyl)-1-butanone-4-(methylnitrosamino)-1-(3-pyridyl)-1-butanone and N-nitrosonornicotine in lacZ upper aerodigestive tissue and liver and inhibition by green tea. *Carcinogenesis, 22*, 203-206.

[50] Wexler, J.A. (2011). Approach to the thyroid cancer patient with bone metastases. *The Journal of Clinical Endocrinology and Metabolism , 96*, 2296-2307.

[51] Xing, M. (2010). Genetic alterations in the phosphatidylinositol-3 kinase/Akt pathway in thyroid cancer. *Thyroid:Official Journal of the American Thyroid Association*, *20,* 697-706.

[52] Yamamura, T., Nakanishi, K., Hiroi, S., Kumaki, F., Sato, H., Aida, S., Kawai, T. (2002). Expression of membrane-type-1-matrix metalloproteinase and metalloproteinase-2 in nonsmall cell lung carcinomas. *Lung Cancer:Journal of the International Association for the Study of Lung Cancer, 35,* 249-255.

[53] Yang, H., Landis-Piwowar, K., Chan, T.H., Dou, Q.P. (2011). Green tea polyphenols as proteasome inhibitors: implication in chemoprevention. *Current Cancer Drug Targets, 11,* 296-306.

[54] Yang, J., Wei, D., Liu, J. (2005). Repressions of MMP-9 expression and NFkappa B localization are involved in inhibition of lung carcinoma 95-D cell invasion by (-)-epigallocatechin-3-gallate. *Biomedicine & Pharmacotherapy, 59,* 98-103.

[55] Yuan, J.M., Sun, C., Butler, L.M. Tea and cancer prevention: epidemiological studies. (2011). *Pharmacological Research: the Official Journal of the Italian Pharmacological Society, 64*, 123-135.

Figure Legends

Figure 1

EGCG inhibits thyroid cancer cell proliferation A, MTT assay. FB-2, WRO and FRTL-5 cells, serum starved, were exposed to vehicle (-), or different concentrations of EGCG in medium containing 1% dextran charcoal-stripped FBS for 4d (treatments were renewed every 2d). Results indicate mean of three independent experiments done in triplicate; bars SD ;* $P<0.05$ compared with untreated cells. **B,** ^{3}H thymidine incorporation. FB-2 and WRO cells were exposed to vehicle (-), or different concentrations of EGCG for 18h. Thymidine incorporation assay was performed. Results indicate mean of three independent experiments done in triplicate; bars SD ;* $P<0.05$ compared with untreated cells. **C,** DNA fragmentation. FB-2 cells, serum starved, were exposed to vehicle (-), or different concentrations of EGCG for 24h**.** M, DNA marker. **D**, Immunoblot analysis. FB-2 cells were treated with different concentrations of EGCG for 24 h. The whole-cell lysates were then collected and analyzed by WB using specific Abs. Immunoblot figure results is representative of three independent experiments.

Figure 2

EGCG decreases cyclin D1 and up-regulates p21WAF1/Cip1 and p53 expression in FB-2 cells. A, Immunoblot analysis. FB-2 cells were treated with different concentrations of EGCG for 24 h. The whole-cell lysates were then collected and analyzed by WB using specific Abs. Immunoblot figures results are representative of three independent experiments; columns, mean of three independent experiments in which band intensities were evaluated in terms of optical density arbitrary units and expressed as percentages of the control, which was assumed to be 100%; bars, SD;* $P<0.05$ compared with untreated cells.

B, Real time PCR assay. mRNA expression of p53 and p21 in FB-2 cells treated with vehicle (-) or different concentrations of EGCG for 24 h; 18S was determined as a control. Graphs are the mean of three independent experiments run in triplicate; bars SD ;* $P<0.05$ compared with untreated cells.

Figure 3

EGCG modulates AKT and MAPK signalling in FB-2 and WRO cells. A-B Immunoblot analysis. Cells were treated with 40μM EGCG for different times as indicated. The whole-cell lysates were then collected and analyzed by WB using specific Abs. Columns mean of three independent experiments in which band

intensities were evaluated in terms of optical density arbitrary units and represent the average fold change in p-ERK/ERK and pAKT/AKT levels; bars, SD;* P<0.05 compared with untreated cells.

Figure 4

EGCG inhibits motility in FB-2 and WRO cells. A Serum-starved FB-2 and WRO cells were scrape wounded (t0h) and then treated as indicated. Images are representative of the process of wound-healing after 24h of treatment. **B** FB-2 and WRO cells were serum starved for 48 h. Synchronized cells were then seeded on polylisine-coated Boyden chambers and treated as indicated. Columns mean of number of migrated cells after 12h EGCG treatment of three independent experiments; bars, SD;* P<0.05 compared with untreated cells.

Figure 5

EGCG reduces MMP-9 protein secretion and activity in thyroid cells

A, Immunoblot analysis. FB-2 cells were treated with different concentrations of EGCG for 24 h. The whole-cell lysates were then collected and analyzed by WB using specific Abs. Immunoblot figures results are representative of three independent experiments; columns, mean of three independent experiments in which band intensities were evaluated in terms of optical density arbitrary units and expressed as percentages of the control, which was assumed to be 100%; bars, SD;* P<0.05 compared with untreated cells.

B,.Real time PCR assay. mRNA expression of SNAIL, ZEB1, ZEB2 and Twist in FB-2 cells treated with vehicle (-) or different concentrations of EGCG for 24 h; 18S was determined as a control. Graphs are the mean of three independent experiments run in triplicate; bars SD ;* P<0.05 compared with untreated cells. **C,** Gelatin zymography Conditioned medium from FB-2 cells treated as indicated for 24 h were collected and total protein concentration was determined. One microgram (mg) of protein for each treatment was resolved by SDS-PAGE followed by zymography. Areas of MMP9 enzymatic activity appeared as clear bands over the dark background. Results are representative of three independent experiments.

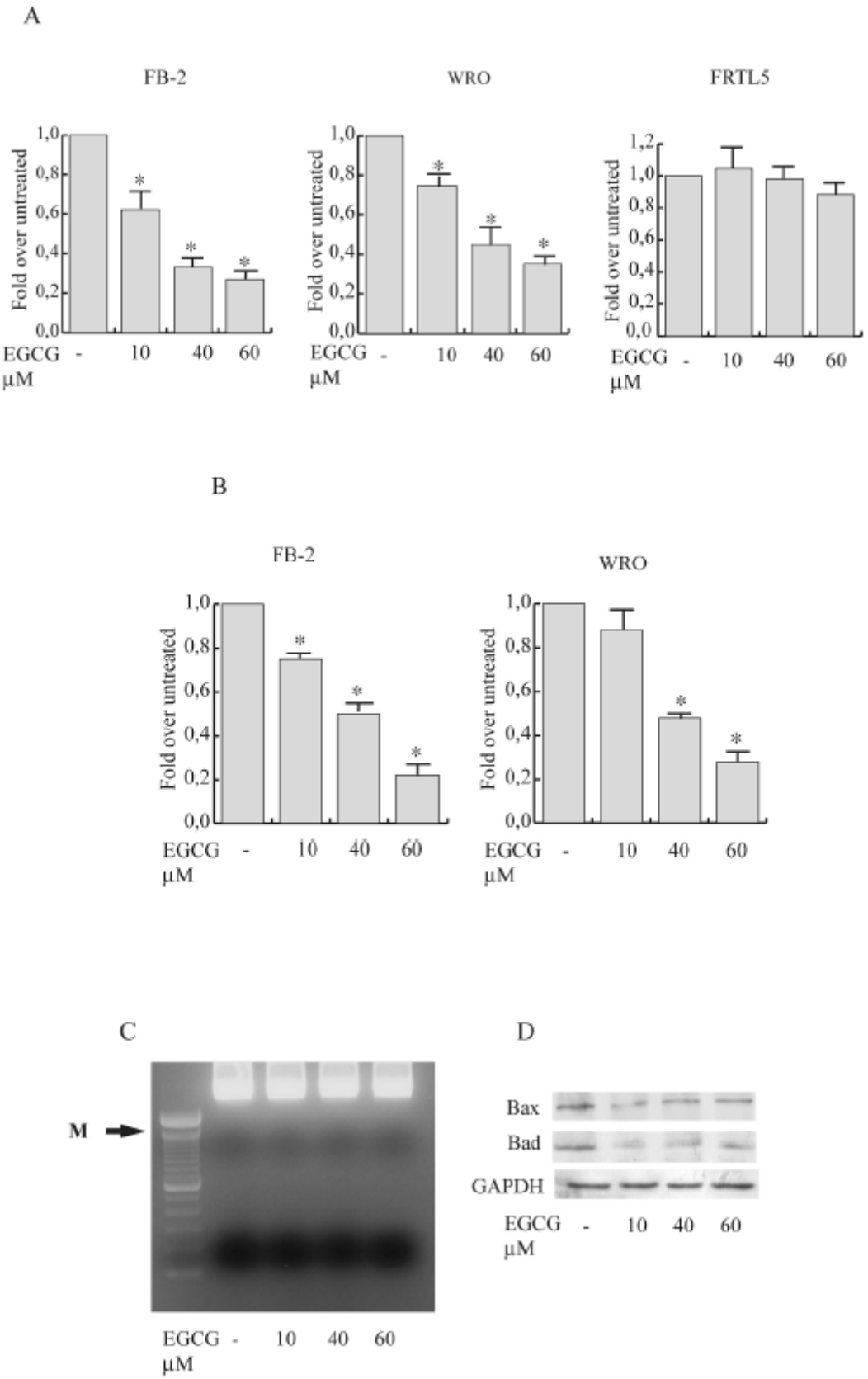

Figure 1

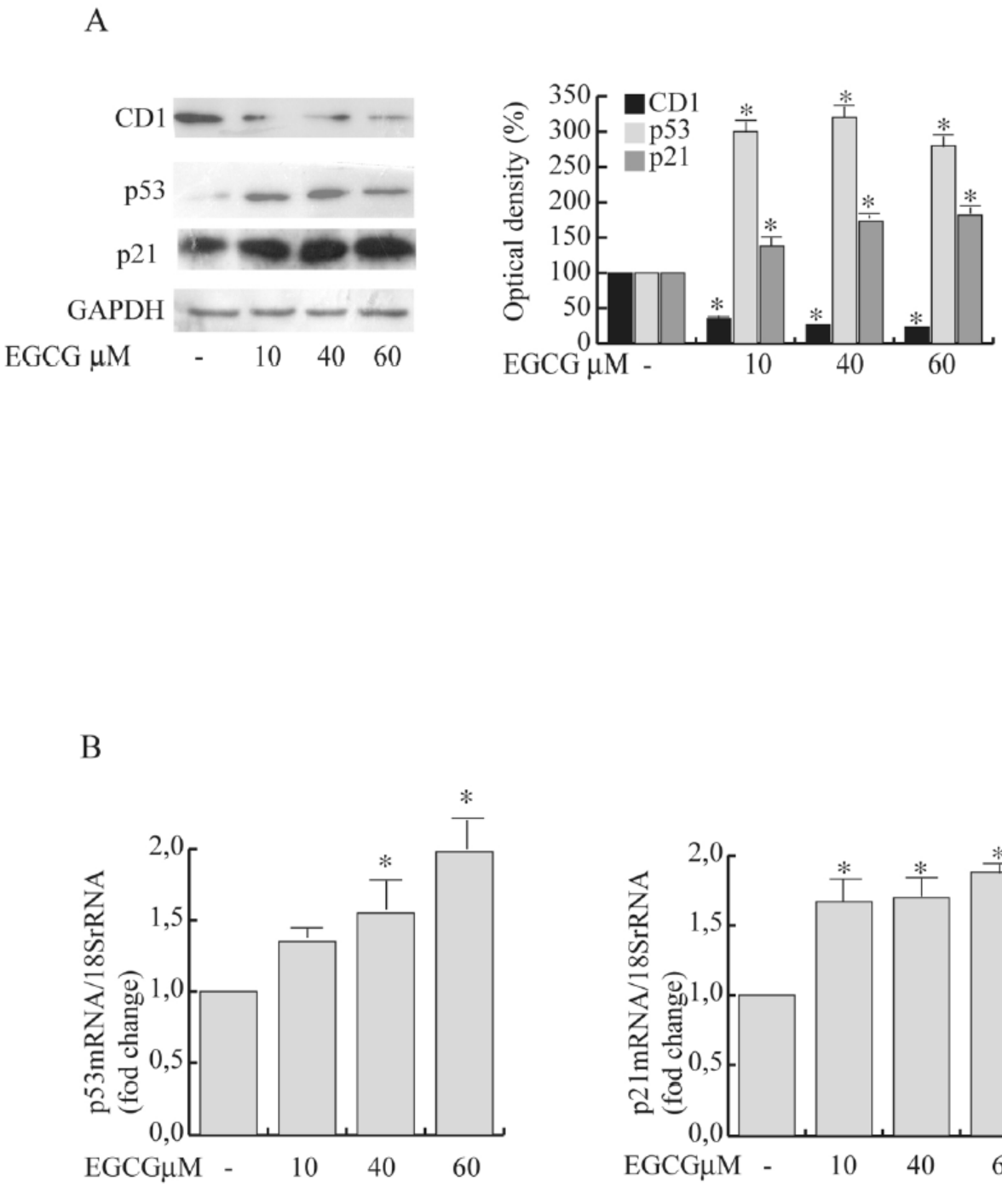

Figure 2

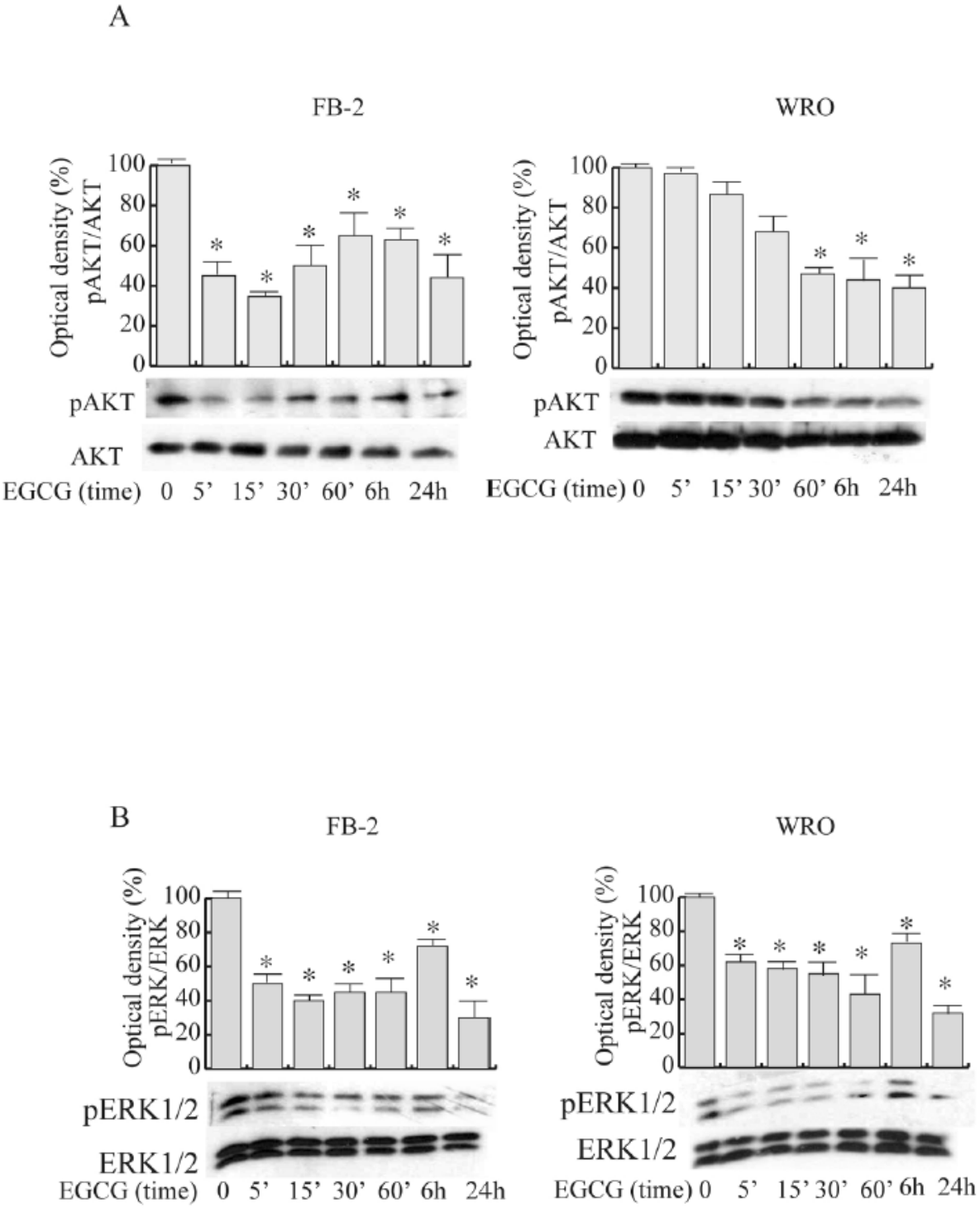

Figure 3

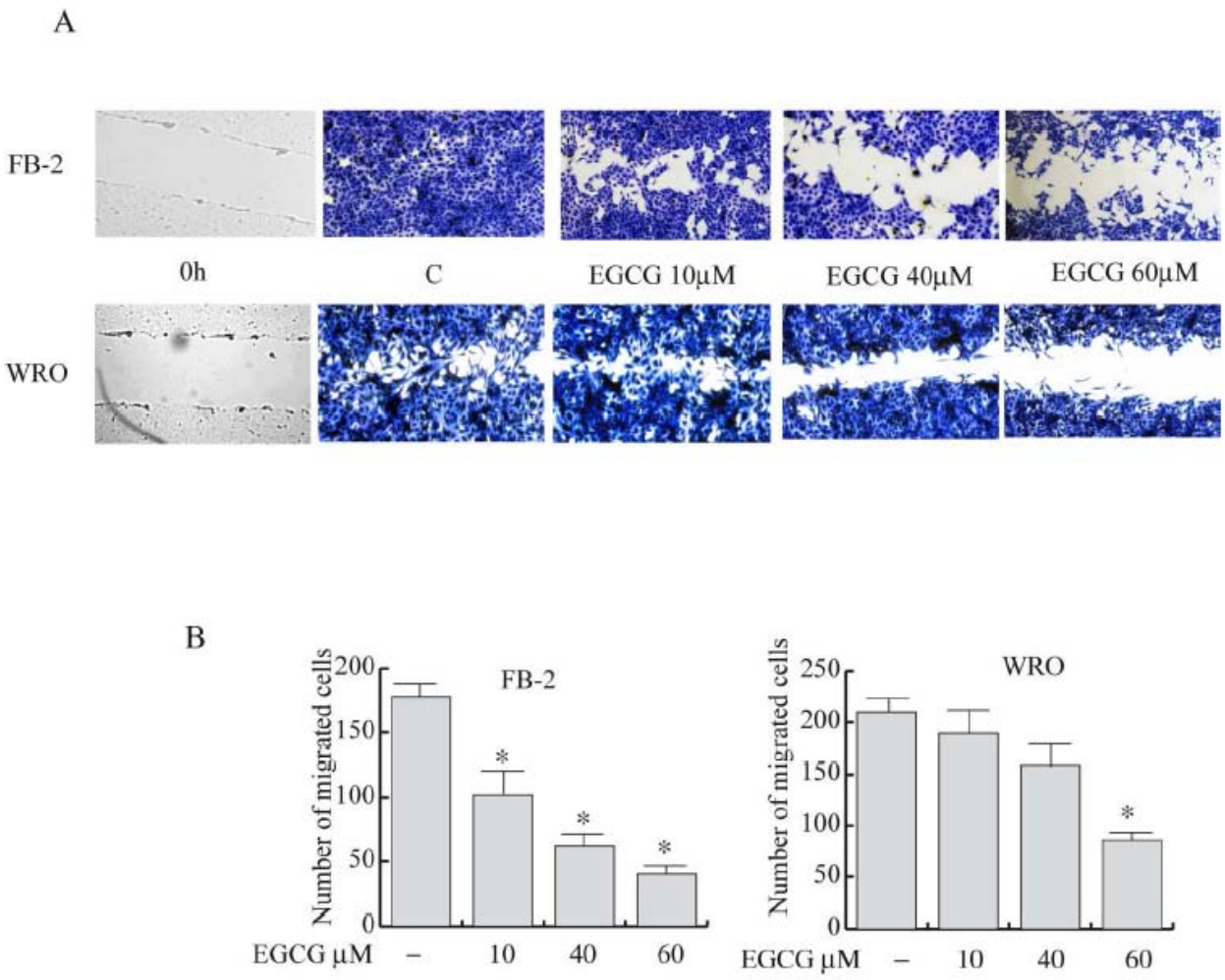

Figure 4

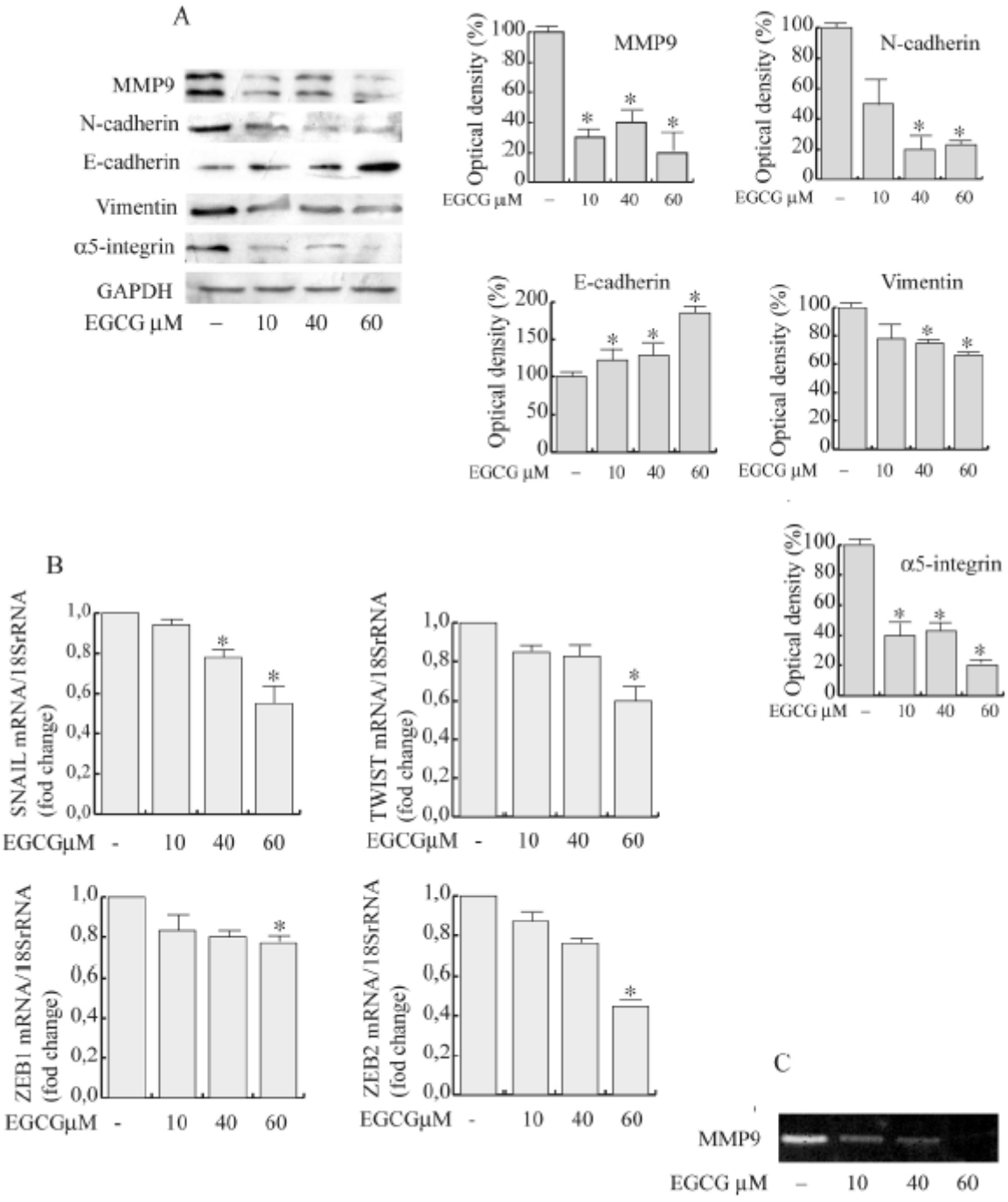

Figure 5